The Dissertation Committee for Taiwen Tang
certifies that this is the approved version of the following dissertation:

Multiple Antenna Downlink: Feedback Reduction, Interference Suppression and Relay Transmission

Committee:

Robert W. Heath, Jr., Supervisor

Jeffrey G. Andrews

Gustavo de Veciana

Scott M. Nettles

Lili Qiu

Multiple Antenna Downlink: Feedback Reduction, Interference Suppression and Relay Transmission

by

Taiwen Tang, B.E.; M.S.

DISSERTATION

Presented to the Faculty of the Graduate School of

The University of Texas at Austin

in Partial Fulfillment

of the Requirements

for the Degree of

DOCTOR OF PHILOSOPHY

THE UNIVERSITY OF TEXAS AT AUSTIN

August 2006

Dedicated to my parents

Acknowledgments

I would like to thank my parents Youxian Tang and Zifang Liu for their love and encouragement to me. Thank my Father for being a moral example to me and thank my Mother for being caring and giving to me. My gratitude goes to them especially for their encouragement and support during the difficult times of my Ph.D. study. Without those, this dissertation will not be possible. I also would like to thank my Uncle, Steve Tang and my Aunt, Qing Wang for their help and support. Those were essential for me to start and continue my graduate study.

I am indebted to my advisor, Prof. Robert W. Heath, Jr. Without his trust and help, I would not be able to start the Ph.D. study at UT. Thank him for his guidance and support throughout my life at UT. Thank him for helping me make improvements in research, writing and presentation. All these are important for the success of my Ph.D. and will have important influence on my career. I would like to thank my committee members at UT, Prof. Jeffrey G. Andrews, Prof. Gustavo de Veciana, Prof. Scott M. Nettles and Prof. Lili Qiu for their suggestions on my research and feedback on my dissertation. I also owe my gratitude to the professors at UT and Colorado State University, who have kindly accommodated me in their classes. I appreciate the classroom learnings from them.

I really want to express my gratitude to the past and current group members at the Wireless Networking and Communications Group for their friendship and help, especially Zukang Shen, Runhua Chen, Wei Wu, Roopsha Samanta, Manish Airy, Antonio Forenza, Johann Chiang, Bishwarup Mondal, Chan-Byoung Chae, Kaibin Huang and Caleb Lo. I also wish to thank Minyoung Park, Ketan Mandke and Chan-Byoung Chae for the collaboration on the research.

Multiple Antenna Downlink: Feedback Reduction, Interference Suppression and Relay Transmission

Publication No. _____

Taiwen Tang, Ph.D.
The University of Texas at Austin, 2006

Supervisor: Robert W. Heath, Jr.

Multiple input multiple output (MIMO), which uses multiple antennas at both the transmitters and the receivers, is an emerging technology that greatly improve the data rate of wireless systems. This dissertation focuses on the downlink of a cellular system, where a base station transmits data to multiple users. It proposes design solutions on how to combat the impairments in the system and improve the data rate or error rate performance with multiple antennas at the base station and/or the users.

In the downlink, the scheduling decisions, which determine how to transmit data from the base station to the users, usually depend on users' channel conditions, e.g., the gains or the coefficients of the channels. Reducing the system resource, e.g., transmission time or radio frequency band, used for feeding back the channel information from the downlink MIMO users, which works with scheduling algorithms and different MIMO transmitter and receiver

configurations, has been recently recognized as an important design issue. The first part of this dissertation proposes a scheduling and feedback strategy that exploits multiuser diversity with significant reduction of the amount of resource for feedback of channel information.

The second contribution of this dissertation studies the problem of interference suppression. Combatting interference from adjacent base stations that use the same radio frequency band (cochannel interference) requires signal processing techniques at the transmitters and/or the receivers. In particular, in orthogonal frequency division multiplexing (OFDM) systems, dealing with cochannel interference that is not synchronized in carrier frequency and propagation time poses challenges to the receiver design. This dissertation studies the design problem for suppressing the asynchronous cochannel interference at an OFDM receiver.

In the third part of this dissertation, a technique for improving coverage for the downlink users under heavy signal attenuation is investigated. The basic idea is to use relays that are deployed at fixed locations in the downlink to receive and forward signals from the base station to mobile users. This dissertation studies the design of different signal processing components for the system where both the base station and the relay have multiple antennas.

Table of Contents

List of Tables

List of Figures

Chapter 1

Introduction

This chapter introduces MIMO communications, discusses using multiple antennas for the downlink of cellular systems, and outlines main contributions of this dissertation. In Section 1.1, a brief introduction of the background on MIMO communications is presented. Then Section 1.2 summarizes the prior research on different MIMO communication scenarios. Section 1.3 introduces several issues that may challenge the system deployment and throughput performance of the multiple antenna downlink. These challenges include feedback reduction, interference suppression and relay-aided broadcast that will be addressed in details in Section 1.3.The main scope of this dissertation is on solutions to overcome these challenges. Main results are outlined in Section 1.4. Finally, notation used in this dissertation is described in Section 1.5.

1.1 Background on MIMO Communications

Wireless communication has developed rapidly worldwide over the past two decades. Demands on data service and multimedia communications over wireless media has driven wireless technology to support higher and higher data rates. For cellular systems, where mobile users communicate with the

centralized controllers of each local cell (the base station), migration from second generation wireless technology that mainly supports low data rate voice communications, to third and fourth generation broadband communications that promise high speed services such as high rate data transfer and digital video broadcasting, has been taking place worldwide.

High data rate communications most aggressively exploit the radio frequency resource. For many wireless systems, the radio frequency band is specified before deployment and it has a limited capacity or bandwidth. Improving the spectral efficiency, which defines the number of bits per second that can be transmitted per unit bandwidth, becomes more and more important. Multiple input multiple output (MIMO), which uses multiple antennas at the transmitters and receivers, has been well recognized as a promising approach to improve the spectral efficiency [1–5]. By sophisticated antenna array configuration and advanced array signal processing, utilization of spatial degrees of freedom becomes possible in multiple antenna systems. By sufficiently spacing the antenna elements, the signals traversed between any transmit and receive antenna pair become distinct from each other. Advanced array signal processing at both the transmitters and the receivers is able to exploit advantages such as higher system capacity, more reliable communication and spatial suppression of interfering transmissions.

Utilizing MIMO technology for a variety of wireless communication systems has received significant interest. For several communication standards of The Institute of Electrical and Electronics Engineers (IEEE), MIMO technol-

ogy has been incorporated into the draft standards or under active discussion. The IEEE 802.16 standards for fixed wireless broadband communications in cellular networks specifies different MIMO design options to improve the spectral efficiency of the system [6]. MIMO is also under formal development process in The Third Generation Partnership Project (3GPP) that works on standardization of the third generation cellular networks [7]. For wireless local area networks (WLAN), significant standardization efforts for MIMO technology have also been developed. The IEEE 802.11n [8] study group is currently working on standardizing a high throughput WLAN that uses MIMO technology.

1.2 Research on MIMO Channels

Different wireless communication scenarios are usually abstracted by "channel" models used in the context of information theory. These models include the *point-to-point channel*, where a source transmits data to a destination, *the broadcast channel*, where a source sends messages to multiple users, *the multiple access channel*, where multiple sources sends messages to a destination, *the relay channel*, where a source cooperates with a relay to send data to a destination, and *the interference channel*, where sources transmit messages to destinations and interfere with each other [9].

MIMO channels are the models used to abstract those communication scenarios when multiple antennas are used at the network nodes. Any transmission between a source with multiple transmit antennas and a destination

with multiple receive antennas in wireless local area networks can be viewed as a point-to-point MIMO channel. Similarly, the cellular downlink with multiple antennas, where the base station transmits data to multiple users, is an instance of the MIMO broadcast channel. The cellular uplink with multiple antennas at both the base station and users, where multiple users send data to the base station, can be modelled by a MIMO multiple access channel. In ad hoc networks where nodes communicate with each other without centralized coordination, relay transmissions and simultaneous interfering transmissions often take place. If multiple antennas are also used on the nodes of the ad hoc networks, the relay transmissions and the interfering transmissions can be modelled using MIMO relay channels and MIMO interference channels respectively.

Prior work on MIMO technology for different communication scenarios has been seen for *the point-to-point MIMO channel* [2, 3, 10–13], *the MIMO multiple access channel* [14], *the MIMO broadcast channel* [15–19], *the MIMO relay channel* [20–22], and *the MIMO interference channel* [23]. In this dissertation, we study several MIMO channels in a cellular communication context, including *the MIMO broadcast channel, the MIMO interference channel* and *the MIMO relay channel*. A brief overview of the related MIMO channels is presented in this subsection.

A main research focus in the past has been on the point-to-point MIMO channel. Studies on information theoretic aspect of the point-to-point MIMO channel reveal significant capacity improvement compared to the single input

single output channel [2]. Point-to-point MIMO transmission strategies such as space-time coding [10, 11, 24], beamforming [25], spatial multiplexing [25] and precoding [26, 27] have been investigated. The fundamental principles of these strategies lie in achieving either more reliable communication or higher data rate with MIMO technology. Details of these strategies are available in the literature.

Research on the multiple antenna broadcast channel shows that significant capacity improvement can be achieved by using multiple antennas in the broadcast channel, i.e., placing multiple antennas at both the source and the destinations [16, 18, 28]. Studies on design aspects of the MIMO broadcast channel remain very active, aiming to bridging the gap between the results from the theory and the practice [4]. Important issues include making decisions of selecting one or multiple users for data transmission (scheduling) and determining the transmission for the selected users and the corresponding reception strategies (transceiver design) at the user side. Techniques such as multiuser antenna selection, beamforming with user selection and multiuser precoding have been seen in [26, 29–35].

The MIMO interference channel, where sources send data to destinations and cause interference between each other's transmission, is another active research area. Using multiple antennas at both the sources and the destinations makes the system capable of dealing with interference with sophisticated array signal processing techniques at both the transmitters and the receivers. The capacity of the MIMO interference channel remains un-

known, however, bounds on the channel capacity have been derived in [23].

MIMO relay channels are also under active investigation. The conventional MIMO relay channel usually refers to a point to point MIMO transmission through a relay node with multiple antennas. The challenging problem for this system is how to coordinate the source and the relay to deliver more information to the destination. Results on rate bounds have been studied in [20–22]. Signal processing methods for the MIMO relay channels have also been investigated in [36–40]. The general concept of relay transmission can be extended to scenarios where a single source sends data to multiple destinations via relay nodes or multiple sources send data to multiple destinations via relay nodes. These communication channels still need to be understood.

1.3 Motivation of this Dissertation

MIMO is an ideal technology for improving data rate in next generation cellular networks. The downlink of a cellular network where data is transmitted from the base station to multiple destinations is an important part of the cellular system. Designing the downlink system with multiple antennas, however, is a challenging task. This dissertation studies solutions for several design challenges. Communication systems usually operate based on protocols defined for different protocol layers [41]. The first aspect of the research in this dissertation is oriented to the joint design of different protocol layers (cross-layer) for the multiple antenna downlink. The second aspect is on how to design sophisticated physical layer under interference or heavy signal atten-

uation for the downlink. Addressing these challenges for the MIMO downlink is the main motivation of this dissertation.

A major question that concerns the design of the MIMO downlink is how to exploit the benefits of MIMO in different protocol layers. A simple layering approach that designs each layer separately does not seem to effectively exploit the advantages of MIMO in the downlink. This limitation is especially recognized for the design of the medium access control (MAC) layer and the physical (PHY) layer of the downlink. The former is mainly concerned with controlling to accessing the wireless medium and the latter is mainly concerned with physical signaling.

In the MIMO downlink, the user scheduling that is part of the MAC functionality should take advantage of MIMO to serve one or multiple users at the same time with certain MIMO transmission strategies [29]. Throughput gain called multiuser diversity can be achieved by making the scheduling decision based on users' instantaneous channel state information [42][30]. User scheduling interacts with the MIMO transmission strategy and the receiver design. A joint design of all these components is a viable approach.

In addition, feedback of channel state information is another important issue. Availability of MIMO channel information for mobile users at the base station is critical for the overall system performance. However, the limited resource of the uplink feedback channel may prohibit real-time feedback of MIMO channel state information for a large number of downlink users [43]. The problem of reducing feedback for the downlink interacts with the schedul-

ing problem and the transceiver design problem. This again emphasizes the importance of a joint design approach to engineer the downlink system.

The challenge of cross-layer design for the MIMO downlink motivates the study of a scheduling and feedback strategy with certain transceiver configurations. This research aims to propose a framework to exploit the advantages of MIMO with reduced feedback and simple scheduling algorithms. The proposed framework is the first contribution for the MIMO downlink design problem.

The second question for designing a MIMO downlink is how to deal with the impairments of this wireless system. This includes the effects of interference and heavy signal attenuation. The main focus is on how to design the physical layer of the downlink. In cellular systems with multiple cells configured in the network (multicell scenario), cochannel interference from adjacent base stations that use the same frequency band has harmful effects on the system performance. Users at cell edges or under significant shadowing are exposed to heavy signal attenuation, therefore, these users are barely able to decode data transmitted from the base station.

Combatting cochannel interference for the MIMO downlink requires careful design of the transceivers for this system [44]. The downlink multicell scenarios resembles the interference channel in the information theory context. Furthermore, non-perfect synchronization in time and carrier frequency between the base station and the users magnifies the harmful effects of cochannel interference [45][46]. This motivates the study of the transceiver

design problem to combat asynchronous cochannel interference. This study is performed for a broadband system with orthogonal frequency division multiplexing (OFDM) that uses subcarriers in the frequency domain to transmit information. Under the assumptions about interference and propagation channels, the receiver design problem is studied. The interference suppression technique called space-time equalization that uses filters at all receive antennas to suppress the cochannel interference is used [45, 47, 48]. Design of the space-time equalizers to suppress cochannel interference is investigated in Chapter 3.

In dealing with the heavy attenuation of signals in the downlink, relays with multiple antennas that are deployed at fixed locations in the cellular network can be used to help the signal transmission [49, 50]. Since data may be distributed to multiple users from the base station, this relay system differs from conventional point-to-point relay systems. Design of the transceivers of this system at the physical layer is challenging since both the MIMO channel between the base station and the relay and the broadcast channel between the relay and the users need to be considered. The study for this problem focuses on the transceiver design aspect and on understanding the performance limits from an information theoretic perspective. This serves as the third contribution of this dissertation, which deals with the relay-aided broadcast system.

1.4 Outline of Contributions

This dissertation proposes solutions for the three problems of the multiple antenna downlink including scheduling with reduced feedback, suppression of cochannel interference, and relay-aided broadcast. These solutions aim to improve the throughput or error rate performance of this system. The proposed techniques could be used for the broadband cellular applications with fixed wireless access (ex. IEEE 802.16) and mobile wireless access (ex. IEEE 802.20). The contributions are summarized as the following:

- A scheduling and feedback strategy to improve the data rate with reduced feedback for the multiple antenna downlink employing linear receivers
  - Developing a feedback strategy that can significantly reduce the data rate for feeding back users' channel state information. This feedback strategy can be controlled by several control parameters.
  - Developing a scheduling algorithm that maps any transmit antenna at the base station to a downlink user (per-antenna scheduling) with the channel information obtained from the proposed feedback strategy.
  - Formulating and solving an optimization problem on how to select the feedback control parameters under different assumptions about the channel distribution information.

- An OFDM receiver for the downlink users with multiple antennas that can suppress the cochannel interference from adjacent base stations.
  - Developing a signal model to include the effects of carrier frequency offsets and propagation delays for this system under cochannel interference.
  - Deriving a condition for selecting the equalizer order and deriving a criterion to consider error-rate performance in the equalizer design.
  - Formulating and solving a space-time equalizer design problem when perfect channel and synchronization parameters are available at the receiver.
  - Formulating and solving a frequency estimation problem and a space-time equalizer design problem with known training sequences.
- Design of a MIMO fixed relay system with linear signal processing at the relay that uses two-hop transmissions to help the downlink broadcast.
  - Proposing a system architecture for the fixed relay system using two-hop transmission from the base station to the users through a fixed relay. The relay only applies linear signal processing to forward the received signal to the users. Proposing a mathematical model for this system.
  - Deriving lower and upper bounds on achievable sum rates of this system in the information theory context.

– Proposing an algorithm that selects multiple users with good channel conditions from all the downlink users for the fixed relay system.

– Proposing a feasible encoding strategy for this system and developing algorithms to design the signal processing components of this system.

1.5 Notation

The following notation is used throughout the dissertation. Matrices or vectors are denoted by bold-face letters, e.g., $\mathbf{A}$ or $\mathbf{a}$. The scalars are denoted by plain letters. The superscript T and $*$ denote the transpose and conjugate operations, respectively, and superscript H stands for conjugate transpose. The matrix trace operator is denoted by $tr(\cdot)$ and matrix inversion is expressed as $(\cdot)^{-1}$.

Chapter 2

Feedback Reduction in the MIMO Downlink with Linear Receivers

This chapter presents a framework for scheduling with reduced feedback for the multiple antenna downlink. A system that employs spatial multiplexing at the base station and linear receivers at the mobile users of the MIMO downlink is first presented. Reducing feedback has become an important issue for deploying multiuser diversity based scheduling. To resolve this problem, a novel feedback strategy that reduces the feedback of channel information for the scheduling framework in the MIMO downlink is proposed. The proposed strategy employs contention based feedback that achieves high multiuser diversity gain and leads to significant feedback reduction. An optimization problem for selection of the feedback control parameters is formulated. Further, iterative search algorithms are proposed to solve the optimization under two different system operation scenarios. The proposed feedback and scheduling framework serves as the main technical contribution of this chapter.

This chapter is organized as follows. In Section 2.1, background on

feedback reduction in the MIMO downlink is discussed and our main contributions are summarized. In Section 2.2, signal models for the downlink data channel and the uplink feedback channel are presented. The protocol is proposed in Section 2.3. In this section, the joint optimization problem for selection of the feedback control parameters is formulated and solved. Section 2.4 presents simulation results of the proposed protocol in different simulation scenarios.

2.1 Introduction

In the downlink of a cellular system, the base station transmits data to mobile users. The base station schedules the service to different mobile users based on the channel state information and the quality of service requirement of the users. Feedback of channel quality information from the mobile users to the base station is required for multiuser diversity [30]. This chapter concerns the problem of feedback of MIMO channel state information for the multiple antenna downlink.

2.1.1 Background on Feedback Reduction in the MIMO Downlink

Research on the MIMO Gaussian broadcast channel capacity has shown that multiuser transmission with dirty paper coding (DPC) can achieve optimum sum capacity under the assumption that complete MIMO channel state information of each user is available to the base station [15–19]. The major issue lies in that an optimal selection of a subset of users along with non-causal

channel coding for these users is required. However, while the sum capacity increases, the amount of feedback also increases with the number of users. Further, the wireless channel is time-varying due to mobility of users and scattering in the environment. Consequently frequent updates of the channel state information are required. Given the high number of channel parameters, the limited volume of the feedback channel seems likely to become a deterrent to system deployment.

An attractive approach that simplifies transmit processing and reduces feedback requirements was proposed in [29] and further studied in [51][52]. The idea is to use a variation of spatial multiplexing at the transmitter where the transmitted streams are independently scheduled to different users. A linear receiver is used at the receivers to provide low complexity detection. An advantage of this approach is that it converts the MIMO broadcast channel into a set of parallel single input single output (SISO) channels, one for each transmit stream. Scheduling decision consequently can be made by the transmitter to the user with the best post-processing SNR for each stream. This substantially reduces the number of channel parameters required at the transmitter. A bonus is that this strategy has the same capacity scaling as the optimal DPC capacity yet with finite rate feedback for each user [51].

Threshold-based quantization to reduce the amount of feedback generated by each user is one approach to lower the feedback requirements for multiuser diversity [43, 53, 54]. The threshold is used to quantize users' channels [53][54] or classify the users into different groups for scheduling [43]. Users

report to the base station whether the channel quality is better than a threshold value. In real systems, however, this approach does not necessarily lead to substantial reduction of the amount of feedback. The reason is that the overhead associated with packaging the quantized channel quality information may be significant. This overhead may include physical layer (PHY) and medium access control (MAC) headers such as training sequence, pilots and MAC addresses, etc. Independent dedicated feedback channels for each user are required to carry the feedback of the channel information and the associated overhead. The number of dedicated feedback channels increases linearly with the number of users [43].

An alternative approach to reduce the feedback is to find the user with the best channel quality from all users using a tree search algorithm. An opportunistic splitting protocol based on this idea was proposed to find the user with the best channel quality among uplink users in a SISO system [55]. It can be applied to the downlink in a similar way. This scheme, though, requires handshakes between the base station and mobile users to split the user set into smaller subsets. The iterative handshaking procedure increases the scheduling latency, and may be vulnerable to link failure. The extension to MIMO scheduling where multiple users are selected is not straightforward.

Contention based feedback, where all users contend for opportunities to send feedback on a shared common medium, is another alternative to reduce feedback load. Contention based feedback was mentioned in [43], however, no contention-based feedback protocols were proposed. A novel contention based

feedback protocol for SISO systems was proposed in [56] by the authors. In this protocol, users contend for feedback of their channel quality information. A channel quality threshold and a random access probability are used to jointly control the contention. These parameters are jointly optimized to achieve good throughput. This provides better performance than just controlling the channel quality threshold. Contention based feedback for SISO downlink has also been studied in [57]. This protocol statically splits users into groups and associates each group with a contention minislot for feedback.

2.1.2 Main Contributions

This chapter proposes a novel framework of multiuser scheduling and feedback in multiple input multiple output (MIMO) downlink that achieves multiuser diversity with reduced feedback requirements. The base station sends multiple independent data streams from the transmit antennas [29, 52, 58, 59]. On the mobile user side, multiple receive antennas are deployed and linear zero-forcing receivers are used to separate the transmitted data streams and decode the desired one. Under this framework, each transmit antenna at the base station can be considered as an independent spatial channel [29]. The base station independently selects a user for each spatial channel. We propose a contention-based feedback protocol that assigns an independent contention channel for each spatial channel to carry the feedback based on our work in [56]. A channel quality threshold and a random access probability are used on each spatial channel to control the feedback. When a user's channel quality

on one spatial channel is better than a threshold, the user sends a feedback message to the base station with the random access probability.

The channel quality metric that is used in this chapter is the tail probability of cumulative distribution functions (CDF) [60]. Using this channel quality metric enables the scheduler to deal with the heterogeneity of users and achieves temporal fairness. As a further enhancement, MIMO capture is proposed to support simultaneous feedback from multiple users on the same channel. This improves the efficiency of the uplink feedback channel by exploiting the spatial degrees of freedom. This assumes mobile users have perfect knowledge of their channel distribution information. The base station, however, may know or may not know the channel distribution of the users. Iterative algorithms are proposed, aiming to find good selections of the feedback parameters via offline or online optimization for both scenarios. The proposed protocol can achieve high multiuser diversity gain for the MIMO downlink despite a significant reduction of feedback. These performance advantages are illustrated in simulations.

The proposed scheme supports simultaneous transmission of multiple data streams to different users and combines multiuser scheduling with a feedback protocol that leads to significant feedback reduction. Previous work on scheduling in MIMO downlink in [31, 58, 61–65] mostly concerns scheduling one MIMO user at each scheduling instant and does not study the issue of feedback reduction. Multiuser MIMO scheduling is investigated in [19, 34, 66, 67]. In these works, multiple users are selected based on certain utility maximiza-

tion rules or low complexity user selection algorithms with the assumption that channel quality information of all users is available at the base station. The issue of feedback reduction for large number of users has not been studied in these papers.

2.2 System Model

In this section, a general per-antenna based scheduling framework is first discussed. Then we focus on the narrowband MIMO channel model and present the discrete-time signal models for the downlink data transmission channel and the uplink multiple access feedback channel.

2.2.1 Overview of the Multiple Antenna Downlink with Linear Receivers

In the cellular system under consideration, multiple antennas are available at both the base station and the mobile users. The number of transmit antennas at the base station is denoted by M_t and the number of antennas at each receiver is denoted by M_r. For the downlink transmission, the base station uses spatial multiplexing. It sends independent data streams to potentially different users from each transmit antenna. Each transmit antenna can be considered as an independent spatial channel. The receivers at the mobile user side use linear receivers. This corresponds to linear filtering operations at the receiver that aims to suppress interferences and separate the transmitted data streams. This entire transceiver architecture decouples the multiple

antenna downlink into parallel spatial channels. In terms of scheduling, the base station maps each spatial channel to a mobile user according to the given scheduling algorithms. As we motivated earlier, feedback reduction is an important issue for this system. Our key contribution in this chapter is a novel proposal for the MIMO downlink scheduling with reduced feedback.

This system model presented in the later description follows the assumption of a narrowband MIMO system without the presence of cochannel interference for the purpose of simplicity and clarity. The main results, however, can be generalized to a variety of scenarios, such as broadband systems, with or without cochannel interference and the downlink system with the presence of fixed relays. We will also comment on the possible extensions of our framework in the later description.

2.2.2 Downlink Transmission Model

In this chapter, we consider a narrowband MIMO system and denote the MIMO channel between the base station and the j^{th} user by matrix $\mathbf{H}_j$. For broadband systems with OFDM (orthogonal frequency division multiplexing) modulation, the channel in the frequency domain can be divided into adjacent subchannels, multiuser diversity can be exploited on individual subchannels [68]. These subchannels are analogous to narrowband channels. The framework that will be proposed in this chapter, however, can be readily generalized to OFDM systems.

We assume that the base station allocates equal power to each transmit

antenna. Ideally, when the channel powers on all spatial channels are available to the base station, sophisticated power allocation such as water-filling improves the throughput performance. This, however, adds complexity to the algorithm and only leverages slight performance gain since multiuser diversity is exploited on all spatial channels. In this chapter, we simply assume equal power allocation for all transmit antennas to simplify the analysis. We also make the assumption that the data queues of different users are infinitely backlogged [69] and our analysis does not involve any queueing dynamics. This assumption approximates systems that serve large data packets, e.g., data file transfer or audio/video streaming. This also characterizes the throughput region of any queue-dependent scheduling policies.

The channel is assumed to be block-wise time invariant for each frame and to vary independently from frame to frame (block stationary). Here each frame has approximately the duration of channel coherence time [41]. Research on the length of block stationarity for MIMO channels has been reported in [70]. Further, we assumption that the cumulative distribution functions of users does not change for R frames, but may change every R frame. This assumptions simplifies our analysis. When users are located in approximately stationary environments, the quantity R can be a large number. To simplify the notation, we focus on the first R frames and index the frames within every R frames by $l = 1, ..., R$.

The MIMO signal model for the j^{th} user has the following form

$$\mathbf{x}_j = \mathbf{H}_j\mathbf{s} + \mathbf{n}_j \tag{2.1}$$

where $\mathbf{x}_j$ denotes the received signal at the j^{th} user and $\mathbf{s}$ is the transmitted signal from the base station. The noise term is denoted by $\mathbf{n}_j$, which is assumed to follow an i.i.d complex Gaussian distribution with zero mean and variance σ_n^2.

To decode the transmitted data streams, the mobile users employ a linear receiver that uses a linear matrix multiplication of the received signal to separate the transmitted data streams. We denote the operation matrix by $\mathbf{W}_j$ of a size $M_t \times M_r$. Only the desired data streams are decoded after the matrix multiplication. Notice that in frequency selective channels, this separation corresponds to equalization of the frequency selective MIMO channel in both time and space. For simplicity, we do not address this space-time equalization architecture in this chapter, but study it in the next chapter. There may be one or multiple streams that are intended for each mobile user depending on the scheduling decision.

In the scenario where $M_r \geq M_t$, the receiver has enough degrees of free to null interference. Zero-forcing receiver may be used [29]. In this case, we have $\mathbf{W}_j = (\mathbf{H}_j^H \mathbf{H}_j)^{-1} \mathbf{H}_j^H$. We primarily focus on this option in this chapter. It simplifies the analysis. The signal after the zero-forcing operation can be expressed as

$$\begin{aligned} \mathbf{y}_j &= (\mathbf{H}_j^H \mathbf{H}_j)^{-1} \mathbf{H}_j^H \mathbf{x}_j \\ &= \mathbf{s} + \mathbf{z}_j \end{aligned} \tag{2.2}$$

where $\mathbf{z}_j = (\mathbf{H}_j^H \mathbf{H}_j)^{-1} \mathbf{H}_j^H \mathbf{n}_j$ is the noise component after the zero-forcing

operation. The noise term $\mathbf{z}_j$ follows a complex Gaussian distribution with zero mean and covariance matrix $\sigma_n^2(\mathbf{H}_j^H\mathbf{H}_j)^{-1}$. Zero-forcing receivers separate the transmitted streams from the received signals, thus detection is performed independently for each stream.

A more general approach for designing the receiver filter is to maximize the signal to noise and interference ratio (SINR) for each desired transmit stream [19]. This formulation does not impose restrictions on the number of receive antennas. It can be also applied to the scenario with the presence of cochannel interference. For simplicity, we do not address it in this chapter.

2.2.3 The Uplink MIMO Feedback Channel

To make the scheduling decision in the downlink, the base station needs to obtain the channel quality information for each mobile user. This can be achieved by sending back the channel matrix $\mathbf{H}_j$ via a uplink feedback channel. With MIMO transmission, the amount of channel information grows with the MIMO channel dimension. On the other hand, the uplink MIMO multiple access channel can be used to carry feedback of users' channel quality information [71]. MIMO based feedback allows multiple users to send the feedback simultaneously. This takes advantage of the MIMO multiple access channel spectral efficiency.

In this chapter, we propose to use a contention channel in the uplink to carry feedback from users. Users share a common feedback channel in the uplink and contend to send back their channel quality. We assume that

each user uses only one transmit antenna to send a feedback message that contains its channel quality. Here capture of multiple feedback messages can be leveraged at the base station assuming that the multiple antennas deployed at the base station can also be used for reception.

Justification for the capture effect is the following. We make the assumption that users are perfectly synchronized to the base station in time and carrier frequency for the uplink transmission. This is a common assumption in TDMA (time division multiplexing access) cellular systems. One approach that supports MIMO capture is to assign distinct CDMA (code division multiplexing access) nonorthogonal spreading codes to different users [72]. When multiple feedback messages are received at the base station, the base station searches over the space of the codes to identify the ones that are used for the feedback messages. Using distinct training sequences for different users is another useful approach to enable MIMO capture [73][74]. This requires coordination at the MAC layer to distribute training sequences to users. A third approach that enables MIMO capture is using blind methods. Algorithms such as constant modulus algorithm (CMA), known modulus algorithm (KMA) and blind equalization have been proposed in literature [75, 76].

We also assume that the reception of the feedback messages is robust to the uplink propagation impairment. This usually involves error coding to protect the feedback messages from corruption. The maximum number of feedback messages that can be simultaneously decoded is assumed to be M_t. *A user succeeds in a feedback attempt if there are no greater than* M_t

simultaneous feedbacks from different users. This abstracts the physical layer of the uplink feedback channel. Investigation of the reception errors caused by the uplink propagation impairments is a topic of future work.

2.3 Proposed Feedback Strategy

In this section, we describe the proposed feedback protocol. We formulate and solve an optimization problem to select the feedback control parameters.

2.3.1 Basic Feedback Protocol

We illustrate the proposed framing structure in Fig. 2.1. Users share the uplink feedback channel and contend to send back their channel quality through random access minislots. To control the feedback load, i.e., the amount of feedback information, two parameters are used: a channel quality threshold and a contention probability. They are selected to achieve certain performance guarantee and they are broadcast to all users at the beginning of the frame. The broadcast message is followed by M_t contention channels that are used for user selection for the M_t transmit antennas. Each contention channel consists of K minislots in time.

We denote the channel quality threshold by η_m and contention probability by p_m for $m = 1, 2, ..., M_t$. The system performs the same operation in each contention channel. We elaborate the operation of the system in the m^{th} contention channel here. Within each minislot of any contention chan-

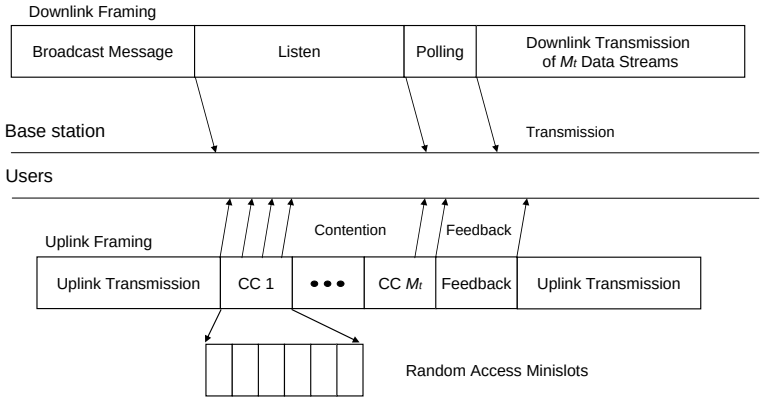

Figure 2.1: Example of a framing structure for use with MIMO opportunistic feedback.

nel, when a user finds that its channel quality is better than the threshold η_m, it randomly sends a feedback message containing its ID information with probability p_m, otherwise, it does not contend for that spatial channel. The feedback message includes the user ID information and the associated physical layer and medium access layer overheads. The base station monitors the feedback packages in the minislots. If the base station decodes at least one feedback messages, the base station randomly selects one user corresponding to the decoded messages for data transmission. If the base station decodes no users' feedback messages, it randomly selects one user from the set of all users for that spatial channel. Once the desired user is selected, the base station polls this user to request its transmission rate of the spatial channel in the

polling slot. This is required since only user ID information is fed back in the contention stage. The base station also informs the antenna assignment to the desired users in the polling stage.

2.3.2 Channel Quality of Users and Statistical Assumptions

One of the key issues in our system design is to properly choose the random access probability p_m and the channel quality threshold η_m after the linear operation at the receivers. Our approach is to formulate an optimization problem to maximize the sum throughput with respect to these parameters subject to the temporal fairness constraint. Here temporal fairness implies all users are served with equal probability. Notice that throughput is a specific form of utility function. A more general formulation can be performed by maximizing the sum utility under certain fairness constraints [69]. In this chapter, we focus on using user's throughput as the utility function and only dealing with temporal fairness. This formulation yields clean solutions for the parameter selection problem.

Let us denote the energy per symbol period for each antenna at the base station by $\frac{E_s}{M_t}$, where E_s is the total transmit energy per symbol period at the transmitter. Thus the signal energy $E\|\mathbf{s}\|^2 \leq E_s$. The post-processing SNR for the j^{th} user at the m^{th} spatial channel, which we denote by $\xi_{m,j}$, has the following form [29]

$$\xi_{m,j} = \frac{E_s}{M_t \sigma_n^2 [(\mathbf{H}_j^H \mathbf{H}_j)^{-1}]_{m,m}}. \tag{2.3}$$

The cumulative distribution function can be derived as

$$F_{\xi_{m,j}}(x) = \int_0^x f_{\xi_{m,j}}(s)ds \tag{2.4}$$

where $f_{\xi_{m,j}}$ is the probability density function of $\xi_{m,j}$.

We stack the SNR's of the m^{th} spatial channel of all users as $\boldsymbol{\xi}_m = [\xi_{m,1}, ..., \xi_{m,N}]^T$. We denote the marginal probability density of the j^{th} user by $f_{\xi_j}(\mathbf{x})$. Assuming that users' channels are mutually independent, the joint density function can be written as

$$f_{\boldsymbol{\xi}_m}(\mathbf{x}) = \prod_{j=1}^{N} f_{\xi_{m,j}}(x_j). \tag{2.5}$$

We use the tail probability of the CDF of the signal to noise ratio (SNR) after zero-forcing on the spatial channels for each user as the channel quality metric. It is denoted by $\alpha_{m,j}$ for the j^{th} user at the m^{th} spatial channel, where $0 \leq \alpha_{m,j} \leq 1$. Thus the relation between the random variables $\xi_{m,j}$ and $\alpha_{m,j}$ is

$$\alpha_{m,j} = 1 - F_{\xi_{m,j}}(\xi_{m,j}). \tag{2.6}$$

Notice that the random variable $\alpha_{m,j}$ is uniformly distributed in $[0, 1]$. This channel quality metric has also been used in [60][57], where it has shown to guarantee temporal fairness for heterogeneous users. It implies that users are equally likely to be served. In our proposed scheme, temporal fairness can also be achieved by using this channel quality metric. The reason is that users' channel quality $\alpha_{m,j}$'s on the m^{th} spatial channel are independently and identically distributed. In any frame, users' channel qualities are equally

likely to be above the channel quality threshold. Further when their channel qualities are above a threshold, they are equally likely to succeed in feedback contention. Finally, the selection at the base station is uniform among successful candidates.

2.3.3 Analysis of the Average Sum Rate

In this subsection, we derive the average sum rate expression for the proposed system. Here we focus on the first spatial channel without loss of generality. The reason is that using zero-forcing receivers for spatial multiplexing decouples the MIMO channels into parallel spatial channels and the analysis holds for all spatial channels in the same manner. The main result is summarized in the following proposition.

Proposition 1. The average sum rate of the system on the first spatial channel can be expressed as follows

$$\begin{aligned} C(p_1, \eta_1) &= \sum_{j=1}^{N} C_j(p_1, \eta_1) \\ &= \sum_{j=1}^{N} (\bar{C}_j(p_1, \eta_1) + \underline{C}_j(p_1, \eta_1)) \end{aligned} \tag{2.7}$$

where $C_j(p_1, \eta_1)$ is the average sum rate of the j^{th} users. The quantity $\bar{C}_j(p_1, \eta_1)$ denotes the average sum rate that the system can achieve when the base station selects user j and its channel quality is better than the threshold η_1

$$\bar{C}_j(p_1, \eta_1) = \bar{R}_j \sum_{m=1}^{N} \left(\begin{array}{c} N-1 \\ m-1 \end{array} \right) \eta_1^{m-1} (1-\eta_1)^{N-m} \left\{ \frac{1}{m} + (\frac{1}{N} - \frac{1}{m})[1 - P_c(m)]^K \right\}. \tag{2.8}$$

We denote the integration of the rate of the j^{th} user in the region where its channel quality is below the threshold η_1 by $\bar{R}_j$. Thus $\bar{R}_j = \int_0^{\eta_1} \log_2(1 + F_{\xi_{1,j}}^{-1}(1-\alpha))d\alpha$. The term $\underline{C}_j(p_1, \eta_1)$ denotes the average sum rate that the system achieves when the base station selects user j and its channel quality is worse than the threshold η_1,

$$\underline{C}_j(p_1, \eta_1) = \underline{R}_j \sum_{m=0}^{N-1} \left(\begin{array}{c} N-1 \\ m \end{array} \right) \eta_1^m (1-\eta_1)^{N-m-1} \frac{1}{N} [1 - P_c(m)]^K. \tag{2.9}$$

We denote the integration of the rate of the j^{th} user in the region where its channel quality is above the threshold η_1 by $\underline{R}_j$, where $\underline{R}_j = \int_{\eta_1}^{1} \log_2(1 + F_{\xi_{1,j}}^{-1}(1-\alpha))d\alpha$. The term $P_c(m)$ denotes the probability that there is at least one user out of the total m users, whose channel quality is better than the threshold, successfully sends back its feedback message in one of the minislots.

$$P_c(m) = \sum_{u=1}^{\min\{M_t, m\}} \left(\begin{array}{c} m \\ u \end{array} \right) p_1^u (1-p_1)^{m-u} \tag{2.10}$$

where $m = \sum_{u=1}^{N} I\{\alpha_{1,u} < \eta_1\}$ and $I\{\cdot\}$ denotes the indicator function.

Proof. See Appendix A.1. □

Notice that to derive the closed-form expression of the average sum rate for any pair of p_1 and η_1, information of the channel distribution, the number of transmit antennas M_t, the number of active users N and the number of feedback minislots K are needed. Depending on how the system is engineered, the CDF's of users may not be known at the base station. In the rest of this section, we will design the system to perform an optimization of the average

sum rate with respect to p_1 and η_1 in the settings where the CDF information of all users is known or not known to the base station.

2.3.4 Optimization Based on Global CDF Information at the Base Station

In the downlink, the CDF's of the channels of mobile users can be estimated at the user side. When the downlink and uplink channels are statistically reciprocal, the base station may estimate the CDF's of users' channels via the uplink reception. In this subsection, we assume that the global CDF information for different users is available at the base station. We study an algorithm of selecting the feedback parameters p_1 and η_1 with such information.

The average sum rate of the system is a function of both p_1 and η_1 given the CDF's of users and the quantities N, M_t and K. We propose to solve the optimization problem to find a good choice of p_1 and η_1

$$\begin{aligned} &\min_{p_1,\eta_1} -C(p_1,\eta_1) \\ \text{s.t.} \quad &0 \le p_1 \le 1,\ 0 \le \eta_1 \le 1. \end{aligned} \tag{2.11}$$

Clearly, joint optimization of the parameters p_1 and η_1 offers higher average sum capacity than optimizing only with respect to one variable p_1 or η_1 (for example, optimizing η_1 with $p_1 = 1$).

In (2.11), the feasible set on (p_1, η_1) (denoted by $\mathfrak{F}$) is convex. The cost function, however, is not convex. We do not have a closed form solution

to this problem. The steepest descent algorithm with back-track line search is used to iteratively approach a locally optimal solution [77]. Notice that the cost function is continuous and bounded (since the receive SNR is bounded in real systems) on a convex set. The derivatives of the cost function with respect to variables p_1 and η_1 are expressed in the following

$$\frac{\partial C}{\partial p_1} = \sum_{j=1}^{N} \frac{\partial C_j}{\partial p_1} = \sum_{j=1}^{N} \left(\frac{\partial \bar{C}_j}{\partial p_1} + \frac{\partial \underline{C}_j}{\partial p_1} \right) \tag{2.12}$$

$$\frac{\partial C}{\partial \eta_1} = \sum_{j=1}^{N} \frac{\partial C_j}{\partial \eta_1} = \sum_{j=1}^{N} \left(\frac{\partial \bar{C}_j}{\partial \eta_1} + \frac{\partial \underline{C}_j}{\partial \eta_1} \right) \tag{2.13}$$

where $\frac{\partial \bar{C}_j}{\partial p_1}$, $\frac{\partial \underline{C}_j}{\partial p_1}$, $\frac{\partial \bar{C}_j}{\partial \eta_1}$, $\frac{\partial \underline{C}_j}{\partial \eta_1}$ are calculated in Appendix A.2.

For each iteration, the algorithm computes

$$\begin{aligned} p_1^{(k+1)} &= p_1^{(k)} + \delta_k \frac{\partial C}{\partial p_1} \Big|_{(p_1^{(k)}, \eta_1^{(k)})}, \quad \text{and} \\ \eta_1^{(k+1)} &= \eta_1^{(k)} + \delta_k \frac{\partial C}{\partial \eta_1} \Big|_{(p_1^{(k)}, \eta_1^{(k)})}. \end{aligned} \tag{2.14}$$

We use the standard back-tracking line search to select the step size δ_k [77]. We have two parameters ν and β, with $0 < \nu < 0.5$ and $0 < \beta < 1$. The algorithm is described as follows for each iteration.

Compute $\frac{\partial C}{\partial p_1} \Big|_{(p_1^{(k)}, \eta_1^{(k)})}$ *and* $\frac{\partial C}{\partial \eta_1} \Big|_{(p_1^{(k)}, \eta_1^{(k)})}$

Let $\delta_k = 1$

Compute $(p_1^{(k+1)}, \eta_1^{(k+1)})$ *based on (2.14)*

While $(p_1^{(k+1)}, \eta_1^{(k+1)}) \notin \mathcal{F}$ or

$$-C(p_1^{(k+1)}, \eta_1^{(k+1)}) > -C(p_1^{(k)}, \eta_1^{(k)}) - \nu\delta_k \left(\left| \frac{\partial C}{\partial \eta_1} \mid_{(p_1^{(k)}, \eta_1^{(k)})} \right|^2 + \left| \frac{\partial C}{\partial p_1} \mid_{(p_1^{(k)}, \eta_1^{(k)})} \right|^2 \right)$$

$\delta_k := \beta\delta_k$

Perform *(2.14)*

end

This algorithm guarantees that a locally optimal solution to the problem (2.11) can be found. The reason is that we guarantee that there is a decrease of cost in each iteration according to the line search [78][77]. When the base station has all the information about the channel quality distribution $f_{\xi_j}(x)$, the derivatives can be evaluated in closed-form, and a good selection of p_1 and η_1 can be determined for the first spatial channel. Then this pair of parameters can be broadcast to the mobile users.

2.3.5 Online Optimization and Online Feedback Without Global CDF Information

In the previous subsection, we studied the algorithm of selecting feedback control parameters p_1 and η_1 when the global CDF information of users is available at the base station. When the reciprocity does not hold (for example, different types of bandwidths or multiple access techniques are used for the uplink or downlink), the base station may not be able to estimate the CDF's of users' channels. In this case, the CDF's of users are not available to the base station. We propose an online feedback and optimization procedure to determine the feedback control parameters: η_m and p_m.

For simplicity, we assume that the CDF's are perfectly known at the user side, but unknown to the base station. Note that we do not analyze the effects of measurement accuracy. Monte Carlo sampling can be used to obtain good estimates of various statistics of users, such as the CDF's of users' channels, $\bar{R}_j$'s and $\underline{R}_j$'s [79]. For example, the CDF's may be estimated using histograms based on the collected samples. As the number of samples of channel power collected at the base station increases, the estimates turn to be more and more close to the quantities evaluated with the closed-form CDF.

From (2.12) and (2.13), we observe that to compute the derivatives, the base station must obtain the derivatives of all users. The parameters N, K, M_t, p_1 and η_1 can be broadcast to the mobile users at the beginning of the frame. Thus mobile users may compute the derivatives $\frac{\partial C_j}{\partial p_1}$ and $\frac{\partial C_j}{\partial \eta_1}$ individually with their CDF's.

The procedure of contention and user selection follows the description in Section 2.3.1 for each frame. The protocol is modified slightly here: *after the user has been selected, it is required to send back not only its instantaneous transmission rate, but also the derivatives* $\frac{\partial C_j}{\partial p_1}$ *and* $\frac{\partial C_j}{\partial \eta_1}$. These quantities can be represented in high precision using long bit sequences. We neglect the quantization issue here.

Based on our previous assumption on the variation of the CDF's of users in Section 2.2.2, we describe the algorithm for a block length of R frames. Within the R frames, the base station collects the feedback information from the users in every P frames. Notice that R can be much larger than P and

for simplicity we assume that $R = PU$, where U is an integer number. By our assumption, the channels of the users do not change within these P frames. We denote the derivatives fed back in the $((l-1)P+t)^{th}$ frame by $g^p[t,l]$ and $g^\eta[t,l]$ (with respect to p_1 and η_1 respectively), where $l = 1, 2, ...$ and $t = 1, 2, ..., P$. Then the base station may estimate the derivatives in (2.12) and (2.13) using the following formula

$$\tilde{g}^p[l] = \frac{N}{P}\sum_{t=1}^{P} g^p[t,l] \tag{2.15}$$

$$\tilde{g}^\eta[l] = \frac{N}{P}\sum_{t=1}^{P} g^\eta[t,l] \tag{2.16}$$

where $\tilde{g}^p[l]$ is the estimate to the derivative $\frac{\partial C}{\partial p_1}$ in (2.12) and $\tilde{g}^\eta[l]$ is the estimate to the derivative $\frac{\partial C}{\partial \eta_1}$ in (2.13). We state the following proposition about the derivative estimates (2.15) and (2.16).

Proposition 2. The quantities $\tilde{g}^p[l]$ and $\tilde{g}^\eta[l]$ are unbiased estimates of (2.12) and (2.13) respectively.

Proof. We denote the probability that the j^{th} user is selected at the $((l-1)P+t)^{th}$ frame as $Pr_j[t,l]$. Since all users are equally likely to be selected based on the basic protocol in Section 2.3.1, $Pr_j[t,l] = \frac{1}{N}$. Taking the expectation of $\tilde{g}^p[l]$, we have the following

$$\begin{aligned} E(\tilde{g}^p[l]) &= \frac{N}{P}\sum_{t=1}^{P} E(g^p[t,l]) \\ &= \frac{N}{P}\sum_{t=1}^{P}\sum_{j=1}^{N} \frac{\partial C_j}{\partial p_1} Pr_j[t,l]. \end{aligned} \tag{2.17}$$

Using the fact $Pr_j[t,l] = \frac{1}{N}$, we obtain that $E(\tilde{g}^p[l]) = \frac{\partial C}{\partial p_1}$. Similarly we can show that $E(\tilde{g}^\eta[l]) = \frac{\partial C}{\partial \eta_1}$. □

A stochastic gradient search algorithm is adopted to find optimal p_1 and η_1 for the problem (2.11). We use the search rule with variable step size δ_l for the l^{th} iteration. The quantities γ $(0 < \gamma < 1)$ and β $(0 < \beta < 1)$ are parameters of the algorithm. The initial step size δ_1 is set to be $\delta_1 = \gamma$. The parameter T_o specifies the tolerance of the algorithm. For each iteration the parameters can be updated via the following

$$\begin{aligned} p_1^{(l+1)} &= \Pi_{\mathcal{F}} \left(p_1^{(l)} + \delta_l \tilde{g}^p[l]|_{(p_1^{(l)}, \eta_1^{(l)})} \right) \\ \eta_1^{(l+1)} &= \Pi_{\mathcal{F}} \left(\eta_1^{(l)} + \delta_l \tilde{g}^\eta[l]|_{(p_1^{(l)}, \eta_1^{(l)})} \right) \end{aligned} \tag{2.18}$$

where $\Pi_{\mathcal{F}}$ projects the point outside the feasible set $\mathcal{F}$ to the nearest point in $\mathcal{F}$. The algorithm is described as follows

While $\left| \tilde{g}^p[l]|_{(p_1^{(l)}, \eta_1^{(l)})} \right|^2 + \left| \tilde{g}^\eta[l]|_{(p_1^{(l)}, \eta_1^{(l)})} \right|^2 > T_o$ ***and*** $l \leq U$

Let $\delta_l = \gamma / l$

Perform (2.18)

Let $l := l + 1$

end

The parameter U specifies the maximum number of iterations that can be performed within the R frames. We should also emphasize that the stepsize δ_l is re-initialized for every R frames. Since (2.12) and (2.16) are

unbiased estimators for the derivatives, the algorithm is the Robbins-Monro procedure to find the roots of the derivatives [80][81]. For the case that $R = \infty$ (the CDF's of users do not change over time), convergence of the algorithm is guaranteed under the conditions that the set $\mathfrak{F}$ is a closed and convex set and the stepsize is chosen such that $\sum_{l=1}^{\infty} \delta_l = \infty$ and $\sum_{l=1}^{\infty} \delta_l^2 < \infty$.

The algorithm is intended to be performed online and enables to optimize the cost function with decentralized information. Only one user is requested to send back its rate and the derivatives after it is selected. This only introduces a slight increase of the amount of feedback for each frame. Significant reduction of feedback load is still achieved compared with using dedicated feedback channels for different users. We also observe that with derivative feedback, the base station may consistently update the parameters p_1 and η_1.

2.4 Simulations

In this section, we illustrate the average sum rate for the proposed random access protocol for different scenarios using Monte Carlo simulations. These simulations are conducted using MATLAB. We first assume that the CDF's of users' channels do not change over time and known to the base station. The online simulation is then studied in the last part of this section. The elements of the channel matrix $\mathbf{H}_j$ for the j^{th} user are assumed to be independently and identically Gaussian distributed with zero mean and variances σ_j^2, where σ_j^2's are chosen uniformly within the interval $[0, 1]$ to model the

heterogeneity of users. We fix the transmit power to make the receive signal to noise ratio (SNR) at the receive antennas of the j^{th} user be $6 + 10\log_{10}(\sigma_j^2)$ dB. The marginal density function of the SNR [29] can be expressed as

$$f_{\xi_{m,j}}(x) = \frac{\lambda_j^{M_r - M_t + 1} x^{M_r - M_t} e^{-\lambda_j x}}{\Gamma(M_r - M_t + 1)} \tag{2.19}$$

where $\lambda_j = \frac{M_t \sigma_n^2}{E_s \sigma_j^2}$.

We first assume that the channel distributions are fully known at the base station and apply the steepest descent algorithm with the back-tracking line search in Section 2.3.4 to find an optimizer of (2.11). We initialize the (p_1, η_1) at $(1/(0.05N), 0.05)$ and set the parameters $\nu = 0.001$ and $\beta = 0.5$ for the steepest descent algorithm with the back-tracking line search.

Fig. 2.2 illustrates the results of average sum rate vs. the number of active users when both the number of minislots K and the number of transmit antennas M_t are fixed. For this simulation, we conduct Monte Carlo simulations for 10 times and collect the data samples from the simulations to compute the means and the standard deviations. We use 2000 channel realizations for each point and illustrate the sample means of the performance curves with error bars (the range of one standard deviation) in Fig. 2.2.

The performance of the proposed protocol is compared with the polling-based protocol. In this scheme, the base station randomly polls KM_t users out of the total N users, then selects the one with the smallest $\alpha_{m,j}$ for the m^{th} channel from these users to send data to. Here we use MIMO to effectively create more polling slots. We show the performance of the ideal scheme

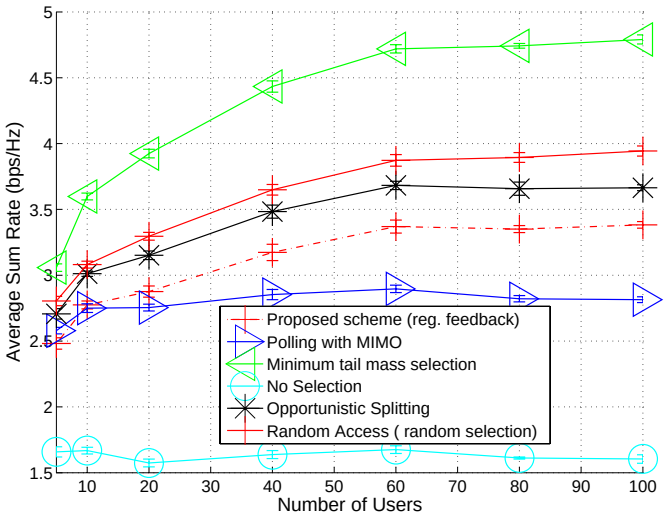

Figure 2.2: Performance of the proposed feedback protocol versus different number of active users for $K = 2$, $M_t = 2$ and $M_r = 2$. Users' channels are heterogenous in this experiment.

that always selects the user with the best tail probability (minimum tail mass selection) as a performance benchmark. The proposed protocol performs significantly better than polling. Using MIMO capture utilizes the spatial resources to reduce collision probability and effectively creates more feedback minislots to carry the feedback. We observe that a good throughput gain has been achieved by using MIMO capture (MIMO feedback) than the scenario that there is no MIMO capture (reg. feedback). Regular feedback refers to the scheme that feedback is successful when there is only one user sends a feedback message [56].

Compared to the opportunistic splitting algorithm [55] (here the channel quality is measured by tail probability of the CDF of the post-processing SNR after zero-forcing instead of the channel power in the original version algorithm by [55]), the proposed scheme with MIMO feedback outperforms the opportunistic splitting for this experiment. The number of handshakes in the opportunistic splitting algorithm and the number of random access minislots in our proposed scheme are both two.

Since the standard deviations collected from the data samples in the previous result are small, we only conduct the simulations for one time using 2000 channel realizations for each simulation. As we know that DPC-based scheme is sum-rate optimal, it, however, does not achieve temporal fairness for heterogeneous users. For the case that users' channels follow i.i.d. Rayleigh fading, we compare the DPC-based scheme [28] with the proposed scheme in Fig. 2.3. The performance gap is due to the suboptimal MIMO downlink

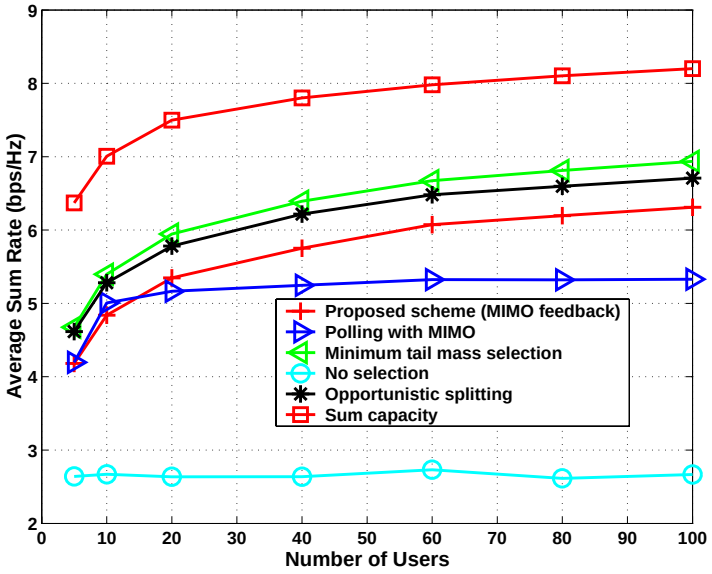

Figure 2.3: Comparison of the DPC-based scheme with the proposed scheme for $K = 5$, $M_t = 2$ and $M_r = 2$. The elements of users' channel matrices follow i.i.d. Rayleigh fading with zero mean and unit variance in this experiment.

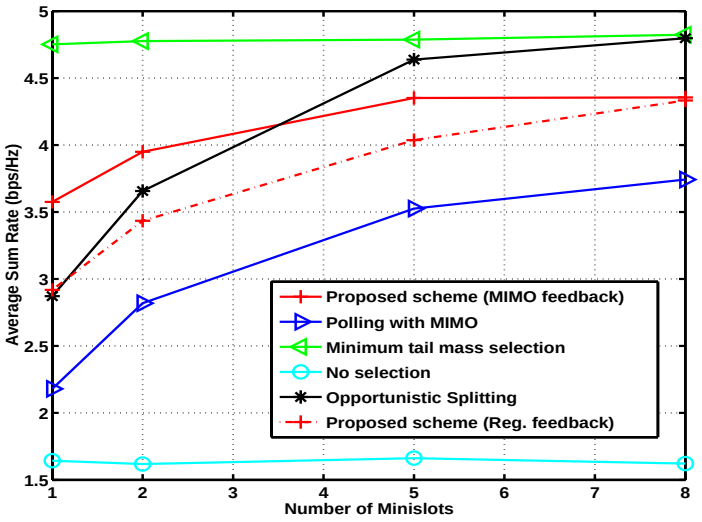

Figure 2.4: Performance of the proposed feedback protocol versus the number of minislots for $N = 100$, $M_t = 2$ and $M_r = 2$.

architecture that uses per-antenna scheduling with linear receivers. Multiuser diversity is still achieved with the proposed framework.

We use the heterogeneous channels in (2.19) in the subsequent simulation experiments. We show the system performance of the throughput versus the number of minislots in Fig. 2.4. The system throughput increases with the number of minislots. Using MIMO capture significantly benefits the system throughput in the region of small number of minislots. Compared to an opportunistic splitting algorithm, the proposed protocol with MIMO capture performs better when the number of minislots is small. When the number of minislots is large, the proposed protocol performs worse than the opportunistic splitting.

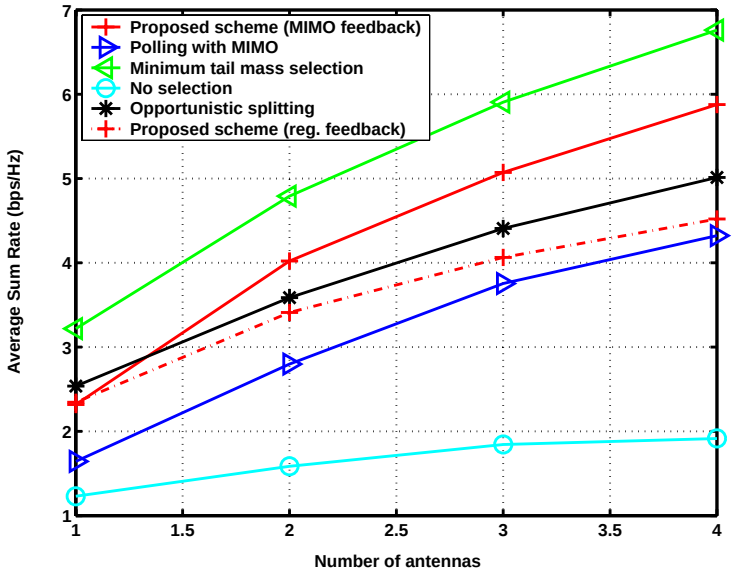

Figure 2.5: Performance of the proposed feedback protocol versus the number of antennas for $N = 100$ and $K = 2$.

Fig. 2.5 illustrates the system throughput versus the number of antennas used in the system. Here we assume that equal number of transmit/receive antennas are deployed at the base station and the mobile users. The system throughput increases with the number of antennas for all schemes. Using MIMO feedback significantly outperforms the strategy of regular contention based feedback. It also performs better than the opportunistic splitting when there is more than one transmit antennas in this setting.

When CDF's of the users are not available to the base station, the online algorithm in Section 2.3.5 can be used. Here we set the search parameter $\eta = 0.01$ and use the initial selection of feedback parameters (p_1, η_1) to be $(1/(0.05N), 0.05)$. We plot the dynamics of the search algorithm over 5000

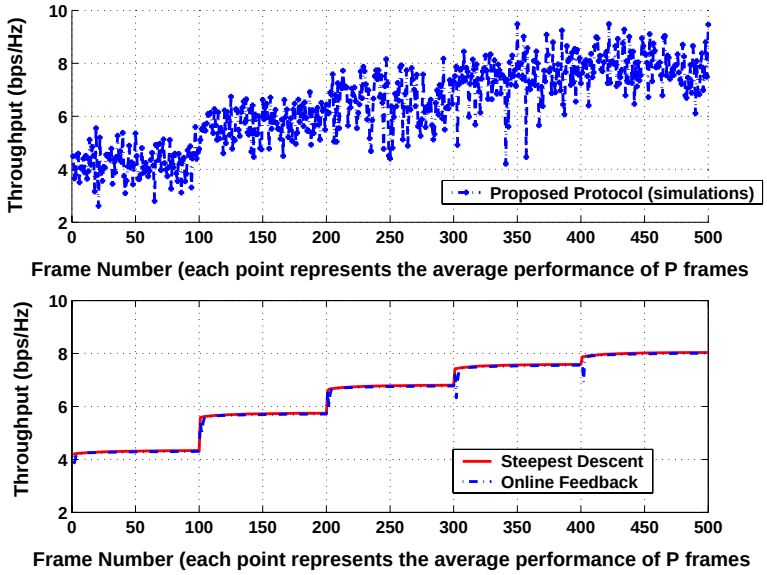

Figure 2.6: Performance of the online optimization algorithm for $N = 100$, $K = 5$, $M_t = 2$ and $M_r = 2$. We plot the evolution of the average sum rates (varying with the updated parameters p_1 and η_1) for the proposed algorithms and the actual throughput for the simulation.

frames with a window size $P = 10$ for 100 users in Fig. 2.6. Here a simple modelling of the channel evolution is adopted. The parameter R is set to be $R = 1000$. Therefore, for every 1000 frames, we regenerate the parameters σ_j^2 for all users uniformly within the interval $[0, u]$ for the u^{th} group of 1000 frames ($u = 1, 2, ..., 5$). Thus the channel distributions of users change for every 1000 frames because a different set of σ_j^2's are used. A comparison of the online algorithm and the steepest descent algorithm in Section 2.3.4 is presented. We observe that both algorithms converge. The online algorithm performs well even when there are only a small number of users that send back their derivatives.

2.5 Summary of Contributions

In this chapter, a novel framework of multiuser scheduling with reduced feedback in the MIMO downlink is proposed. The base station uses per-antenna transmission whereas the mobile users employ linear receivers. This decouples the MIMO downlink channel into parallel SISO channels that can be assigned to different users. For each spatial channel, independent contention channels are used to carry the feedback of users' channel quality. As a further enhancement, MIMO capture is adopted to improve the spatial utilization of the feedback channel. We control the uplink feedback behavior by two parameters: the feedback probability and the channel quality threshold.

In terms of algorithm development for this proposed system, we formulated an optimization problem to maximize the system throughput with re-

spect to the feedback parameters subject to the temporal fairness constraint. We proposed search algorithms to select these parameters for the scenarios that the channel distribution information of users is fully known or unknown to the base station. Simulations showed that the proposed algorithms achieve multiuser diversity in the MIMO downlink despite significant reduction in feedback. It significantly outperforms the polling based scheme and performs better than an opportunistic splitting algorithm when the number of feedback minislots is small.

Chapter 3

Suppression of Cochannel Interference in the Downlink

In this chapter, a receiver that can suppress asynchronous cochannel interference in an OFDM downlink multicell scenario is presented. The effects of asynchronism caused by carrier frequency offsets and propagation delays are considered in this framework. To combat the various interferences in this system, the proposed receiver uses two stages of equalization in both the time domain and the frequency domain.

Main contributions of this chapter are the algorithms for the equalizer design under the scenarios where the channel and the synchronization parameters are known or unknown to the receiver. The first part of this chapter concerns the equalizer design when perfect channel and synchronization parameters are known to the receiver. A novel space-time equalization algorithm based on the channel state information is proposed. This algorithm aims to null the co-channel interference and combat asynchronism as well as minimize a lower bound to the symbol error rate. In the second part of this

chapter, a training-based minimizing mean square error (MMSE) algorithm to jointly obtain the frequency offsets and the equalization delays is proposed. This algorithm does not acquire the knowledge of channel and synchronization parameters. The performance of the proposed algorithms is evaluated via simulations.

This chapter is organized in the following way. Section 3.1 presents background on the problem of downlink cochannel interference suppression and summarizes our contributions. In Section 3.2, we propose the space-time/space-frequency signal model for the multiuser MIMO-OFDM systems with synchronization parameters. In Section 3.3, we discuss the equalizer design issues for such system based on channel information and the synchronization parameters. In Section 3.4, we propose a direct-training based synchronization architecture and a direct training based equalizer design algorithm. We set up the optimization problems, and propose optimization algorithms. In Section 3.5, we present simulation results for our proposed receiver.

3.1 Introduction

Future broadband cellular wireless communications systems feature high data rate and high spectral efficiency. Aggressive frequency reuse where adjacent cells use the same time-frequency channels may improve spectral efficiency, however, poses challenges on dealing with the cochannel interference [45][82] as illustrated in Fig. 3.1. OFDM is a promising physical layer technology for high data rate communications [83][6]. It is an efficient means

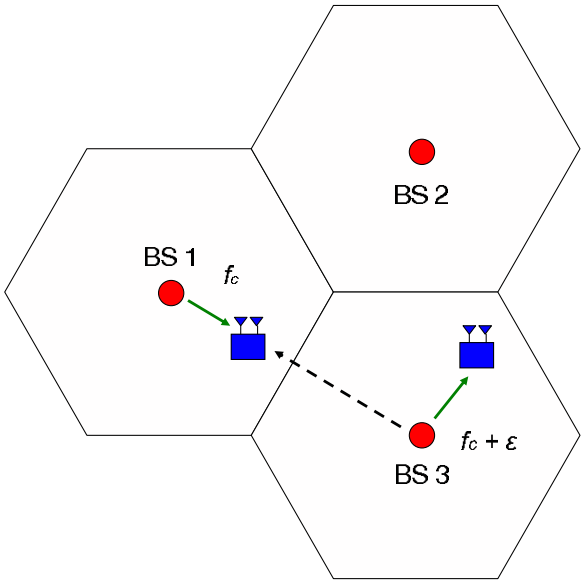

Figure 3.1: The downlink data transmission from BS 1 is interfered by the adjacent BS 3. These cells take aggressive frequency reuse. There exists a difference in the propagation delay and the carrier frequency between these links.

of combatting multipath fading in wireless systems and it achieves very high spectral efficiency [84]. In OFDM systems, the propagation delays between the transmitted signals from different BS and the small differences in carrier frequencies of different BS may also cause inter-carrier interference (ICI). These effects significantly deteriorate the performance of these systems[85]. Equalization in the time domain is an attractive option to deal with various sources of interferences. Previous work on space-time interference cancellation [45, 82] focuses on equalizer design algorithms that combat cochannel interference and the interference caused by different propagation delays of users. The effects of carrier frequency offsets, however, are not addressed in these papers.

The first contribution of this chapter is to propose an equalizer design principle based on channel information that achieves interference cancellation and deals with the effects of residual frequency offsets. A similar idea has been used for single user systems without cochannel interference [86, 87]. In this chapter, we design equalizers to suppress various sources of interferences and consider the symbol error rate performance.

To design the equalizer based on the channel and synchronization information, estimates of the channel and the synchronization parameters are needed for not only the desire stream but also the cochannel interferences. In particular, obtaining accurate estimates of the frequency offsets is an important issue. Related results on frequency offset estimation have been presented in [88–92]. In OFDM system with frequency selective channel and cochannel interference, this problem, however, is relatively unaddressed.

For the second contribution in this chapter, we propose a training based algorithm that uses known training sequences to obtain the synchronization parameters and the equalizer coefficients. We present a two stage feedforward receiver architecture to perform joint synchronization and equalization. A direct-training based MMSE (minimizing mean square error) algorithm is proposed to estimate the frequency offsets and the equalization delays in this system. A novel direct training based method is later used to fine-tune the space-time equalizer based on the design principles with channel information, after obtaining the synchronization parameters.

3.2 System Model

This section presents the system model of the downlink multicell scenario. An overview of the system is first discussed, then the channel model and the space-time signal model are given.

3.2.1 System Overview

We assume that one local oscillator is present at each base station and at the downlink user. Therefore, there is only one frequency offset between any base station and any downlink user. The users are equipped with M_r receive antennas. The base station of the current cell and neighboring cells are transmitting data to the users in these cells using only one transmit antenna [45]. The total number of active transmit antennas in this system is M_t, which corresponds to M_t active base stations. There may be one or multiple streams intended to the mobile users from the base stations. For example, handoff in the downlink may require the receiver to decode signals from multiple base stations. The intended streams are considered as desired signals, and the rest of the active streams consist of cochannel interference.

Each OFDM symbol has N subcarriers and a length L_{CP} cyclic prefix. Each data stream transmitted by one active antenna may only use some portion of the OFDM subcarriers for data transmission. We denote the index set of the subcarriers used for data transmission of the i^{th} stream as $\mathcal{S}_i$. We can also use a diagonal matrix $\boldsymbol{\mathcal{T}}_i$ consisting of 0's and 1's in its diagonal axis to select these subcarriers.

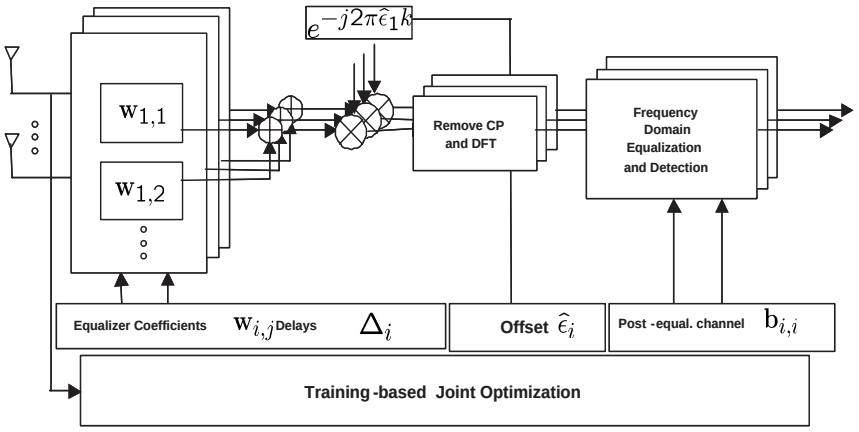

Figure 3.2: The block diagram of the receiver. The space-time equalization is followed by frequency offset compensation.

We illustrate the proposed receiver structure in Fig. 3.2. A space-time equalizer is deployed at the frontend to suppress co-channel interference and shorten the channel response in the case that the channel response is longer than the cyclic prefix. By performing interference cancellation at the equalizer bank, various interferences are suppressed. After space-time equalization, we use a two step feedforward scheme to achieve frequency offset and timing synchronization for each transmitted data stream. The first step is to estimate the frequency offset and timing based on training sequences for each stream independently. The second step is to correct the phase rotation and the timing for this particular data stream after equalization.

The space time equalizer at the j^{th} receive antenna for the i^{th} output data stream of the space-time equalizers is represented by a vector $\mathbf{w}_{i,j} = [w_{i,j}(0), ..., w_{i,j}(L)]^T$ of $L+1$ taps, where $(\cdot)^T$ denotes transpose. Each finite im-

pulse response (FIR) equalizer $\mathbf{w}_{i,j}$ may have a different equalization decision delay $\Delta_{i,j}$. The equalizer set $\{\mathbf{w}_{i,1}, ..., \mathbf{w}_{i,M_r}\}$ forms a space-time filter bank for the i^{th} output data stream. The frequency domain signal of the b^{th} OFDM symbol of the m^{th} data stream is denoted by $\mathbf{v}_m(b) = [v_m(0,b), ..., v_m(N-1,b)]^T$. The time domain signal is transformed by a Discrete Fourier Transformation (DFT) basis matrix $\mathbf{Q}$ of a size $N \times N$ as $\mathbf{s}_m(b) = \mathbf{Q}\mathbf{v}_m(b)$, where $\mathbf{Q}$ is the DFT basis matrix, and $\mathbf{s}_m(b) = [s_m(0,b), ..., s_m(N-1,b)]^T$. For the sample $s_m(p,b)$, the relation between b, p and k is that $k = b(N + L_{CP}) + p + L_{CP}$, which is the universal time in the system.

3.2.2 Channel Model

The channel is assumed to be frequency selective and block-wise time invariant over the duration of multiple OFDM symbols. We denote the channel response by $h_{j,m}(l)$ for the l^{th} tap of the channel between the m^{th} transmit antenna and the j^{th} receive antenna, where $l = 0, 1, 2..., \nu$, $m = 1, 2, ..., M_t$, and $j = 1, 2, ..., M_r$. Note that $\nu + 1$ is considered as the length of the channel response between the m^{th} transmit antenna and the j^{th} receive antenna. We assume that ν is known at the receiver, and it takes into account the maximal span of the channels in the time domain between all active M_t transmit antennas and the receive antennas over different channel realizations. The absolute propagation delay of the link between the m^{th} transmit antenna and the j^{th} receive antenna is denoted by $d_{j,m}$. We model the effects of propagation delays as part of the channel response. The first $d_{j,m}$ taps of the channel response are

considered to be zeros. Assume that the number of nonzero taps of the channel response between the j^{th} transmit antenna and the m^{th} receive antenna is $\nu_{j,m}+1$. We have $\nu_{j,m}+d_{j,m}+1 \leq \nu+1$. The frequency offset between the m^{th} transmit antenna and the j^{th} receive antenna is denoted by ϵ_m, which is normalized by the sampling interval T_s. We make the assumption that ν is less than the number of OFDM subcarriers N, but ν may be less than or greater than L_{CP}.

3.2.3 MIMO Signal Model

Received Signal Model Let $s_m(k)$ be the signal of the data stream transmitted by the m^{th} antenna at discrete time k. The basic discrete time system equation, extended from the SISO case in [88] to the MIMO scenario can be written as

$$r_j(k) = \sum_{m=1}^{M_t} \sum_{l=0}^{\nu} h_{j,m}(l) s_m(k-l) e^{j2\pi\epsilon_m k} + n_j(k), \tag{3.1}$$

where $n_j(k)$ is the noise for receive antenna j at time k.

We construct a Toeplitz channel matrix $\mathbf{H}_{j,m}$ of a size $(L+1)\times(L+\nu+1)$ for the m^{th} transmit antenna and the j^{th} receive antenna constructed from $h_{j,m}(l)$'s, where

$$\mathbf{H}_{j,m} = \begin{bmatrix} h_{j,m}(\nu) & h_{j,m}(\nu-1) & ... & h_{j,m}(0) & 0 & 0 & ... & 0 \\ 0 & h_{j,m}(\nu) & h_{j,m}(\nu-1) & ... & h_{j,m}(0) & 0 & ... & 0 \\ \vdots & \vdots & \ddots & \ddots & \ddots & \ddots & \vdots & \vdots \\ 0 & 0 & 0 & ... & h_{j,m}(\nu) & h_{j,m}(\nu-1) & ... & h_{j,m}(0) \end{bmatrix} \tag{3.2}$$

Notice that the first $d_{j,m}$ taps $(h_{j,m}(l), \quad l=0,1,...,d_{j,m}-1)$ are zeros in this Toeplitz matrix to account for the effects of propagation delays.

We also define a diagonal matrix $\mathbf{\Gamma}(\epsilon_m, L)$ to represent the phase rotation introduced by the frequency offset, which has the following form

$$\mathbf{\Gamma}(\epsilon_m, L) = \text{diag}\{e^{-j2\pi\epsilon_m L}, e^{-j2\pi\epsilon_m (L-1)}, ..., 1\}. \tag{3.3}$$

We stack $L + \nu + 1$ (the length of the effective channel response after equalization) samples of the transmitted signal into a vector $\mathbf{s}_m(k - L - \nu : k) = [s_m(k - L - \nu), ..., s_m(k)]^T$, where $p : q$ denotes the p^{th} to the q^{th} sample of the signal in MATLAB notation. The signal vector at the j^{th} receive antenna, denoted by $\mathbf{r}_j(k - L : k)$, is given as

$$\begin{aligned} \mathbf{r}_j(k - L : k) &= \sum_{m=1}^{M_t} \mathbf{\Gamma}(\epsilon_m, L)\mathbf{H}_{j,m}\mathbf{s}_m(k - L - \nu : k)e^{j2\pi\epsilon_m k} \\ &+ \mathbf{n}_j(k - L : k) \end{aligned} \tag{3.4}$$

where $\mathbf{n}_j(k - L : k) = [n_j(k - L), ..., n_j(k)]^T$ is the noise vector at the j^{th} receive antenna.

Remark 1: As addressed earlier, with additional spatial dimensions leveraged by multiple receive antennas, time domain equalization with multiple antennas can be applied to suppress the co-channel interference caused by interfering data streams. We may combine this step with joint channel shortening to constrain the post equalization channel response to be less than or equal to $L_{CP} + 1$.

Remark 2: An important observation is that the effects caused by the frequency offset and propagation delay (equivalently equalization delay) can be

adjusted after the space-time equalization for each stream since the cochannel interference can be nulled by the equalizers.

Based on these observations, we propose a receiver to support joint space-time interference cancellation and the correction to the frequency offset and the propagation delay. The receiver needs to obtain an estimate for the frequency offset ϵ_m, which we denote by $\hat{\epsilon}_m$. The phase rotation caused by the effects of frequency offsets can thus be corrected with the frequency offset estimate after space-time equalization. The propagation delay for the desired stream can be adjusted with the equalization delay.

Post-Equalization Space-Time Model The k^{th} sample of the i^{th} output data stream after the space-time equalization and the correction to the frequency offset, denoted by $x_i(k)$, can be written as

$$\begin{aligned} x_i(k) &= \sum_{j=1}^{M_r} \mathbf{w}_{i,j}^T \mathbf{r}_j(k+\Delta_{i,j}-L:k+\Delta_{i,j}) e^{-j2\pi\hat{\epsilon}_i k} \\ &= \sum_{j=1}^{M_r} \mathbf{w}_{i,j}^T \mathbf{\Gamma}(\epsilon_i, L)\mathbf{H}_{j,i} e^{j2\pi\epsilon_i\Delta_{i,j}} \mathbf{s}_i(k+\Delta_{i,j}-L-\nu:k+\Delta_{i,j}) e^{j2\pi(\epsilon_i-\hat{\epsilon}_i)k} \\ &+ \sum_{m=1,m\neq i}^{M_t} \sum_{j=1}^{M_r} \mathbf{w}_{i,j}^T \mathbf{\Gamma}(\epsilon_m, L)\mathbf{H}_{j,m} e^{j2\pi\epsilon_m\Delta_{i,j}} \mathbf{s}_m(k+\Delta_{i,j}-L-\nu:k+\Delta_{i,j}) \\ &\times e^{j2\pi(\epsilon_m-\hat{\epsilon}_i)k} + \sum_{j=1}^{M_r} \mathbf{w}_{i,j}^T \mathbf{n}_j(k+\Delta_{i,j}-L:k+\Delta_{i,j}). \end{aligned} \tag{3.5}$$

We write the effective channel between the m^{th} transmit antenna and the j^{th} receive antenna as

$$\mathbf{H}_{j,m}^e = \mathbf{\Gamma}(\epsilon_m, L)\mathbf{H}_{j,m} e^{j2\pi\epsilon_m\Delta_{i,j}}. \tag{3.6}$$

Remark 3: From (3.5), we observe that the effective channels are time-invariant, thus it is possible to use time-invariant space-time equalizers ($\mathbf{w}_{i,j}$)

to null the other transmitted data streams. This is equivalent to having

$$\sum_{j=1}^{M_r} \mathbf{w}_{i,j}^T \mathbf{H}_{j,m}^e = \mathbf{0}^T. \tag{3.7}$$

Remark 4: The equivalent channel response after the space-time equalization has a length of $L + \nu + 1$, which might be larger than $L_{CP} + 1$. In this case, the signal from adjacent OFDM symbols might propagate, and thus cause inter-OFDM-symbol interference (IOSI). If we can constrain the number of the nonzero taps of the effective channel out of the total $L + \nu + 1$ taps to be $L_{CP} + 1$, such problem can be avoided.

After the frequency and timing adjustment, the receiver discards the cyclic prefix and performs the DFT. Detection happens in parallel for all sub-carriers in frequency after the DFT.

Post-Equalization Space-Frequency Model From (3.4), we stack the received signal vectors at the j^{th} receive antenna into a matrix $\mathbf{R}_j(b, \Delta_{i,j})$ of a size $N \times (L + 1)$ with delay parameter $\Delta_{i,j}$ for the b^{th} OFDM symbol, which has the following form

$$\begin{aligned} \mathbf{R}_j(b, \Delta_{i,j}) &= \begin{bmatrix} \mathbf{r}_j(b(L_{CP}+N) + L_{CP} - L + \Delta_{i,j} : b(L_{CP}+N) + L_{CP} + \Delta_{i,j})^T \\ \vdots \\ \mathbf{r}_j((b+1)(L_{CP}+N) - L + \Delta_{i,j} - 1 : (b+1)(L_{CP}+N) + \Delta_{i,j} - 1)^T \end{bmatrix} \\ &= \sum_{m=1}^{M_t} \mathbf{Q}\mathbf{\Theta}(\epsilon_m, N, b)\mathbf{S}_m(b, \Delta_{i,j})\mathbf{H}_{j,m}^T \mathbf{\Gamma}(\epsilon_m, L) e^{j2\pi\epsilon_m \Delta_{i,j}} \\ &+ \mathbf{N}_j(\Delta_{i,j}) \end{aligned} \tag{3.8}$$

where the matrix $\mathbf{S}_m(b, \Delta_{i,j})$ is generated by stacking the transmitted data vector $\mathbf{s}_m$ with the delay parameter $\Delta_{i,j}$. The matrix $\mathbf{N}_j(\Delta_{i,j})$ denotes the

stacked noise matrix at the j^{th} receive antenna. The matrix $\mathbf{\Theta}(\epsilon_i, N, b)$ is a $N \times N$ diagonal matrix, defined as

$$\mathbf{\Theta}(\epsilon_i, N, b) = e^{j2\pi\epsilon_i(N+L_{CP})b}\text{diag}\{1, e^{j2\pi\epsilon_i}, ..., e^{j2\pi\epsilon_i(N-1)}\}. \tag{3.9}$$

The space-frequency model can then be derived as follows

$$\begin{aligned} \mathbf{y}_i(b) &= \textstyle\sum_{j=1}^{M_r} \mathbf{Q}\mathbf{\Theta}(\hat{\epsilon}_i, N, b)^*\mathbf{R}_j(b, \Delta_{i,j})\mathbf{w}_{i,j} \\ &= \mathbf{V}_i(b)\underbrace{\bar{\mathbf{Q}}\mathbf{b}_{i,i}}_{\mathbf{f}_{i,i}} + \underbrace{\text{ICI} + \text{IOSI} + \text{CCI} + \text{Noise}}_{\mathbf{e}_i(b)} \end{aligned} \tag{3.10}$$

where $\mathbf{y}_i(b)$ is a $N \times 1$ vector, which has the samples of the b^{th} OFDM symbol of the i^{th} output data stream. The matrix $\mathbf{R}_j(b, \Delta_{i,j})$ is the stacked version of the data matrix at the j^{th} receive antenna with delay parameter $\Delta_{i,j}$ of a size $N \times (L+1)$.

We define $\mathbf{V}_m(b) = \text{diag}\{v_m(0, b), ..., v_m(N-1, b)\}$, which has the b^{th} frequency domain samples of the data stream transmitted by the m^{th} active transmit antenna. Notice that only those subcarriers whose indices belong to the set $\mathcal{S}_m$ have non-zero values. The vector $\mathbf{f}_{i,i}$ is the frequency domain effective channel response for the i^{th} output stream, the partial DFT basis is denoted by $\bar{\mathbf{Q}}$ which has a size of $N \times (L_{CP}+1)$, and $\mathbf{b}_{i,i}$ is the shortened channel response of a size $(L_{CP}+1) \times 1$ for the shortened effective channel between the i^{th} transmit antenna and the i^{th} output data stream. Note that $\sum_{j=1}^{M_r} \mathbf{H}_{j,m}^T \mathbf{\Gamma}(\epsilon_i, L)\mathbf{w}_{i,j}$ which is of a size $(L+\nu+1) \times 1$ is the post equalization channel response for the m^{th} transmit antenna and the j^{th} receive antenna. The quantity $\mathbf{e}_i(b)$ includes the colored noise, and the intercarrier interference due to the frequency offset estimation error, the possible inter-OFDM-symbol

interference due to the long channel response after equalization, and also the residual co-channel interference due to imperfect interference cancellation.

3.3 Space-Time Equalizer Design

In this section, we focus on the space-time equalizer design for the downlink multicell scenario, given the ideal channel information and synchronization parameters such as frequency offsets and propagation delays. We address the design constraints and formulate optimization problems to meet these constraints. The equalizer design methods based on channel information as we propose here are the rationales for the training based algorithms addressed in Section 3.4. They also provide baseline performance as compared to the training based algorithms in Section 3.5.

3.3.1 Min-SER Equalizer Design

In general, it is very costly to optimize the equalizer delays $\Delta_{i,j}$ for all receive antennas. We make the following assumption that $\Delta_{i,j} = \Delta_i$ for all $j = 1, ..., M_r$ to simplify the M_r variable optimization to a single variable optimization. Let us define a vector channel response after the space-time equalization as
$\bar{\mathbf{b}}_{m,i}^T = \sum_{j=1}^{M_r} \mathbf{w}_{i,j}^T \mathbf{\Gamma}(\epsilon_m, L)\mathbf{H}_{j,m} e^{j2\pi\epsilon_m\Delta_i}$.

Constraint 1 — Nulling Cochannel Interference To guarantee that there is no co-channel interference on the selected subcarriers for the i^{th} output

data stream, we must have the following

$$\mathbf{\mathcal{T}}_i \tilde{\mathbf{Q}} \bar{\mathbf{b}}_{m,i} = \mathbf{0}_{N\times 1}, \quad m \neq i, \tag{3.11}$$

where $\tilde{\mathbf{Q}}$ is the partial DFT matrix to transform the time domain channel repsonse into the frequency domain channel response. This implies that the equivalent channel response of the interferers in the frequency domain after the space-time equalization should be null. We assume that rank$\{\mathbf{\mathcal{T}}_i\} \geq L+\nu+1$, which is equivalent to using more than $L+\nu+1$ subcarriers for the i^{th} data stream. Since the matrix $\mathbf{\mathcal{T}}_i\tilde{\mathbf{Q}}$ is a tall matrix, then the condition of cancelling co-channel interference is equivalent to

$$\sum_{j=1}^{M_r} \mathbf{w}_{i,j}^T \mathbf{\Gamma}(\epsilon_m, L)\mathbf{H}_{j,m} e^{j2\pi\epsilon_m \Delta_i} = \mathbf{0}_{L+\nu+1}^T,$$
$$\forall m \neq i, \quad m = 1, ..., M_t. \tag{3.12}$$

Notice that there are $\nu_{j,m}+1$ nonzero taps for the channel $\mathbf{H}_{j,m}$. The rank of the effective channel matrix $\mathbf{\Gamma}(\epsilon_m, L)\mathbf{H}_{j,m}$ is $\min\{M_r(L+1), L+\nu_{j,m}+1\}$.

Constraint 2 — Shortening Channel to Mitigate ICI Another constraint is to make the non-zero taps of the effective channel response be no longer than the length of the cyclic prefix plus one after equalization, where $\bar{\mathbf{b}}_{m,i} = [\mathbf{0}_{\Delta_i}^T, \mathbf{b}_{i,i}^T, \mathbf{0}_{L+\nu-L_{CP}-\Delta_i}^T]$. This guarantees that no ICI arises after the DFT operation following space-time equalization.

Matrix Formulation for Constraint 1 and 2 Define an aggregated effective channel matrix

$$\mathcal{H} = \begin{bmatrix} \mathbf{\Gamma}(\epsilon_1, L)\mathbf{H}_{1,1}e^{j2\pi\epsilon_1\Delta_i} & ... & \mathbf{\Gamma}(\epsilon_{M_t}, L)\mathbf{H}_{1,M_t}e^{j2\pi\epsilon_{M_t}\Delta_i} \\ \vdots & \ddots & \vdots \\ \mathbf{\Gamma}(\epsilon_1, L)\mathbf{H}_{M_r,1}e^{j2\pi\epsilon_1\Delta_i} & ... & \mathbf{\Gamma}(\epsilon_{M_t}, L)\mathbf{H}_{M_r,M_t}e^{j2\pi\epsilon_{M_t}\Delta_i} \end{bmatrix}. \tag{3.13}$$

We aggregate the equalizers ($\mathbf{w}_{i,j}$) on all receive antennas into a vector $\mathbf{w}_i = [\mathbf{w}_{i,1}^T, ..., \mathbf{w}_{i,M_r}^T]^T$. We define a matrix $\mathcal{C}_i$ to be a binary diagonal matrix which selects the samples in a certain window of length $L_{CP}+1$ of the effective channel response $\mathcal{H}$ after space-time filtering for the i^{th} data stream. The matrix $\bar{\mathcal{C}}_i$ selects the samples outside the window. Both selection matrices are determined by the equalization delay Δ_i. Then we have the following constraint

$$\mathbf{w}_i^T\mathcal{H}\bar{\mathcal{C}}_i = \mathbf{0}^T_{(M_t(L+\nu+1)-L_{CP}-1)\times 1}. \tag{3.14}$$

Also the equivalent channel response for the i^{th} stream after space-time equalization can be written as

$$\mathbf{b}_{i,i}^T = \mathbf{w}_i^T\mathcal{H}\mathcal{C}_i. \tag{3.15}$$

Parameter Selection Condition To avoid the degenerate solution that the equalizer coefficients are all zeros, we further introduce a total power constraint on the equalizer response $\sum_{j=1}^{M_r}\|\mathbf{w}_{i,j}\|^2 = 1$. Notice that the equalizer order L and the number of receive antennas M_r are fixed parameters before system deployment, thus we must select them offline for various channel conditions. We present a simple condition for selecting these parameters.

Proposition 3. A necessary and sufficient condition of existence of equalizer $\mathbf{w}_i$ to satisfy (3.14) for all $\mathcal{H}$'s, and the constraint on the equalizer power is that

$$M_r(L+1) \geq M_t(L+1) + \sum_{m=1}^{M_t} \nu_m - L_{CP}. \tag{3.16}$$

Proof. From linear algebra, we know that there exists a nonzero solution of $\mathbf{w}_i$ to satisfy (3.14) if and only if $M_r(L+1) > \text{rank}(\mathcal{H}\bar{\mathcal{C}}_i)$. Then to find a feasible $\mathbf{w}_i$ and make (3.14) hold for all $\mathcal{H}$, it is equivalent to having $M_r(L+1) > \max_{\mathcal{H}}\{\text{rank}(\mathcal{H}\bar{\mathcal{C}}_i)\}$.

Clearly $\text{rank}(\mathcal{H}\bar{\mathcal{C}}_i) \leq T_d$, where

$$T_d = M_t(L+1) + \sum_{m=1}^{M_t} \nu_m - L_{CP} - 1, \tag{3.17}$$

and the equality holds when the channel vectors $\mathbf{h}_{j,m}$'s ($\mathbf{h}_{j,m} = [h_{j,m}(0), ..., h_{j,m}(\nu)]^T$) are linearly independent to each other. Thus we conclude that the order of the equalizer should be selected to satisfy (3.16). □

Constraint 3 — Minimize a Symbol Error Rate Bound Let us define a Toeplitz matrix $\mathbf{W}_{i,j}$ of size $N \times (N+L)$ generated by the equalizer $\mathbf{w}_{i,j}$ as

$$\mathbf{W}_{i,j} = \begin{bmatrix} w_{i,j}(L) & ... & w_{i,j}(0) & ... & 0 \\ \vdots & \vdots & \ddots & \ddots & \vdots \\ 0 & ... & w_{i,j}(L) & ... & w_{i,j}(0) \end{bmatrix}. \tag{3.18}$$

Assume the noise on each receive antenna follows i.i.d. Gaussian distribution with zero mean and σ_n^2. The noise covariance matrix after the space-

time equalization and DFT operation can be obtained as

$$\mathbf{G}_i = \sigma_n^2 \sum_{j=1}^{M_r} \mathbf{Q}\mathbf{\Theta}(\epsilon_i, N, 0)^* \mathbf{W}_{i,j} \mathbf{W}_{i,j}^H \mathbf{\Theta}(\epsilon_i, N, 0)\mathbf{Q}^H. \tag{3.19}$$

Hence the noise power on subcarrier p for the i^{th} output data stream can be represented as $\mathbf{G}_i(p,p)$, i.e., the p^{th} diagonal element of the matrix $\mathbf{G}_i$.

If the equalizer satisfies the condition (3.14), another design goal is to optimize the average uncoded symbol error rate (SER) using the extra degrees of freedom $\mathcal{D}_e$ in the system, where

$$\mathcal{D}_e = M_r(L+1) - M_t(L+1) + \sum_{m=1}^{M_t} \nu_m - L_{CP}. \tag{3.20}$$

Given a QAM modulation scheme, the average symbol error probability of the OFDM system $\bar{P}_e$ can be approximated by the following expression [93]

$$\bar{P}_e \approx \frac{\text{constant}_1}{N} \sum_{p=1}^{N} Q\left(\frac{\text{constant}_2}{\sqrt{\text{SNR}_p^{-1}}}\right), \tag{3.21}$$

where constant_1 and constant_2 both only depend on the chosen QAM constellation, and $Q(\cdot)$ is the error probability function. In [94] it has been shown that the complementary error function is convex with respect to SNR^{-1} in the moderate-to-high SNR region. It is also shown in [94] that the average SER can be tightly lower bounded by the following at moderate-to-high SNR's for BPSK modulation

$$\bar{P}_e \geq \text{constant}_1 \cdot Q\left(\frac{\text{constant}_2}{\sqrt{\frac{1}{N}\sum_{p=1}^{N} \text{SNR}_p^{-1}}}\right). \tag{3.22}$$

This SER lower bound can be extended to any general QAM modulation with the approximate SER expression in (3.21) using the convexity result established in [94]. Our rationale of designing the equalizer is to minimize this tight lower bound of the average error probability $\bar{P}_e$. This gives

$$g_i(\mathbf{w}_i, \Delta_i) = \frac{1}{|\mathcal{S}_i|} \sum_{p \in \mathcal{S}_i} \frac{\mathbf{G}_i(p,p)}{|\mathbf{f}_{i,i}(p)|^2}, \tag{3.23}$$

where $|\mathcal{S}_i|$ denotes the cardinality of the set $\mathcal{S}_i$.

This performance metric that takes the summation of the inverse per-subcarrier signal to noise and interference ratio can also be related to information theoretic capacity. Notice that by convexity of the $\log_2(1+1/x)$ function, the average sum capacity for the OFDM system can be tightly lowered bounded by the expression $\log_2(1+1/\overline{\mathrm{SNR}^{-1}})$, where $\overline{\mathrm{SNR}^{-1}}$ denotes the average inverse of the per-subcarrier SNR. Indeed, the performance metric that we use here reflects both symbol error rate performance and the performance in terms of average sum capacity.

The Linear Constraint Define the matrix $\mathbf{K}_i = \bar{\mathcal{C}}_i \mathcal{H}^T$, we apply the singular value decomposition (SVD) to this matrix, and obtain the following

$$\mathbf{K}_i = \mathbf{Z}_i \mathbf{\Sigma}_i \mathbf{U}_i^H. \tag{3.24}$$

Clearly, we can write $\mathbf{U}_i$ as the following

$$\mathbf{U}_i = [\mathbf{U}_i^n, \mathbf{U}_i^s] \tag{3.25}$$

where $\mathbf{U}_i^n$ and $\mathbf{U}_i^s$ are of sizes $M_r(L+1) \times T_d$ and $M_r(L+1) \times [M_r(L+1) - T_d]$ respectively (T_d is defined in (3.17)). The matrix $\mathbf{U}_i^n$ generates the subspace corresponding to all singular values in $\mathbf{\Sigma}_i$, and the matrix $\mathbf{U}_i^s$ generates the null space to the subspace generated by $\mathbf{U}_i^n$. Any equalizer vector $\mathbf{w}_i$ lying in the subspace generated by $\mathbf{U}_i^s$ satisfies the constraint $\mathbf{K}_i \mathbf{w}_i = \mathbf{0}$. To avoid the degenerate solution $\mathbf{w}_i = \mathbf{0}$, we further restrict $\mathbf{w}_i$ to be of the following form

$$\mathbf{w}_i = \mathbf{U}_i^s \begin{bmatrix} 1 \\ \mathbf{t}_i \end{bmatrix} = \mathbf{U}^s(:,1) + \mathbf{U}_i^s(:, 2 : (D_e + 1))\mathbf{t}_i \tag{3.26}$$

where $\mathbf{t}_i$ is of length $D_e = M_r(L+1) - T_d - 1$, and the $\mathbf{U}_i^s(:, p:q)$ denotes the p^{th} to the q^{th} column of the matrix $\mathbf{U}_i^s$ in the standard MATLAB notation.

The Min-SER Problem Formulation and the Proposed Optimization Algorithm We phrase the optimization problem of equalizer design as

$$\min_{\mathbf{t}_i, \mathcal{C}_i} g_i(\mathbf{t}_i, \mathcal{C}_i). \tag{3.27}$$

We can solve it by applying the steepest descent method [95]. We describe the optimization algorithm in Appendix B.1. The gradient of the cost function is also given in Appendix B.1. Since any nonzero scalar multiplication to the optimal equalizer vector is still optimal, we normalize the optimal solution in (3.27) by its norm, thus the optimal equalizer vector is given as follows

$$\mathbf{w}_i \rightarrow \frac{\mathbf{U}_i^s [1, \mathbf{t}_i^T]^T}{1 + \|\mathbf{t}_i\|^2}. \tag{3.28}$$

The Min-SER method is robust to the variation of interference power level since the interferers' channels are perfectly cancelled. Given the con-

straint of perfectly nulling the interference, the more extra degrees of freedom D_e the receiver has, the better symbol error rate performance may be achieved.

3.3.2 Maximizing Power Ratio Design (MaxPwr)

The MaxPwr algorithm proposed in [45] uses the power ratio of the desired signal to the interference and noise as the cost function for optimization. We generalize this approach to deal with different frequency offsets in this subsection.

Given the channel estimates in (3.13), we state the problem of maximizing the signal to interference ratio (henceforth the MaxPwr method introduced in [45]) as

$$\max_{\mathbf{w}_i, \mathcal{C}_i} \frac{\mathbf{w}_i^H \boldsymbol{\mathcal{H}}^* \mathcal{C}_i^T \mathcal{C}_i \boldsymbol{\mathcal{H}}^T \mathbf{w}_i}{\mathbf{w}_i^H \boldsymbol{\mathcal{H}}^* \bar{\mathcal{C}}_i^T \bar{\mathcal{C}}_i \boldsymbol{\mathcal{H}}^T \mathbf{w}_i} \quad s.t. \|\mathbf{w}_i\|^2 = 1. \tag{3.29}$$

Thus by performing the optimization over $\mathbf{w}_i$ and $\mathcal{C}_i$, the energy of the post equalization channel response will be mainly concentrated in the selected window, and the energy outside the selected window is minimized. When the length of the window is set to be equal to $L_{CP} + 1$, a joint channel shortening and co-channel interference suppression is performed through the optimization.

As we can see that under the condition (3.16), the interference term can be nulled. Thus the MaxPwr method can be simplified as maximizing the energy of the post equalization channel response under the constraint of

nulling the cochannel interference,

$$\max_{\mathbf{w}_i, \mathcal{C}_i} \|\mathbf{w}_i^T \mathcal{H} \mathcal{C}_i\|^2$$
$$\text{s.t.} \quad \mathbf{w}_i^T \mathcal{H} \bar{\mathcal{C}}_i = \mathbf{0}^T_{(M_t(L+\nu+1)-L_{CP}-1)\times 1}, \quad \|\mathbf{w}_i\|^2 = 1. \tag{3.30}$$

As addressed earlier, we may only use the subcarriers which belong to the set $\mathcal{S}_i$ for the i^{th} data stream, therefore, the cost function is modified as

$$\max_{\mathbf{w}_i, \mathcal{C}_i} \sum_{p \in \mathcal{S}_i} |\mathbf{f}_{i,i}(p)|^2$$
$$\text{s.t.} \quad \mathbf{w}_i^T \mathcal{H} \bar{\mathcal{C}}_i = \mathbf{0}^T_{(M_t(L+\nu+1)-L_{CP}-1)\times 1}, \quad \|\mathbf{w}_i\|^2 = 1 \tag{3.31}$$

where $\mathbf{f}_{i,i} = \bar{\mathbf{Q}} \mathcal{C}_i \mathcal{H}^T \mathbf{w}_i$. We perform an optimization for every $\mathcal{C}_i$. When $\mathcal{C}_i$ is given, by the use of change of variables, we define $\mathbf{w}_i = \mathbf{U}_i^s \mathbf{d}_i$. The optimization problem can be restated as

$$\max_{\mathbf{d}_i} \sum_{p \in \mathcal{S}_i} |\mathbf{f}_{i,i}(p)|^2, \quad \text{s.t.} \quad \|\mathbf{d}_i\|^2 = 1. \tag{3.32}$$

This method of designing equalizer does not give the best uncoded performance, but the optimization is much more simpler to solve than the Min-SER approach. The optimal solution to the problem in (3.32) is the eigenvector corresponding to the maximal eigenvalue of the matrix $(\mathbf{U}_i^s)^H \mathcal{H}^* \mathcal{C}_i \bar{\mathbf{Q}}^H \mathcal{T}_i \bar{\mathbf{Q}} \mathcal{C}_i \mathcal{H}^T \mathbf{U}_i^s$.

3.4 Direct Training Based Synchronization and Equalizer Design

The methods proposed in the previous section are all based on the utilization of channel knowledge. In real systems, the equalizer can be designed

based on the estimated channel responses and frequency offsets. Complexity, however, may be a main concern for this approach because the complexity of jointly obtaining channel responses and frequency offsets is high in MIMO systems. Also, such a design strategy leads to the propagation of the estimation noise to the equalizers. Further, this approach is not possible when the training sequences are not all known to the receiver, i.e., the case of having certain interferers or jammers whose transmitted data sequences are unknown to the receiver.

To deal with these problems, we propose a direct-training based two-stage architecture for synchronization and equalizer design. The first stage utilizes an MMSE joint synchronization and interference cancellation scheme (based on the rationale of MaxPwr) to obtain the synchronization parameters — frequency offsets and equalization delays, and the coarse equalizer coefficients and the post equalization channel response. In the second stage, we refine the design to the equalizer and the post equalization channel response by a direct training based approach based on the rationale of Min-SER.

3.4.1 MMSE Joint Equalization Delay and Frequency Offset Estimation

In this subsection, we propose an MMSE joint synchronization and interference cancellation scheme to estimate equalization delays and frequency offsets.

Define two matrices $\mathbf{P}_{j,i}(\epsilon_i, \Delta_i, b)$ of a size $N \times (L+1)$ as

$$\mathbf{P}_{j,i}(\epsilon_i, \Delta_i, b) = \mathbf{Q}\mathbf{\Theta}(-\epsilon_i, N, b)\mathbf{R}_j(b, \Delta_i), \tag{3.33}$$

and $\mathbf{D}_i(b)$ of a size $N \times (L_{CP}+1)$ as

$$\mathbf{D}_i(b) = \mathbf{V}_i(b)\bar{\mathbf{Q}}. \tag{3.34}$$

Based on the space-frequency model (3.10), the residual error term $\mathbf{e}_i(\epsilon_i, \Delta_i, b)$ has the following form

$$\mathbf{e}_i(\epsilon_i, \Delta_i, b) = \sum_{j=1}^{M_r} \mathbf{P}_{j,i}(\epsilon_i, \Delta_i, b)\mathbf{w}_{i,j} - \mathbf{D}_i(b)\mathbf{b}_{i,i}. \tag{3.35}$$

The mean square error over K training symbol duration amounts to be $\frac{1}{K}\sum_{b=1}^{K} \|\mathbf{e}_i(\epsilon_i, \Delta_i, b)\|^2$. We introduce a matrix $\mathbf{P}(\epsilon_i, \Delta_i)$ defined as

$$\mathbf{P}_i(\epsilon_i, \Delta_i) = \begin{pmatrix} \mathbf{P}_{1,i}(\epsilon_i, \Delta_i, 0) & \cdots & \mathbf{P}_{M_r,i}(\epsilon_i, \Delta_i, 0) \\ \vdots & \ddots & \vdots \\ \mathbf{P}_{1,i}(\epsilon_i, \Delta_i, K-1) & \cdots & \mathbf{P}_{M_r,i}(\epsilon_i, \Delta_i, K-1) \end{pmatrix} \tag{3.36}$$

and a matrix $\mathbf{D}_i$ as

$$\mathbf{D}_i = [\mathbf{D}_i(0)^T, ..., \mathbf{D}_i(K-1)^T]^T. \tag{3.37}$$

The equalizer vectors are stacked into a vector $\mathbf{w}_i = [\mathbf{w}_{i,1}^T, ..., \mathbf{w}_{i,M_r}^T]^T$.

The objective of joint synchronization and interference cancellation is to fine-tune all parameters to minimize the mean square error of the residual error term after equalization, thus we have

$$\min_{\mathbf{w}_i, \mathbf{b}_{i,i}, \Delta_i, \epsilon_i} \|\mathbf{P}(\epsilon_i, \Delta_i)\mathbf{w}_i - \mathbf{D}_i\mathbf{b}_{i,i}\|^2 \quad \text{s.t.} \quad \|\mathbf{b}_{i,i}\|^2 = 1 \tag{3.38}$$

where we use the constraint $\|\mathbf{b}_{i,i}\|^2 = 1$ to avoid degenerate solutions to the optimization. Let us define a matrix $\mathbf{M}_i(\epsilon, \Delta)$ as follows

$$\mathbf{M}_i(\epsilon, \Delta) \;=\; \mathbf{D}_i^H \mathbf{D}_i - \mathbf{D}_i^H \mathbf{P}_i(\epsilon, \Delta)(\mathbf{P}_i(\epsilon, \Delta)^H \mathbf{P}_i(\epsilon, \Delta))^{-1} \mathbf{P}_i(\epsilon, \Delta)^H \mathbf{D}_i.$$

Applying the technique of separation of variables, the offset and equalizer delay estimator can be derived as the following

$$(\epsilon_i^{opt}, \Delta_i^{opt}) = \arg\min_{\epsilon, \Delta} \{\min\{\lambda(\mathbf{M}_i)\}\} \tag{3.39}$$

where $\{\lambda(\cdot)\}$ denotes the set of all eigenvalues of a matrix. Given any integer delay, we use the steepest descent method with Armijo step size selection [95] to find a locally optimal estimate to the frequency offset. The derivative of the eigenvalue of the matrix function $\mathbf{M}_i(\epsilon, \Delta)$ is derived in Appendix B.2.

3.4.2 Direct Training based Min-SER Space-time Equalizer Design

After obtaining the equalization delay Δ_i and the frequency offset ϵ_i based on the MMSE method addressed earlier, we can compensate the effects of asynchronism with these estimated parameters. To further improve the symbol error rate performance, we refine the space-time equalizer coefficients based on the Min-SER principle in Section 3.3. By (3.10), the residual error term has the form

$$\tilde{\mathbf{e}}_i(\epsilon_i, \Delta_i, b) = \sum_{j=1}^{M_r} \mathfrak{T}_i[\mathbf{P}_{j,i}(\epsilon_i, \Delta_i, b)\mathbf{w}_{i,j} - \mathbf{D}_i(b)\mathbf{b}_{i,i}]. \tag{3.40}$$

We also define a matrix $\mathbf{\Lambda}_i$ as

$$\mathbf{\Lambda}_i(\mathbf{b}_{i,i}) = \text{diag}\{|\mathbf{f}_{i,i}(0)|^{-2}, ..., |\mathbf{f}_{i,i}(N-1)|^{-2}\} \tag{3.41}$$

where $\mathbf{f}_{i,i} = \bar{\mathbf{Q}}\mathbf{b}_{i,i}$. The cost function takes the form of the summation of the inverse of the per-subcarrier signal to noise and interference ratio

$$\phi_i(\mathbf{w}_i, \mathbf{b}_{i,i}) = \sum_{b=0}^{K-1} \tilde{\mathbf{e}}_i(\epsilon_i, \Delta_i, b)^H \mathbf{\Lambda}_i \tilde{\mathbf{e}}_i(\epsilon_i, \Delta_i, b). \tag{3.42}$$

The design objective to is to minimize the cost function with certain constraint on $\mathbf{b}_{i,i}$ to avoid degenerate solution, i.e.,

$$\min_{\mathbf{w}_i, \mathbf{b}_{i,i}} \phi_i(\mathbf{w}_i, \mathbf{b}_{i,i}) \quad \text{s.t.} \quad \|\mathbf{b}_{i,i}\|^2 \neq 0. \tag{3.43}$$

We can apply the technique of separation of variables to reduce the number of variables since the optimal $\mathbf{w}_i$ can be expressed as the following

$$\mathbf{w}_i = (\mathbf{P}_i(\epsilon_i, \Delta_i)^H \bar{\mathbf{\Lambda}}_i \mathbf{P}_i(\epsilon_i, \Delta_i))^{-1} \mathbf{P}_i(\epsilon_i, \Delta_i)^H \bar{\mathbf{\Lambda}}_i \mathbf{D}_i \mathbf{b}_{i,i} \tag{3.44}$$

where $\bar{\mathbf{\Lambda}}_i = \mathbf{I}_{K\times K} \otimes \mathbf{\Lambda}_i$, and $\otimes$ denotes the Kronecker product. Also notice that we assume $K|\mathcal{S}_i| > M_r(L+1)$ to guarantee the invertibility of the matrix $\mathbf{P}_i(\epsilon_i, \Delta_i)^H \bar{\mathbf{\Lambda}}_i \mathbf{P}_i(\epsilon_i, \Delta_i)$. Let us also define a matrix $\mathbf{K}_i$ to be

$$\begin{aligned} \mathbf{K}_i(\epsilon_i, \Delta_i, \mathbf{b}_{i,i}) &= \mathbf{D}_i^H [\bar{\mathbf{\Lambda}}_i - \bar{\mathbf{\Lambda}}_i \mathbf{P}_i(\epsilon_i, \Delta_i)(\mathbf{P}_i(\epsilon_i, \Delta_i)^H \bar{\mathbf{\Lambda}}_i \mathbf{P}_i(\epsilon_i, \Delta_i))^{-1} \\ &\times \mathbf{P}_i(\epsilon_i, \Delta_i)^H \bar{\mathbf{\Lambda}}_i] \mathbf{D}_i. \end{aligned} \tag{3.45}$$

To avoid the degenerate solutions, we constrain the first tap of the $\mathbf{b}_{i,i}$ to be 1 to satisfy that $\|\mathbf{b}_{i,i}\|^2 \neq 0$. Thus we can substitute $\mathbf{b}_{i,i}$ with the vector $[1, \mathbf{p}_i]^T$, where $\mathbf{p}_i$ is of length L_{CP}. The optimization problem can be stated with respect to the variable $\mathbf{p}_i$ as the following

$$\min_{\mathbf{p}_i} [1, \mathbf{p}_i^H] \mathbf{K}_i(\epsilon_i, \Delta_i, \mathbf{p}_i) [1, \mathbf{p}_i^T]^T. \tag{3.46}$$

Again, we solve this optimization by the steepest descent algorithm [95], and the derivative to the cost function in (3.46) is given in Appendix B.3. The same optimization algorithm as the one in Appendix B.1 is used to solve this problem.

We normalize the optimal solution $\mathbf{p}_i$ from (3.46), and obtain the post-equalization response as $\mathbf{b}_{i,i} \rightarrow \frac{[1,\mathbf{p}_i^T]}{\|[1,\mathbf{p}_i^T]\|}$, then the optimal solution to the equalizer is provided in (3.44).

3.5 Simulation Results

3.5.1 Simulation Setup

We assume there are two data streams transmitted individually by two base stations. Each stream is targeted to a different mobile user that corresponds to one of the base stations. Throughout the simulation, we assume that the channel is fixed over a frame which contains certain number of OFDM symbols. For each frame, we observe an independently faded channel. The time domain channel for both streams has 6 $M_r \times M_t$ matrix taps. The coefficients of the channel matrices are all independently generated according to a complex Gaussian distribution with zero mean and unit variance. The simulations are conducted in MATLAB.

We use QPSK modulation and $N = 64$ subcarriers. The cyclic prefix length is $L_{CP} = 16$. In the simulation, we assume that each data stream uses all the subcarriers ($\mathfrak{T}_i = \mathbf{I}$). We select the number of receive antennas M_r and the equalizer order L based on (3.16). For each channel realization, we use one

OFDM symbol for the parameter estimation and equalizer training ($K = 1$). The training sequence is i.i.d. constant modulus with random phase. In the training stage, the synchronization parameters are estimated via the MMSE method. Then the equalizer coefficients and the post-equalization channel response are obtained from the Min-SER method. After the training stage, we apply the equalizer obtained at the training stage to equalize the received signal.

We study the uncoded bit error rate (BER) performance. We assume that there is no interleaving in space for the transmitted data streams. At the receiver, we apply the equalization schemes discussed in the previous sections to obtain the equalizer coefficients and the post equalization channel response. For uncoded streams, we perform detection independently for each subcarrier of any transmitted stream. This allows us to apply maximum likelihood scalar detection. Throughout the simulations, we assume that there is a common time reference in the system, namely time 0. The propagation delays for the two users considered in the rest part of this chapter are the absolute time lags with respect to the common time reference.

3.5.2 BER Comparison of Different Design Methods

In Fig. 3.3, we compare the uncoded BER performance of the proposed schemes. In this comparison, we average the BER over 400 channel realizations. For each channel realization, we randomly generate a normalized frequency offset (normalized by the number of OFDM subcarriers) within the

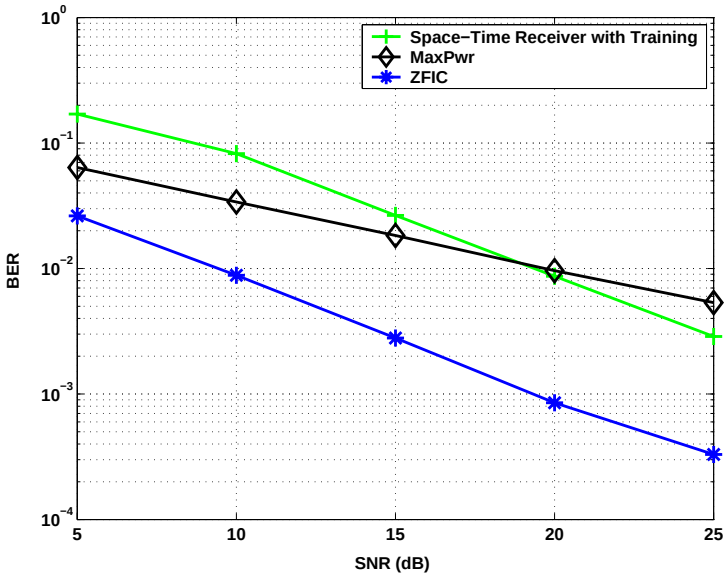

Figure 3.3: BER vs. SNR for the proposed schemes with two transmit data streams. The equalizer memory length is set to be 12. The system uses QPSK modulation. The number of channel taps from the two transmit streams to the receive antennas are both 6.

range of -0.5 to 0.5. The propagation delay difference between both transmitted streams is set to be 0. With ideal channel information and all synchronization parameters, at 20 dB SNR, the Min-SER algorithm outperforms the MaxPwr method by 10 dB. At 20 dB SNR, the BER of the Min-SER algorithm is below 10^{-3}. We also show the BER performance of the proposed space-time receiver with both synchronization and equalization. Notice that with only one training OFDM symbol, this algorithm outperforms the MaxPwr method in high SNR region, and can achieve uncoded BER on the order of 10^{-3} when SNR is higher than 20 dB.

3.5.3 NMSE of the Frequency Offset Estimator

In Fig. 3.4, we illustrate the normalized mean square error (NMSE) versus SNR for the proposed MMSE training algorithm. We average the simulation results over 1000 channel realizations. The normalized frequency offsets are set to be 0.45 and 0.36 in this simulation. The normalized mean square error is defined as the mean square error of the estimated frequency offset normalized by the square of the true frequency offset. Let ϵ_i denotes the true frequency offset, and $\hat{\epsilon}_i$ stands for the estimate to ϵ_i, then the normalized mean square error is

$$NE_i = \frac{E|\hat{\epsilon}_i - \epsilon_i|^2}{\epsilon_i^2} \tag{3.47}$$

where E denotes the expectation with respect to $\hat{\epsilon}_i$. We also plot a lower bound to the NMSE as a baseline for comparison. The bound is obtained in [85]. It is the Cramer-Rao Lower Bound normalized by the true frequency offset for each individual stream using one training OFDM symbol (LCRB), assuming there are no other interfering data streams. The NMSE is monotonically decreasing and is on the order of 10^{-4} for SNR's above 20 dB.

3.5.4 BER Comparison for Different Frequency Offsets

We study the performance of the proposed space-time receiver with different frequency offsets. The propagation delay difference between transmitted data streams is set to be 0, and we average the simulation results over 400 channel realizations. We use two sets of frequency offsets in the simulation. The first pair of frequency offsets for the first and second transmitted streams

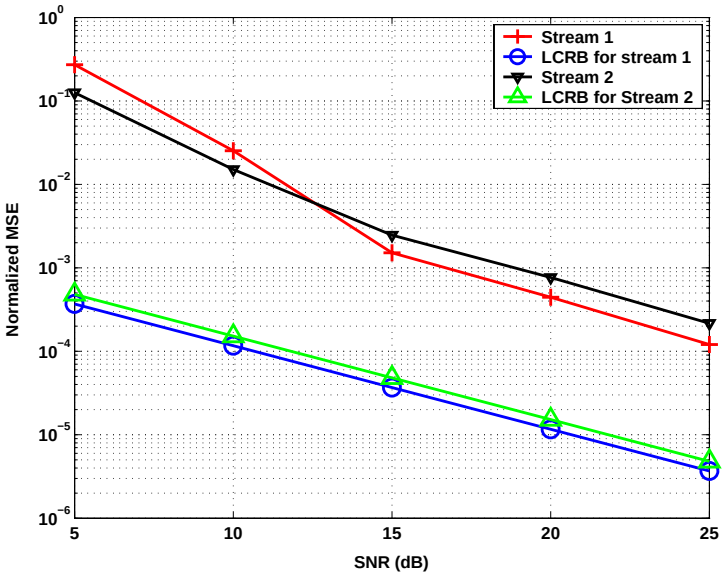

Figure 3.4: Normalized mean square error (NMSE) vs. SNR for the proposed frequency offset estimator for the case of two transmit data streams. The number of channel taps from the two transmit streams to both receive antennas are 3 and 4 respectively.

are 0.05 and -0.03 respectively, and the other pair are set to be $[0.45, -0.36]$. The BER performance for both pairs of frequency offsets is very similar. Thus we can conclude that the space-time receiver is robust to different range of frequency offsets.

3.5.5 BER Comparison for Different Propagation Delays

The performance of the proposed space-time receiver is also studied for different propagation delays between transmitted data streams. we average the BER over 400 channel realizations. For each channel realization, we randomly generate a normalized frequency offset (normalized by the number of OFDM

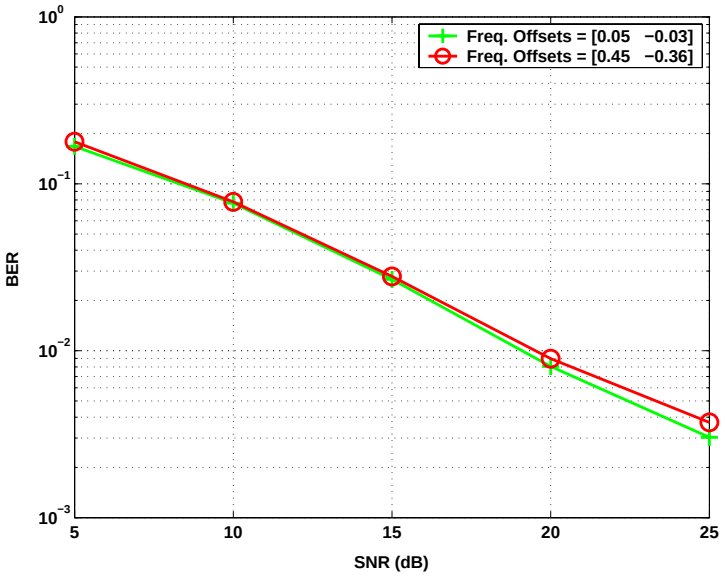

Figure 3.5: BER vs. SNR for the proposed space-time receiver with two transmit data streams with different frequency offsets. Two receive antennas are equipped at the receiver. The equalizer memory length is set to be 12. The system uses QPSK modulation. The number of channel taps from the two transmit streams to the receive antennas are both 6.

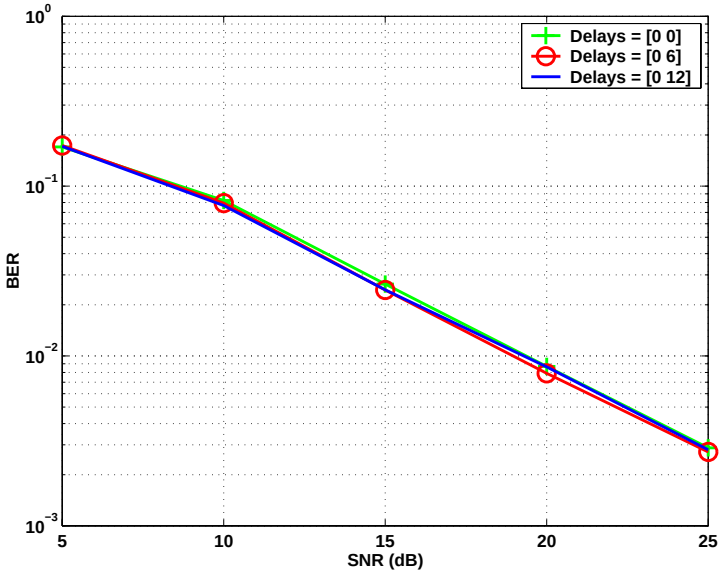

Figure 3.6: BER vs. SNR for the proposed space-time receiver with two transmit data streams with different propagation delays. The equalizer memory length is set to be 12. The system uses QPSK modulation. The number of channel taps from the two transmit streams to the receive antennas are both 6.

subcarriers) within the range of -0.5 to 0.5. The propagation delays between the two transmitted data streams vary from 0 to 12 samples, however, the BER curves under different propagation delays are over close to each other. This concludes that the space-time receiver is robust to different ranges of propagation delays between users.

3.6 Summary of Contributions

In this chapter, we studied the receiver design problem for suppression of asynchronous cochannel interference in a OFDM multicell scenario. The receiver consists of two stage of equalization in both the time domain and the frequency domain after FFT. The main contributions of this chapter are the problem formulations and algorithms for the space-time equalizer design. We included the efforts of frequency offsets in our problem formulations. The space-time equalizer design approach that we propose takes into account both the symbol error rate performance and information theoretic capacity.

We proposed an equalizer design algorithm when both channel information and synchronization parameters are available to the receiver. We also proposed an MMSE joint frequency and equalization delay estimation algorithm using training sequences. A training-based equalizer design algorithm is studied to refine the design to the space-time equalizers after the MMSE synchronization. Simulation results under various asynchronous scenarios illustrate that the proposed space-time receiver produces desirable bit error rate performance.

Chapter 4

MIMO Fixed Relay-aided Broadcast for the Downlink

This chapter presents a novel relaying strategy that uses multiple input multiple output (MIMO) fixed relays with linear processing to support multiuser transmission in cellular networks. This strategy applies to the two hop relaying scenario for coverage enhancement in the downlink, where the base station transmits data to multiple users through one fixed relay (multiuser transmission). The fixed relay processes the received signal with linear operations and forwards the processed signal to multiple users.

This chapter mainly concerns how to design the transceiver at the base station and the relay for the MIMO fixed relay system. The first part of this research proposes upper and lower bounds on the information theoretci achievable sum rate for the proposed architecture. Reduced complexity algorithms based on the sum rate lower bounds are used to select a subset of users. In the second part of this chapter, an implementable multiuser precoding strategy is proposed. This framework combines Tomlinson-Harashima precoding [26]

at the base station and linear signal processing at the relay, adaptive stream selection, and QAM modulation. The MIMO fixed relaying architecture and the proposed design algorithms serve as our contributions in this chapter.

The chapter is organized as the following. An introduction of the background on MIMO downlink with fixed relays and some prior work is first presented in Section 4.1. Main technical contributions are also summarized. The system model of the multiuser relaying system is then presented in Section 4.2. Various design algorithms that jointly optimize the power allocation at the base station and the relay are proposed in Section 4.3. An implementable relaying strategy is presented in Section 4.4.3. Simulations are conducted to illustrate performance of the proposed schemes versus a decode-and-forward model in Section 4.5.

4.1 Introduction

Recently using fixed relays in cellular systems has received significant interest. Fixed relays are low cost and low transmit power elements that receive and forward data from the base station to the users via wireless channels, and vice versa. Using fixed relays boosts coverage in cellular networks when carefully placed at the cell edge or in regions with significant shadowing [49].

Relays do not have wired connection to the backhaul and only process the signal received wirelessly from the base station and forward to the users. Using pico-cells [96] or distributed antennas [97] can also boost coverage for users at the cell edge or in shadowing regions. Using pico-cells increases the

density of the cells by deploying more base stations in the system. In distributed antenna systems, the antennas of the base station are distributed in different sites. Both systems require wired connection to connect the base stations or distributed antennas to the backhaul. Using relays can eliminate the cost and the time to connect the relaying devices to the wired backhaul. Fixed relays are mounted in fixed locations and are part of the infrastructure of the cellular systems. Using fixed relays can avoid the complex operation of routing and medium access control compared to using mobile relays, where the relaying nodes operate in a similar manner to the mobile users.

Using fixed relays is an attractive design option for coverage improvement in the cellular networks. In this chapter, we focus on a downlink broadcast channel that employs MIMO fixed relays. This is a new system framework that differs from the conventional point to point relay channels [49, 50, 98].

4.1.1 Prior Work on Relay Channels

The general relay channel, where relays are used to help send data from a source to a destination, has been studied in [20, 21, 36, 37, 99, 100]. Though the information theoretic capacity of the relay channel remains unknown, several results on capacity bounds are available [20, 21, 37, 99–101]. Design aspects of relaying strategies are addressed [102–104]. Prior work mainly focuses on point-to-point transmission via relays, often considering the mobile relay. Unfortunately, it is likely that only a few fixed relays will be available in each cell. Consequently, each fixed relay will need to support multiple users. This

motivates developing point-to-multipoint relaying solutions, where the relay forwards data to and from multiple users.

The main challenge in the point-to-multipoint fixed relay is providing a high capacity link between the base station and relay, while at the same time providing multiple data links to multiple users. A natural solution to this problem is to exploit the advantages of multiple-input multiple-output (MIMO) communication. It is well known that MIMO communication uses multiple antennas to enhance system capacity and improve resilience against fading [2, 4, 105]. Initial work on MIMO relay channels [20][22], however, deals only with the point-to-point MIMO relay channel. The point-to-multipoint case has received less attention. In this chapter we assume that the base station and fixed relay each have multiple antennas but that the mobile users have only a single receive antenna (the latter assumption is primarily for simplicity). Used in this way a high-throughput MIMO link can be employed between the base station and fixed relay, then the MIMO broadcast channel/MAC channel can be used to deliver the data to/from multiple users.

4.1.2 Main Contributions

In this chapter, we consider the special case of MIMO fixed relays with linear processing to enhance multiuser transmission in the downlink of a cellular system. We assume two-hop communication where in one time-slot the relay stores the message, applies a linear filter, and forwards it to the users in the second timeslot. We assume the case where the relay node does

not decode the signal from the source, but simply process the received signal with matrix multiplication. Further we neglect the direct connection between the source and the users. This is realistic for the case where relays are used to improve coverage and is helpful because it simplifies the analysis.

Our proposed framework that uses MIMO fixed relays for multiuser transmission in the downlink combines concepts from multiuser MIMO broadcast transmission with a fixed relay concept. The MIMO broadcast channel, where a single point with multiple antennas communicates with multiple users with multiple antennas, has been studied in terms of information theory [15–19] and precoding design have been considered [26, 32–35]. Motivated by the research for MIMO broadcast channel, in this chapter we address both the information theoretic and the transceiver design aspects of the multiuser MIMO fixed relay system. We employ zero-forcing dirty paper coding and impose several different structures to design the precoder at the base station and the signal processing unit at the relay. We consider achievable sum rates of this system, which define the sum of the coding rates intended to the downlink users with vanishing decoding error probability as the coding block length grows [15]. We propose to jointly design the precoder at the base station and the signal processing unit at the relay to improve throughput performance. This leads to upper and lower bounds on the achievable sum rate for this architecture neglecting the direct links from the base station to the users. These performance bounds motivate us to propose an implementable multiuser precoding strategy for this system that combines Tomlinson-Harashima precoding at the

base station [26] and linear signal processing at the relay, adaptive stream selection, and QAM modulation [106]. Our framework can also be extended to the MIMO MAC (multiple access channel) where multiple sources send data to a destination via a MIMO fixed relay.

In comparison to decode-and-forward relaying strategies [36–38], a major benefit of our proposed approach is that it does not require decoding and re-encoding of the real-time data at the relay. Compared to prior work on MIMO relay design that uses linear signal processing at the relay [39, 40, 107–109], we consider simultaneous multi-user transmission whereas prior work considers only single user MIMO transmission. We find that the optimizations and their solutions are quite different due to the difficulty in finding closed-form solutions for the MIMO broadcast channel.

We propose sum rate bounds for the point-to-multipoint MIMO relay channel. This differentiates from prior work on information theoretic aspects of the point-to-point relay channel [20–22] and relay networks with multiple source-destination pairs [110]. Compared to the prior work on MIMO broadcast channel[15, 16, 18], we still apply the dirty paper coding to derive achievable sum rates of the multiuser MIMO relay channel, however, we conduct a joint design of the precoder at the base station and the linear processing matrix at the relay. The design needs to satisfy the power constraints at both the source node and the relay node. The proposed implementable relaying strategy using Tomlinson-Harashima precoding is similar to the application of Tomlinson-Harashima precoding in the MIMO broadcast channel [26][32]. Dif-

ferent design and optimization criteria for the Tomlinson-Harashima precoder, however, are proposed in our framework.

4.2 System Model

In this section, we elaborate on the system model of the multiuser fixed relay system. First we describe the system block diagram and main assumptions of the system, then we present the downlink signal model.

4.2.1 System Block Diagram and Main Assumptions

Our relaying strategy supports multiuser transmission as illustrated in Fig. 4.1, i.e., multiple users are served simultaneously through a single fixed relay. We consider only a two-hop relaying, i.e., there is at most one relay between the base station and the mobile users in our system. This is reasonable as more than two hops adds complexity to the system operation, especially routing, and increases transmission latency [49]. We neglect the direct link between the base station and the users in our system model. This is a reasonable assumption when fixed relays are used to extend coverage in highly attenuated propagation environments, where the signal quality of the direct link from the base station to the users is poor.

In this chapter, we consider a narrowband system. Our analysis, however, can be generalized to broadband systems with OFDM (orthogonal frequency division multiplexing), where each subcarrier in the frequency domain can be viewed as a narrowband channel. The base station (BS) is deployed

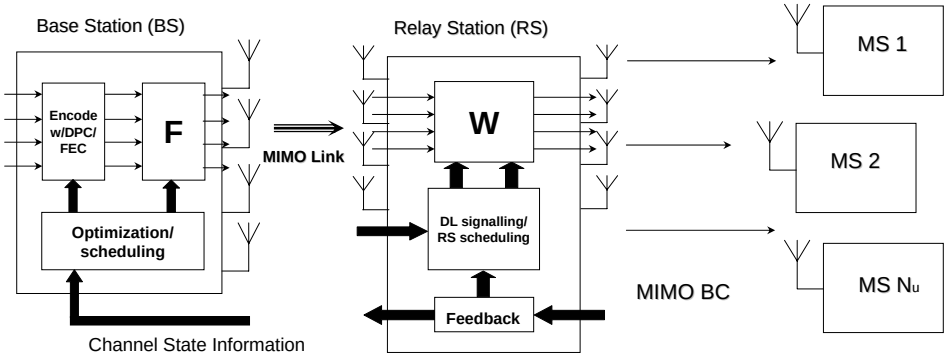

Figure 4.1: The multiuser MIMO relay system with linear processing. The relay uses linear processing. The base station performs error correction coding and dirty paper coding along with adaptive modulation coding.

with M_b transmit antennas and communicates with a fixed relay node that has M_r antennas. A MIMO channel denoted by $\mathbf{H}_1$ is thus created between the base station and the relay. The precoding strategy at the BS includes an encoding operation and a subsequent linear operation with a precoding matrix $\mathbf{F}$ [15]. The base station encodes the data that is targeted to multiple users and sends it to the relay. The relay then broadcasts the data to multiple mobile users.

In this narrowband system, the relaying operation is performed in a half time division duplex (TDD) mode. Each downlink frame consists of two phases of operations. In the first phase, the relay receives the signal from the base station. In the second phase, this signal is processed, then it is forwarded to the users. Both phases span equal time durations. In this chapter, we focus on non-decode-and-forward relays because this does not require encoding and decoding of real-time data at the relays.

Note that other duplex options for the relay, e.g., frequency division duplex (FDD) (the base station and the relay operate on different frequency bands at the downlink) and code division multiple access (CDMA) based duplex (the base station and the relay operate with different CDMA spreading codes at the downlink) [100][111], are also feasible. These, however, may require more bandwidth than the simple half TDD mode. We do not elaborate on these options in this chapter.

4.2.2 Downlink Signal Model

In this subsection, we elaborate on the downlink signal model. We use a linear signal processing unit denoted by a relaying matrix $\mathbf{W}$ of a size $M_r \times M_r$ to process the received signal at the relay. The transmitted signal vector intended for multiple users is denoted by $\mathbf{s}$. Note that $\mathbf{s}$ is the coded data vector. The noise added to the received signal at the relay is represented by $\mathbf{n}_1$. The number of users in the system is denoted by N_u. The relay forwards the signal from the BS to multiple users, each with one receive antenna.

In this system, the users may be classified as relaying users (served through relays) and direct-link users (served directly by the base station). It is a complicated design problem to determine how to schedule multiple relaying users, multiple direct-link users and a mixture of these two in the system. We restrict our study to serving multiple relaying users via one MIMO relay in this chapter. This captures the essence of the design issue for MIMO relays. It is an interesting topic of future work to study scheduling algorithms with the co-existence of relaying users and direct-link users.

The channel between the relay and the i^{th} mobile user can be represented by a vector $\mathbf{h}_{i,2}$ of size $M_r \times 1$. User i observes the following linear combination of the transmitted signals

$$\begin{aligned} x_i &= \mathbf{h}_{i,2}^T \mathbf{W}(\mathbf{H}_1 \mathbf{F}\mathbf{s} + \mathbf{n}_1) + n_{i,2} \\ &= \mathbf{h}_{i,2}^T \mathbf{W}\mathbf{H}_1 \mathbf{F}\mathbf{s} + \mathbf{h}_{i,2}^T \mathbf{W}\mathbf{n}_1 + n_{i,2} \end{aligned} \tag{4.1}$$

where x_i is the scalar received signal at user i. The noise term $n_{i,2}$ is a scalar

at the i^{th} user and $\mathbf{n}_1$ is the noise vector at the relay. The elements of the noise vector $\mathbf{n}_1$ and the noise term $n_{i,2}$ follow i.i.d. complex Gaussian distribution with zero mean and variance σ_1^2 and σ_2^2 respectively.

In this system, the total power at the base station and the relay are P_t and P_r respectively. The input signal vectors are independent inputs that are all with zero mean and unit variance. The signal vector is coded by a linear precoder $\mathbf{F}$ [15]. The signal after the linear precoding satisfies the total power constraint $E\|\mathbf{Fs}\|^2 \leq P_t$, where E denotes expectation. Hence the transmit power constraints at the base station can be written as

$$\mathrm{Tr}\{\mathbf{F}\mathbf{F}^H\} \leq P_t. \tag{4.2}$$

The received signal at the relay is processed by the relay matrix $\mathbf{W}$. Let $\tilde{\mathbf{s}} = \mathbf{W}\mathbf{H}_1\mathbf{F}\mathbf{s} + \mathbf{W}\mathbf{n}_1$. The relay power constraint is expressed as $E\|\tilde{\mathbf{s}}\|^2 \leq P_r$. This power constraint can be written explicitly with respect to $\mathbf{W}$ and $\mathbf{F}$ as follows

$$\mathrm{Tr}\{\mathbf{W}(\mathbf{H}_1\mathbf{F}\mathbf{F}^H\mathbf{H}_1^H + \mathbf{I}\sigma_1^2)\mathbf{W}^H\} \leq P_r \tag{4.3}$$

where $\mathrm{Tr}\{\cdot\}$ denotes the trace of a matrix. The noise power at the i^{th} user is the following

$$v_i = (\mathbf{h}_{i,2})^T\mathbf{W}\mathbf{W}^H(\mathbf{h}_{i,2})^*\sigma_1^2 + \sigma_2^2 \tag{4.4}$$

where $(\cdot)^*$ denotes conjugate operation.

Overall, we model the multiuser MIMO relaying system as a broadcast channel in (4.1) with power constraints at the base station and the relay in (4.2) and (4.3), respectively.

4.3 Achievable Sum Rates with Relay Design Structures

In this section, we derive bounds of achievable sum rates of the MIMO fixed relay system using dirty paper coding, which has been shown to be sum capacity optimal. The sum rate using dirty paper coding can be expressed as a function of the precoding matrix $\mathbf{F}$ and the relay processing matrix $\mathbf{W}$. A brute-force approach is to directly optimize the sum rate with respect to the matrices $\mathbf{F}$ and $\mathbf{W}$, however, this approach optimizes large number of parameters and has very high computational cost. Further, in this formulation, the optimizers may not be unique. Thus finding a globally optimum solution is difficult. To resolve this problem, we introduce several design structures for the parameters $\mathbf{F}$ and $\mathbf{W}$. This leads to sum rate lower bounds that can be computed using low complexity algorithms. In this section, we also discuss a sum rate upper bound for the proposed MIMO relay system and derive the maximum sum rate of the decode-and-forward strategy, neglecting the direct link between the base station and the users.

4.3.1 All-pass Relay with Zero-Forcing Dirty Paper Coding (All-Pass Relay Design)

A simple approach to design the relay is to treat it as an all-pass amplify-forward unit, which we construct as follows $\mathbf{W} = g_w \mathbf{I}_{M_r \times M_r}$, where g_w ($g_w \geq 0$) represents the gain at the relay. All-pass relays have low hardware complexity because they simply amplify the received signal for all antennas.

We stack the channel vectors between the relay and the users into a matrix $\mathbf{H}_2 = [\mathbf{h}_{1,2}, ..., \mathbf{h}_{N_u,2}]^T$. The equivalent channel from the base station side has the following form:

$$\mathbf{H}_{eq} = g_w \mathbf{\Pi} \mathbf{H}_2 \mathbf{H}_1, \tag{4.5}$$

which is a matrix of a dimension $N_u \times M_b$. The matrix $\mathbf{\Pi}$, which consists of zeros and ones, performs permutation of the rows of the matrix $\mathbf{H}_2\mathbf{H}_1$. Applying the QR decomposition [112],

$$\mathbf{H}_{eq} = g_w \mathbf{G}_{eq} \mathbf{Q}_{eq} \tag{4.6}$$

where $\mathbf{G}_{eq}$ is a lower triangular matrix of size $N_u \times M_b$. The rank of the matrix $\mathbf{G}_{eq}$ is less than or equal to $M_u = \min\{M_r, M_b, N_u\}$. The $(M_u + 1)^{th}$ to the M_b^{th} diagonal elements are zeros. The matrix $\mathbf{Q}_{eq}$ is unitary. Thus a maximum of M_u users can be served simultaneously using this scheme. The relaying gain parameter g_w is selected to satisfy the power constraints (4.2) and (4.3).

Let $\mathbf{F}\mathbf{F}^H = \mathbf{Q}_{eq}^H \mathbf{\Theta} \mathbf{Q}_{eq}$, where $\mathbf{\Theta} = \text{diag}\{p_1, ..., p_{M_u}, 0, ..., 0\}$ denotes the powers allocated to the transmit streams. Hence $\mathbf{F} = \mathbf{Q}_{eq}^H \mathbf{\Theta}^{1/2} \mathbf{X}$, where $\mathbf{X}$ is a unitary matrix. We stack the powers in a vector $\mathbf{p} = [p_1, ..., p_{M_u}]^T$ and define $g_s = |g_w|^2$, $d_i = |g_w \mathbf{G}_{eq}(i,i)|^2 = g_s |\mathbf{G}_{eq}(i,i)|^2$, where $\mathbf{G}_{eq}(i,i)$ stands for the i^{th} diagonal element of the matrix $\mathbf{G}_{eq}$. We can compute the noise power at the i^{th} user as $v_i = \|\mathbf{h}_{i,2}\|^2 g_s \sigma_1^2 + \sigma_2^2$.

The relaying system is modelled as an equivalent MIMO broadcast channel in (4.1). Thus coding schemes for the MIMO broadcast channel can

be extended to the proposed system. We employ zero-forcing dirty paper coding [15] for the all pass relay design. This gives a lower bound of the sum capacity (the maximum achievable sum rate of the system). The sum rate with the all pass relay design has the following form

$$\begin{aligned} R(\mathbf{p}, g_s) &= \frac{1}{2}\sum_{i=1}^{M_u} \log_2\left(1 + \frac{d_i p_i}{v_i}\right) \\ &\geq \frac{1}{2}\sum_{i=1}^{M_u} \log_2\left(\frac{d_i p_i}{v_i}\right) \\ &= -\frac{1}{2}\log_2 \prod_{i=1}^{M_u} v_i d_i^{-1} p_i^{-1} \\ &= R_b(\mathbf{p}, g_s). \end{aligned} \tag{4.7}$$

The quantity $R_b(\mathbf{p}, g_s)$ is a lower bound of the sum rate $R(\mathbf{p}, g_s)$ and it closely approximates $R(\mathbf{p}, g_s)$ in the high SNR region. Using this quantity as our cost function for optimization, we can formulate a geometric program, which has a unique optimizer. A geometric program is a class of nonlinear optimization problems characterized by objective and constraint functions that have a special form [77][113]. A geometric program can be transformed into a convex optimization via a bijective mapping. Then the convex optimizaton problem can be solved efficiently.

Optimization Problem for All-Pass Relay Design

For each permutation $\mathbf{\Pi}$, we can formulate a problem to maximize $R_b(\mathbf{p}, g_s)$

subject to the transmit and relay power constraints,

$$\begin{aligned} &\min_{\mathbf{p},g_s} \tfrac{1}{2}\log_2 \textstyle\prod_{i=1}^{M_u} v_i d_i^{-1} p_i^{-1} \\ \text{s.t.}\quad &\mathrm{Tr}\{\mathbf{H}_1\mathbf{Q}_{eq}^H\mathbf{\Theta}\mathbf{Q}_{eq}\mathbf{H}_1^H + \mathbf{I}\sigma_1^2\}g_s \le P_r, \\ &\textstyle\sum_{i=1}^{M_u} p_i \le P_t, \quad p_i \ge 0 \ \ \forall i, \quad g_s \ge 0. \end{aligned} \tag{4.8}$$

We introduce the main result for the all-pass relay design in the following proposition.

Proposition 4. The optimization problem in (4.8) is a geometric program.

Proof of Proposition 4 is given in Appendix C.1. An important observation is that the optimization problem in (4.8) has a unique optimizer since it is a standard geometric program. We describe a standard algorithm to solve this problem in Appendix C.2.

4.3.2 Design of the Eigen-Space of the Relaying Matrix (SVD Relay Resign)

In this subsection, we propose a relay design approach that operates on the eigen-space of the relaying matrix, which we call SVD relay design. This design approach requires slightly more complex operations at the relay than the all-pass structure. By allowing more degrees of freedom in the design, the SVD relay structure provides a higher achievable sum rate than the all-pass structure and thus a better lower bound.

Define $\bar{\mathbf{H}}_2 = \mathbf{\Pi}\mathbf{H}_2$, which is a permutated version of the channel matrix. Applying the QR decomposition and singular value decomposition (SVD) to

the channel matrices $\bar{\mathbf{H}}_2$ and $\mathbf{H}_1$, respectively, we have the following

$$\bar{\mathbf{H}}_2 = \mathbf{G}_2\mathbf{Q}_2 \tag{4.9}$$

where $\mathbf{G}_2$ is a lower triangular matrix and $\mathbf{Q}_2$ is unitary. This directly follows from the QR decomposition [112]. Performing the singular value decomposition,

$$\mathbf{H}_1 = \mathbf{U}_1\mathbf{\Sigma}_1\mathbf{V}_1^H \tag{4.10}$$

where both $\mathbf{U}_1$ and $\mathbf{V}_1$ are unitary, and the nonzero diagonal elements of the matrix $\mathbf{\Sigma}_1$ are placed in descending order ($\sqrt{\nu_1} \geq ... \geq \sqrt{\nu_{\min\{M_b,M_r\}}}$).

We construct a diagonal matrix $\mathbf{K}$ such that $\mathbf{K}\mathbf{K}^H = \text{diag}\{k_1, ..., k_{M_r}\}$. In our design, the linear processing matrix $\mathbf{W}$ is expressed with respect to $\mathbf{K}$ as

$$\mathbf{W} = \mathbf{Q}_2^H\mathbf{K}\mathbf{U}_1^H. \tag{4.11}$$

The precoder is structured such that $\mathbf{F}\mathbf{F}^H = \mathbf{V}_1\mathbf{\Theta}\mathbf{V}_1^H$, where $\mathbf{\Theta}$ is a diagonal matrix as defined earlier for the all-pass relay design. The vector $\mathbf{p}$ includes all nonzero diagonal elements of $\mathbf{\Theta}$. We jointly design $\mathbf{p}$ and $\mathbf{k}$ to adjust the power allocation at the base station and at the relay.

Let $\bar{d}_i = \nu_i k_i |\mathbf{G}_2(i,i)|^2$. The noise term can be written as

$$v_i = \sum_{j=1}^{i} |\mathbf{G}_2(i,j)|^2 k_j \sigma_1^2 + \sigma_2^2. \tag{4.12}$$

The SNR at the i^{th} user is denoted by $\eta_i = \frac{\bar{d}_i p_i}{v_i}$. We assume zero-forcing dirty paper coding for the SVD relay design. The sum rate of the system under the

SVD relay design can be expressed as

$$\begin{aligned}
\bar{R}(\mathbf{p},\mathbf{k}) &= \frac{1}{2}\sum_{i=1}^{M_u}\log_2(1+\eta_i) \\
&= \frac{1}{2}\sum_{i=1}^{M_u}\log_2\left(1+\frac{\bar{d}_i p_i}{v_i}\right) \\
&\geq \frac{1}{2}\sum_{i=1}^{M_u}\log_2\left(\frac{\bar{d}_i p_i}{v_i}\right) \\
&= -\frac{1}{2}\log_2\prod_{i=1}^{M_u} v_i \bar{d}_i^{-1} p_i^{-1} \\
&= \bar{R}_b(\mathbf{p},\mathbf{k}) \qquad (4.13)
\end{aligned}$$

where $\bar{R}_b(\mathbf{p},\mathbf{k})$ is the lower bound to the sum rate $\bar{R}(\mathbf{p},\mathbf{k})$. Notice that with this particular relay structure, the relay power constraint equates

$$\mathrm{Tr}\{\mathbf{W}(\mathbf{H}_1\mathbf{F}\mathbf{F}^H\mathbf{H}_1^H + \mathbf{I}\sigma_1^2)\mathbf{W}^H\} = \sum_{i=1}^{M_u} k_i(\nu_i p_i + \sigma_1^2). \qquad (4.14)$$

Optimization Problem for SVD Relay Design

For each user permutation $\mathbf{\Pi}$, we formulate an optimization problem that jointly maximizes the sum rate with respect to the parameters $\mathbf{p}$ and $\mathbf{k}$ as

$$\begin{aligned}
&\max_{\mathbf{p},\mathbf{k}} \bar{R}_b(\mathbf{p},\mathbf{k}) \\
&\text{s.t.} \quad \textstyle\sum_{i=1}^{M_u} k_i(\nu_i p_i + \sigma_1^2) \leq P_r, \\
&\textstyle\sum_{i=1}^{M_u} p_i \leq P_t, \quad p_i \geq 0, k_i \geq 0 \ \ \forall i. \qquad (4.15)
\end{aligned}$$

This is also a geometric program. Using the transformation $\mathbf{p}^t = \log(\mathbf{p})$ and $\mathbf{k}^t = \log(\mathbf{k})$, we are able to transform the problem in (4.15) into a convex optimization [113]. This can be solved via standard iterative algorithms [77].

The procedure is the same as the one that has been used for the all pass relay design, thus we do not elaborate it here. We select the permutation that provides the highest sum rate over all permutations.

4.3.3 Equal Transmit Power Allocation at the Base Station with Relay Water Filling (Relay Water-filling)

The design algorithms proposed earlier formulate optimization problems that can be solved using geometric programming for all user permutations. The major issue is that using exhaustive search to find the optimum user selection over all permutations is highly costly in computation. In this subsection, we first propose a lower bound of the maximum achievable sum rate with dirty paper coding. We then present a reduced-complexity algorithm for user selection based on this lower bound. Finally we propose a relaying strategy using equal transmit power allocation at the base station with water-filling at the relay. This problem is convex and can be solved using water-filling. The proposed user selection and relay design algorithms lead to much lower computation complexity than the previously proposed algorithms.

A Lower Bound of the Sum Rate We assume that all the users are arranged in a permutation order $\mathbf{\Pi}$. Then the base station selects the first T users out of all users, where $T \leq M_u$ and $M_u = \min\{M_r, M_b, N_u\}$. This corresponds to operate on the first T rows of the aggregated channel matrix $\bar{\mathbf{H}}_2$ in (4.9). Equal power is allocated to the transmitted streams, thus each stream is loaded with power P_t/T. We present the lower bound of the sum

rate in the following proposition.

Proposition 5. A lower bound to the sum rate of the fixed relay system under the consideration with equal power allocation to all streams is $\bar{R}_l(\mathbf{k}) = \frac{1}{2}\sum_{i=1}^{T}\log_2(1+\eta_i^{(l)})$, where $\eta_i^{(l)}$ is a lower bound of the SNR at the i^{th} user

$$\eta_i^{(l)} = c_i k_i, \tag{4.16}$$

where

$$c_i = \frac{\nu_i|\mathbf{G}_2(i,i)|^2 P_t/T}{\|\mathbf{h}_{i,2}\|^2\frac{P_r\sigma_1^2}{\nu_i P_t/T+\sigma_1^2}+\sigma_2^2}. \tag{4.17}$$

Proof. Notice that with equal transmit power allocated to the streams at the transmitter, the noise power at the i^{th} user can be written as

$$\begin{aligned} v_i &= \sum_{j=1}^{i}|\mathbf{G}_2(i,j)|^2 k_j\sigma_1^2+\sigma_2^2 \\ &\leq \sum_{j=1}^{i}|\mathbf{G}_2(i,j)|^2\sum_{j=1}^{i}k_j\sigma_1^2+\sigma_2^2 \\ &\leq \|\mathbf{h}_{i,2}\|^2\frac{P_r\sigma_1^2}{\nu_i P_t/T+\sigma_1^2}+\sigma_2^2. \end{aligned} \tag{4.18}$$

The last step follows from that $\|\mathbf{h}_{i,2}\|^2 = \sum_{j=1}^{i}|\mathbf{G}_2(i,j)|^2$ via the QR decomposition. From the relay power constraint $\sum_{j=1}^{T}k_j\left(\nu_j\frac{P_t}{T}+\sigma_1^2\right) \leq P_r$, since $\nu_1 \geq ... \geq \nu_T$, we have $\sum_{j=1}^{i}k_j(\nu_i\frac{P_t}{T}+\sigma_1^2) \leq \sum_{j=1}^{i}k_j(\nu_j\frac{P_t}{T}+\sigma_1^2) \leq P_r$.

Therefore, the SNR for the i^{th} user denoted by η_i can be derived as

$$\begin{aligned} \eta_i &= \frac{\nu_i k_i|\mathbf{G}_2(i,i)|^2 P_t/T}{v_i} \\ &\geq \frac{\nu_i k_i|\mathbf{G}_2(i,i)|^2 P_t/T}{\|\mathbf{h}_{i,2}\|^2\frac{P_r\sigma_1^2}{\nu_i P_t/T+\sigma_1^2}+\sigma_2^2}. \end{aligned} \tag{4.19}$$

This gives a lower bound to the receive SNR and hence leads to a lower bound of the sum capacity of the system. □

This bound captures the effect of noise amplification for the second link's transmission. The denominator of the SNR does not depend on the relay power allocation to the other streams.

A Greedy Reduced Complexity User Selection Algorithm When the number of users N_u is large or M_u is large, it is costly to search over the permutations of all users. It is of interest to study a user selection algorithm to determine a permutation of the M_u users out of all the users. The algorithm proposed here is a modification to the algorithm in [34][114]. The metric for user selection is based on the lower bound to the SNR in (4.16). The set of users is denoted by $\mathcal{U} = \{1, 2, ..., N_u\}$. We elaborate the selection algorithm here (the description follows [114]).

Algorithm 1: Reduced Complexity User Selection

1. **Initialization**

   - Set $n = 1$.
   - Let $r_{1,u} = \frac{\|\mathbf{h}_{u,2}\|^2}{\|\mathbf{h}_{u,2}\|^2 \frac{P_r \sigma_1^2}{\nu_1 P_t / M_u + \sigma_1^2} + \sigma_2^2}$. Find a user s_1 such that $s_1 = \arg\max_{u \in \mathcal{U}} r_{1,u}$.
   - Let $S_1 = \{s_1\}$.

2. **While** $n \leq M_u$**:**

- Increase n by 1.
- Project each remaining channel vector onto the orthogonal complement of the subspace spanned by the channels of the selected users. The projection matrix is

$$\mathbf{P}_n^{\perp} = \mathbf{I}_{M_r} - \mathbf{H}_2(S_{n-1})^H(\mathbf{H}_2(S_{n-1})\mathbf{H}_2(S_{n-1})^H)^{-1}\mathbf{H}_2(S_{n-1}) \quad (4.20)$$

  where $\mathbf{I}_{M_r}$ is the $M_r \times M_r$ identity matrix, and $\mathbf{H}_2(S_{n-1})$ denotes the row-reduced channel matrix consisting of the channel vectors of the users selected in the first $n-1$ steps

$$\mathbf{H}_2(S_{n-1}) = [\mathbf{h}_{s_1,2}, ..., \mathbf{h}_{s_{n-1},2}]^T. \quad (4.21)$$

  Let $\tau_{n,u} = \|\mathbf{h}_{u,2}^T \mathbf{P}_n^{\perp}\|^2$.
- Find a user s_n such that

$$s_n = \arg\max_{u \in \mathcal{U} \backslash S_{n-1}} \frac{\tau_{n,u}}{\|\mathbf{h}_{u,2}\|^2 \frac{P_r \sigma_1^2}{\nu_n P_t / M_u + \sigma_1^2} + \sigma_2^2}. \quad (4.22)$$

- Set $S_n = S_{n-1} \cup \{s_n\}$

3. **Perform the optimization in (4.15).**

This algorithm aims to select a group of M_u users who have good channel conditions. It has been shown in [34] that using this user selection algorithm with zero-forcing dirty paper coding provides a sum rate that is very close to the sum capacity of the MIMO broadcast channel. We illustrate the performance gain of the proposed user selection algorithm in the simulations.

Equal Power Allocation with Water-filling at the Relay After the desired set of users have been determined, we propose an algorithm for the relay design when equal power allocation is used. We first assume that M_u streams are used in the system. The optimization problem that determines the relay power vector $\mathbf{k}$ is the following

$$\begin{aligned} &\min_{\mathbf{k}} -\tfrac{1}{2}\sum_{i=1}^{M_u}\log_2(1+c_i k_i) \\ &\sum_{i=1}^{M_u} k_i(\nu_i P_t/M_u+\sigma_1^2) \le P_r \\ &k_i \ge 0 \quad \forall i. \end{aligned} \tag{4.23}$$

Let us denote $m_i = \nu_i P_t/M_u + \sigma_1^2$. Using Lagrangian methods, the solution to this problem is water-filling according to

$$k_i = \frac{1}{m_i}\left(\mu - \frac{m_i}{c_i}\right)^+, \quad i = 1, ..., M_u, \tag{4.24}$$

$$\sum_{i=1}^{M_u} m_i k_i = P_r, \tag{4.25}$$

where μ is a constant and $(x)^+$ is defined as

$$(x)^+ = \begin{cases} x & \text{if} \quad x \ge 0 \\ 0 & \text{if} \quad x \le 0 \end{cases}. \tag{4.26}$$

When k_i is determined to be 0 for some streams, we want to conserve power for these channels. The number of streams T can be recomputed as $T = \sum_{i=1}^{M_u} I\{k_i > 0\}$, where $I\{\cdot\}$ is the indicator function. The group of users are identified as $S = \{t_1, ..., t_T\}$ from the M_u users, where $t_i \in \{1, 2, ..., M_u\}$. With this selection of S, we perform the QR decomposition to the matrix

$\mathbf{H}_2(S)$ and we have $\mathbf{H}_2(S) = \mathbf{G}_2(S)\mathbf{Q}_2(S)$. An optimization is formulated as

$$\begin{aligned} &\min_{\mathbf{k}} -\tfrac{1}{2}\sum_{i=1}^{T}\log_2(1+\tilde{c}_i k_i) \\ &\sum_{i=1}^{T} k_i(\nu_i P_t/T+\sigma_1^2) \le P_r, \quad k_i \ge 0 \quad \forall i, \end{aligned} \tag{4.27}$$

where $\tilde{c}_i$ is defined as $\tilde{c}_i = \frac{\nu_i |\mathbf{G}_2(S)(i,i)|^2 P_t/T}{\|\mathbf{h}_{i,2}\|^2 \frac{P_r\sigma_1^2}{\nu_i P_t/T+\sigma_1^2}+\sigma_2^2}$. This optimization problem can be solved using the water-filling algorithm, which provides the optimum solution for the relay coefficients $\mathbf{k}$. In summary, the proposed procedure for the relay design involves a two-step water-filling.

4.3.4 A Sum Rate Upper Bound for the Proposed Relaying Strategies

The ergodic capacity of the MIMO channel, which we denote by $C_1(\mathbf{H}_1)$, can be derived from the following optimization

$$\begin{aligned} &\max_{\mathbf{Q}} \log_2 |\mathbf{I}+\tfrac{1}{\sigma_1^2}\mathbf{H}_1\mathbf{Q}\mathbf{H}_1^H| \\ &\text{s.t.} \quad \mathbf{Q}\succeq\mathbf{0}, \quad \mathrm{Tr}\{Q\}\le P_t. \end{aligned} \tag{4.28}$$

The optimum solution is given by water-filling [2]. An upper bound of the sum rate for the proposed algorithms is presented in the following proposition.

Proposition 6. When the direct connection between the BS and the users is neglected, an upper bound of the sum rate of the non-decode-and-forward relaying is $\frac{1}{2}C_1(\mathbf{H}_1)$.

Proof. We assume that the channel state information $\mathbf{H}_1$ and $\mathbf{H}_2$ is perfectly known. The mutual information of the signal vector transmitted by

the base station $\mathbf{s}$ and the signal vector transmitted by the relay $\tilde{\mathbf{s}}$ is denoted by $I(\mathbf{s};\tilde{\mathbf{s}})$. The mutual information of $\mathbf{s}$ and the received signal at all users is $I(\mathbf{s};x_1,...,x_{N_u})$. By the data processing inequality [9], we have $I(\mathbf{s};x_1,...,x_{N_u}) \leq I(\mathbf{s};\tilde{\mathbf{s}})$. Hence the average sum rate of the non-decode-and-forward relaying is upper bounded by the ergodic capacity of the MIMO channel normalized by the time-sharing factor $\frac{1}{2}$, i.e., $\frac{1}{2}C_1(\mathbf{H}_1)$. □

4.3.5 Maximum Sum Rate of Decode-and-Forward Relaying

The capacity of the second link $C_2(\mathbf{H}_2)$, which is the MIMO broadcast channel, can be derived from the following optimization

$$\max_{\mathbf{D}\in\boldsymbol{\mathcal{A}}} \log_2 |\mathbf{I} + \tfrac{1}{\sigma_2^2}\mathbf{H}_2^H\mathbf{D}\mathbf{H}_2| \tag{4.29}$$

where $\boldsymbol{\mathcal{A}}$ is the set of $N_u \times N_u$ diagonal matrices with $\mathrm{Tr}\{D\} \leq P_r$ [18].

For comparison, we compute the sum rate of decode and forward relaying. Let the time-sharing factor be t $(0 \leq t \leq 1)$, we have an achievable rate for the decode and forward scheme as

$$\begin{aligned} R_{df}(t) &= \min\{tC_1(\mathbf{H}_1),(1-t)C_2(\mathbf{H}_2)\} \\ &= \begin{cases} tC_1(\mathbf{H}_1) & \text{if } \ t \leq \frac{C_2(\mathbf{H}_2)}{C_1(\mathbf{H}_1)+C_2(\mathbf{H}_2)}, \\ (1-t)C_2(\mathbf{H}_2) & \text{otherwise.} \end{cases} \end{aligned} \tag{4.30}$$

The maximum sum rate of decode-and-forward relaying (denoted by C_{df}), is thus

$$\begin{aligned} C_{df} &= \max_{0\leq t\leq 1} R_{df}(t) \\ &= \frac{C_1(\mathbf{H}_1)C_2(\mathbf{H}_2)}{C_1(\mathbf{H}_1)+C_2(\mathbf{H}_2)}. \end{aligned} \tag{4.31}$$

This is the best achievable sum rate for the decode and forward relaying, neglecting the direct link between the base station and the users. We will compare this result with the sum rates derived from the proposed relaying schemes in the simulations. Another comparison is made between the proposed relaying schemes and the minimum of the first and the second link capacity $\frac{1}{2}\min\{C_1(\mathbf{H}_1), C_2(\mathbf{H}_2)\}$. This method is named "Equal-time-sharing Decode-and-forward".

4.4 An Implementation of the MIMO Fixed Relay System

In the previous section, we discussed sum rate bounds based on dirty paper coding. Though information theoretic coding techniques are not implementable in real systems, the proposed relay structures and the concept of using dirty paper coding can be adopted. In this section, we address transceiver design aspects of the MIMO fixed relay system. We first compare the complexity of the MIMO fixed relay system using linear processing with a decode-and-forward relaying model and then discuss feedback of channel state information. These aim to demonstrate the feasibility of the proposed relaying architecture. Then we propose a relay design using Tomlinson-Harashima precoding (THP) [26] as a specific transceiver solution for the system. Using THP follows the idea of zero-forcing dirty paper coding [26], and is implementable in the communication systems. The proposed THP architecture also combines adaptive modulation with square M-QAM modulation and adaptive stream selection

based on instantaneous channel conditions.

4.4.1 Comments on Complexity Reduction at the Relay

The proposed MIMO fixed relay system only requires linear processing on the downlink signal. We compare the complexity of the relay station for the proposed system and a decode and forward relaying system (concatenated system) as illustrated in Fig. 4.2.

The decode-and-forward relaying system concatenates the MIMO transmission from the base station (BS) to the relay station (RS) and the MIMO broadcast transmission (MIMO BC) from the RS to the users. The BS performs MIMO encoding based on the channel information of the link between the BS and the RS. The RS decodes the signal from the base station and performs scheduling for the users' that are within the coverage of the RS. Then it encodes the data for the selected users and broadcasts it using MIMO broadcast channel coding, e.g., dirty paper coding. We assume that MIMO transmission from the BS to the RS is conducted on the eigen-modes of the channel. This requires matrix multiplications at the BS and at the RS using the unitary matrices decomposed from the SVD of the MIMO channel matrix. The complexity of the relay for the proposed system and the concatenated system is compared in the following table. From Table 4.1, we observe that the complexity of the RS is significantly lower for the proposed system compared to the concatenated system.

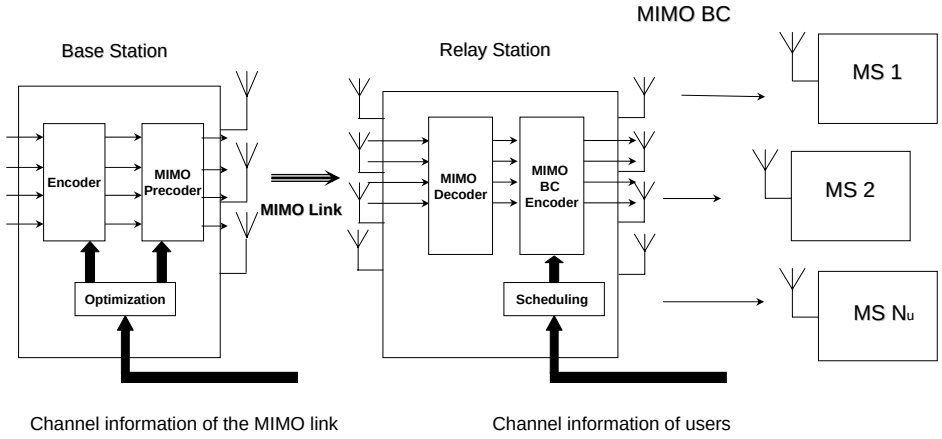

Figure 4.2: A MIMO relay system that concatenates a MIMO channel and a MIMO broadcast channel. At the base station, the encoder performs error correction coding and modulation. At the relay, MIMO decoding is done along with decoding of the error correction code. The MIMO BC encoder performs error correction coding, dirty paper coding and MIMO precoding along with adaptive modulation coding.

Table 4.1: Complexity Comparison of the RS

RS Operation Items	Proposed System	Concatenated System
Matrix Computation	Yes (matrix multiplication)	Yes (SVD operation)
Error decoding (e.g.,Turbo decoding)	No	Yes (high complexity)
Multiuser BC encoding (e.g.,dirty paper coding)	No (BS takes this functionality)	Yes (high complexity)
Scheduling (user selection and adaptive modulation and coding)	Maybe (May use additional scheduling at the BS)	Yes (high complexity)

4.4.2 Feedback of Channel State Information

To design the relay parameters, channel information between the users and the relay and between the relay and the BS is required. We study two scenarios where either the BS performs the optimization or the relay performs the optimization to determine the relaying matrix and the precoding matrix. We propose operational procedures for these scenarios.

In the first scenario, we assume that channel information between the users and the relay and between the relay and the BS can be collected at the BS, and the BS makes centralized decision to determine the relay matrix and the precoding matrix. The relay may use channel reciprocity or a feedback mechanism to convey information about these parameters. For example, the base station sends a channel information inquiry to the mobile users, and the mobile users send the information to the relay; the relay then forwards the data to the base station. A well-known approach for feedback is using vector quantization or limited feedback [13][115]. Each user sends back its channel information in a quantized format. Another method for feedback is via uplink channel sounding. Users feed back their sounding waveforms in the uplink message [116]. In our initial study, we assume that perfect channel information is available at the base station. Once the optimal relay processing coefficients are determined, the base station may configure the relay via downlink signalling.

In the second case, the relay collects the channel information from the mobile users using quantized feedback or uplink channel sounding. It can also

measure the channel between the BS and the relay. Optimization is carried out in the relay. When the precoding matrix is computed, the relay feeds back this quantity to the BS. The relay also configures the relaying matrix using the optimum solution from the optimization. When the number of mobile users is large, feedback of exact channel information between the relay and mobiles users may become a significant overhead. In the second case, channel information between the relay and the mobile users do not need to be fed back to the BS from the relay. Therefore, the amount of feedback from the relay to the BS in the second case is much lower than the first case for large number of mobile users.

4.4.3 Multiuser Tomlinson-Harashima Precoding for Fixed Relay Systems

In this subsection, we discuss adopting Tomlinson-Harashima precoding (THP) in the fixed relay system. We also utilize adaptive modulation with square M-QAM modulation, which works with THP, to maximize the sum spectral efficiency. We call this scheme Tomlinson-Harashima precoding with adaptive modulation (THP-AMC). For simplicity, we do not consider forward error coding for this scheme.

The diagram of the THP is illustrated in Fig. 4.3. We focus on the implementation of the THP along with the SVD based designs at the relay. A feedback loop is employed at the base station to perform the Tomlinson-

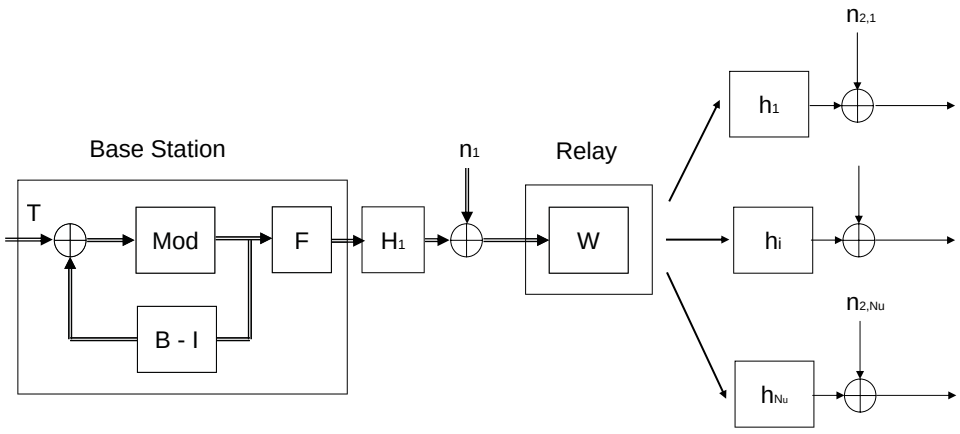

Figure 4.3: The multiuser MIMO relay system using Tomlinson-Harashima precoding.

Harashima precoding. It is constructed based on the following factorization

$$\mathbf{B} = \mathbf{D}_2\mathbf{G}_2 \tag{4.32}$$

where $\mathbf{D}_2$ is a diagonal matrix $\mathbf{D}_2 = \text{diag}\{\mathbf{G}_2(1,1)^{-1}, ..., \mathbf{G}_2(M_u, M_u)^{-1}\}$. This guarantees that the diagonal elements of the matrix $\mathbf{B}$ are ones.

We select the users using the algorithm described in Section 4.3.3. This algorithm significantly lowers the complexity of user selection. In this section, we focus on the algorithms that adaptively determine the QAM modulation of this system.

Given M_u selected users, we assume that equal power is allocated to the input streams of the THP. To simplify the implementation complexity, we do not use different power-loading for the streams in this system. Thus the signal to noise ratio at the i^{th} receiver can be derived as

$$\eta_i = \frac{\bar{d}_i P_t}{M_u v_i}. \tag{4.33}$$

Using the TH precoder enables the base station to multicast data streams to different users. The symbol error rate (SER) with M-QAM modulation for THP can be approximated as [26]

$$\mathrm{SER}_i \approx K_i Q\left(\sqrt{\frac{3\eta_i}{2^{R_i}}}\right) \tag{4.34}$$

where R_i denotes the data rate when the QAM with size $M_i = 2^{R_i}$ is used. Notice that a factor $(\frac{2^{R_i}}{2^{R_i}-1})$ is contained in the SER expression to account for the power penalty of using THP [26]. Here K_i denotes the number of nearest neighbors associated with the periodic extended QAM constellation, and $K_i = 4$ for $M_i \geq 4$. For user i, a target SER is specified as SER_i^t. The condition that $\mathrm{SER}_i \leq \mathrm{SER}_i^t$ is equivalent to $\mathrm{SNR}_i = \frac{3\eta_i}{2^{R_i}} \geq \mathrm{SNR}_i^t$, where SNR_i^t is the target SNR for the i^{th} user. This implies that

$$\begin{aligned} R_i &\leq \log_2\left(\frac{3\eta_i}{\mathrm{SNR}_i^t}\right) \\ &= \log_2(\eta_i) + \log_2(3) - \log_2(\mathrm{SNR}_i^t). \end{aligned} \tag{4.35}$$

Hence the sum rate is bounded by

$$\frac{1}{2}\sum_{i=1}^{M_u} R_i \leq \frac{1}{2}\sum_{i=1}^{M_u} \log_2(\eta_i) + \frac{M_u}{2}\log_2(3) - \frac{1}{2}\sum_{i=1}^{M_u} \log_2(\mathrm{SNR}_i^t), \tag{4.36}$$

where the QAM constellation set is restricted to be $\mathcal{M} = \{1, 2, 4, 16, 64, 256, 1024\}$, hence the rate set $\mathcal{R}_{\mathcal{T}} = \{0, 1, 2, 4, 8, 16, 32\}$.

Clearly, by maximizing the quantity $\sum_{i=1}^{M_u} \log_2(\eta_i)$, we may have higher sum rate. For simplicity of computation, we design the relay coefficients by maximizing the capacity lower bound $\sum_{i=1}^{M_u} \log_2(\eta_i^{(l)})$. This formulation leads to a closed-form solution that can be easily computed.

The optimization problem is formulated as

$$\begin{aligned} &\min_{\mathbf{k}} -\tfrac{1}{2} \textstyle\sum_{i=1}^{M_u} \log_2(c_i k_i) \\ &\text{s.t.} \quad \textstyle\sum_{i=1}^{M_u} k_i(\nu_i P_t/M_u + \sigma_1^2) \le P_r, \quad k_i \ge 0 \quad \forall i. \end{aligned} \tag{4.37}$$

The closed-form solution to this problem is given as $k_i = \frac{P_r}{M_u m_i}$, where $m_i = \nu_i P_t/M_u + \sigma_1^2$.

After we find the optimum $\mathbf{k}$, the rate for the i^{th} user is obtained by truncating $\log_2(\eta_i) + \log_2(3) - \log_2(\text{SNR}_i^t)$ to the nearest point on the feasible rate set $\mathcal{R}_T$ that is no greater than $\log_2(\eta_i) + \log_2(3) - \log_2(\text{SNR}_i^t)$.

We may obtain $R_i = 0$ for some stream. It implies that this user's channel supports no suitable QAM modulation. Therefore, we may drop this stream and update the total number of streams (T) that will be simultaneously served by the base station. Notice that initially $T = M_u$. The entire algorithm is described as follows

Algorithm 2: THP-AMC

Select S (the set of user indices with M_u users) based on the algorithm in Section 4.3.3,

and **let** $T = M_u$.

While Not $(R_i > 0, \forall i \in S)$ or (S is empty)

Update $T \leftarrow \sum_{i=1}^{T} I\{R_i > 0\}$;

Update $S \leftarrow \forall i \in S, R_i > 0$ while preserving the user ordering in the S.

Perform (4.37) with the updated S and T;

Determine R_i by the truncation;

End

Some remarks are given on the multiuser Tomlinson-Harashima precoding in the fixed relay systems.

- The architecture does not require the decoding operation at the relay. The encoding and decoding are carried at the ends — the base station and the users. Therefore, the implementation complexity and the processing latency can be significantly lowered compared to the conventional decode and forward strategy.

- The users are selected by the reduced complexity algorithm (Algorithm 1 in Section 4.3). This is much simpler than an exhaustive search over the entire user set.

- Adaptive modulation is proposed to load the spatial streams of the TH precoder. The number of streams and the QAM modulation are both dynamically selected based on the channel state information.

- The TH precoder is a general architecture for downlink broadcast channel. It can be shared by non-relaying users and the relaying users.

4.5 Simulation Results

We assume that the channel between the BS and the relay $\mathbf{H}_1$ and the channel between the relay and the mobile users $\mathbf{H}_2$ follow i.i.d. complex Gaussian distribution with zero mean and variances α and 1 respectively. The Monte Carlo simulations are conducted in MATLAB. The parameters for the simulations are described in the captions of the simulation results. The parameter α represents the path loss for the first MIMO link. We set it to be 0.05 in the simulations. The total transmit power at the base station is P_t and the total power at the relay is P_r. We set $P_t = P_r = 1$ in the simulations. Here the signal to noise ratio SNR's are defined as $\text{SNR}_1 = \frac{\alpha P_t}{\sigma_1}$ and $\text{SNR}_2 = \frac{P_r}{\sigma_2}$, respectively, representing the average receive SNR's at the receive antennas. The parameters σ_1 and σ_2 are the noise variances. In the simulations, we make the quantities SNR_1 and SNR_2 equal to each other. This implies that the path losses are the same for the first and the second link.

In the simulations, we first compare the sum rate of the relaying strategies with the upper bound derived earlier. We illustrate the sum rate of the proposed schemes in Fig. 4.4. For this result, ten simulations are performed and each of the simulation is averaged over 100 channel realizations. We illustrate the means of the 10 data samples obtained from the simulations versus the SNR. The standard deviations are also computed with these data samples

and are illustrated in the figure. The proposed two algorithms (all pass relay design and SVD relay design) give sum rate performance that is close to the upper bound derived earlier. The SVD relay design outperforms the all pass relay design by having more degrees of freedom in designing the relay. When the capacity of the second link becomes higher than the first link, the performance gap of the decode-forward and the upper bound increases. The reason is that using optimal time sharing, a larger portion of time is allocated to the poor link. This eases the bottle neck effects caused by the poor link. We also compare the achievable sum rates of the proposed relay designs with the rate achieved by $\frac{1}{2}\min\{C_1(\mathbf{H}_1), C_2(\mathbf{H}_2)\}$ (equal-time-sharing decode-and-forward). The performance gap between the proposed schemes and the equal-time-sharing decode-and-forward method is not significant as the SNR increases.

To observe the sum rate increase with multiple antennas, we fix equal number of transmit antennas at the base station and receive antennas at the relay. For this result, we also perform ten simulations and each of the simulation is averaged over 100 channel realizations. From Fig. 4.5, we observe that the average capacities of the proposed schemes increase with the number of antennas as expected for all schemes. The performance gap between the SVD based design and the relay water-filling algorithm, however, increases with the number of antennas. The sum rate of the relay design that uses equal power transmission at the BS with relay water-filling is close to the SVD based design. It is a good strategy to use equal power allocation at the base station

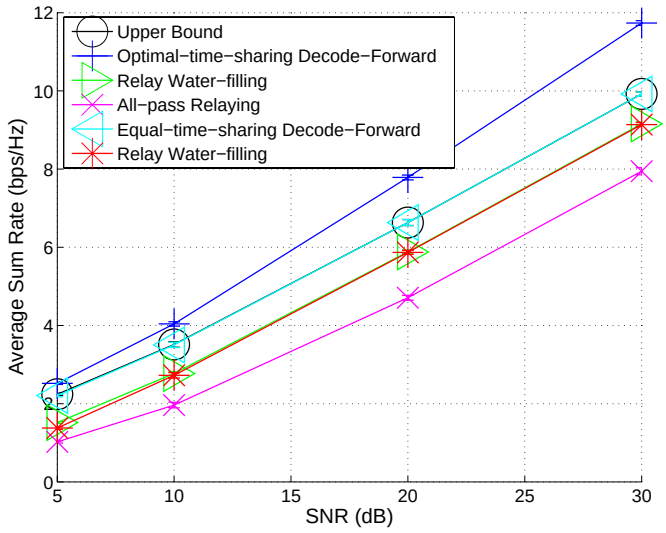

Figure 4.4: Sum rate vs. SNR of the proposed schemes for the number of antennas at the BS $M_b = 2$, the number of antennas at the RS $M_r = 3$ and the number of users $N_u = 5$.

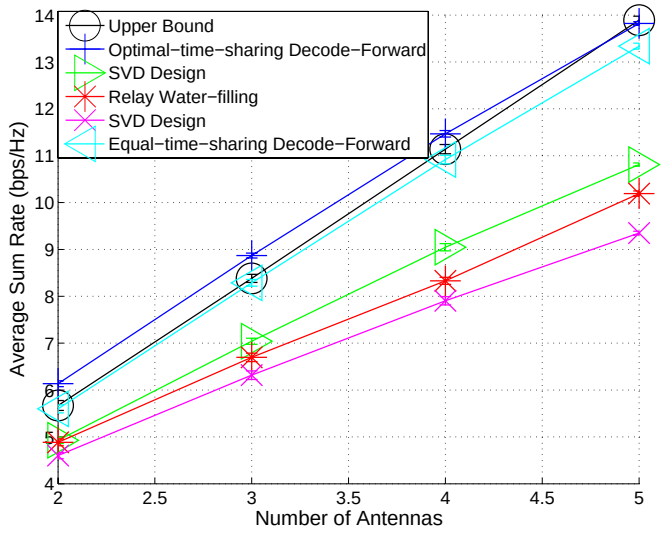

Figure 4.5: Sum rate vs. number of antennas of the proposed schemes vs. the number of antennas at the relay for $M_b = M_r$ (the BS and the RS have equal number of antennas), the number of users $N_u = 5$ and the signal to noise ratio for the first and second link SNR $= 20dB$.

and only allocate power of the relay based on the channel conditions.

For the rest of the results, we conduct Monte Carlo simulations over 200 channel realizations for one time. Because the standard deviation is very small as observed from the previous experiments with 100 channel realizations for each simulation, we avoid the extensive simulation execution for computing the standard deviations over data samples.

We simulate the performance of the relaying THP with adaptive modulation. The sum rate of this scheme is compared with the information theoretic sum rates as illustrated in Fig. 4.6. This characterizes the average sum spectral efficiency of the relaying THP. The target symbol error rates for all streams

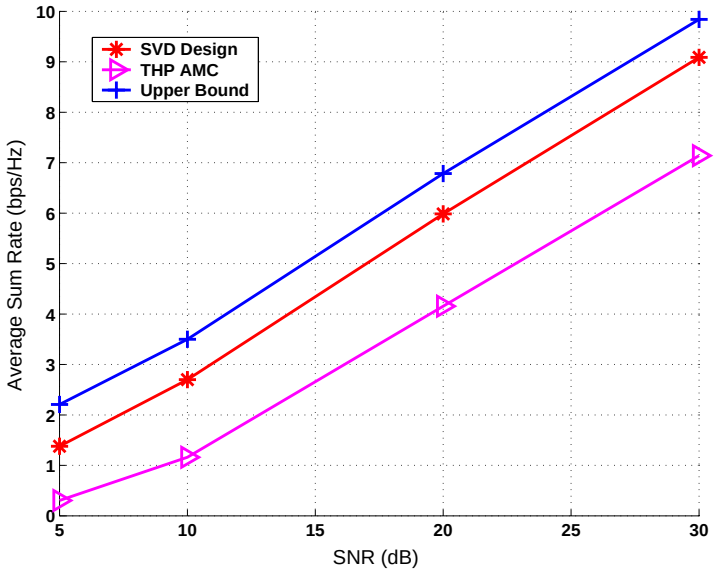

Figure 4.6: The performance of the Tomlinson-Harashima precoding with adaptive modulation and stream selection in the fixed relay system for the number of antennas at the BS $M_b = 2$, the number of antennas at the RS $M_r = 3$ and the number of users $N_u = 5$. The target SER is 10^{-2} for all users.

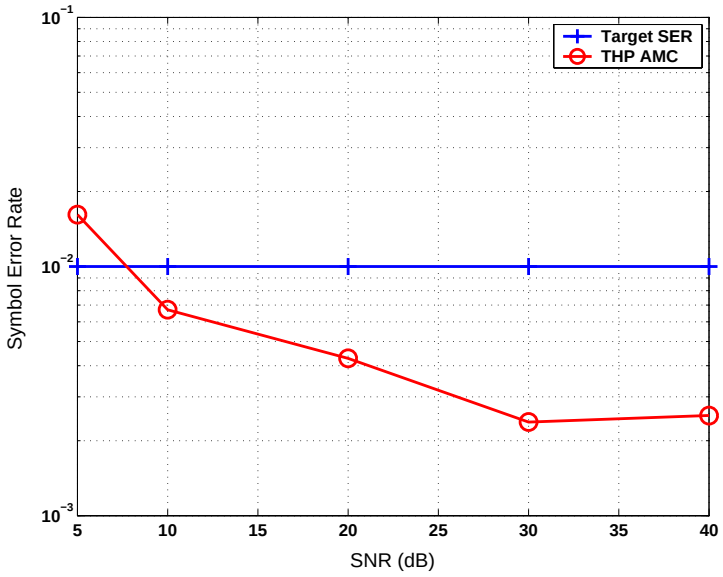

Figure 4.7: The symbol error rate performance of the Tomlinson-Harashima precoding with adaptive modulation and stream selection in the fixed relay system for the number of antennas at the BS $M_b = 2$, the number of antennas at the RS $M_r = 3$ and the number of users $N_u = 5$.

are set to be 10^{-2} in this experiment. The sum rate gap arises from the use of discrete QAM modulation. We perform Monte Carlo simulation to study the SER performance. The SER is controlled to be less than the target SER from Fig. 4.7. This shows that the adaptation meets the SER requirements in most of the SNR region.

We plot the sum rate vs. the number of users in Fig. 4.8. The sum rate increases with the number of users. The user selection algorithm captures good multiuser diversity gain in this scenario. We also observe that the rate adaptation based on the reduced complexity user selection algorithm and the THP with AMC is a good strategy to achieve good multiuser diversity gain.

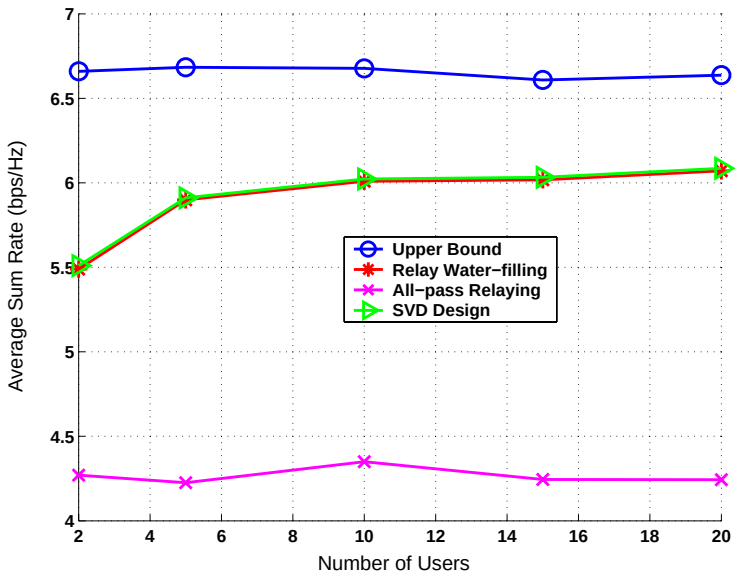

Figure 4.8: Sum rate vs. number of users of the proposed schemes for the number of antennas at the BS $M_b = 2$ and the number of antennas at the relay $M_r = 3$. The SNR is fixed to be 20 dB for both links.

4.6 Summary of Contributions

In this chapter, we investigated the design problem of using two hop transmission through one non-decode-and-forward MIMO fixed relay for coverage enhancement in cellular networks. The relay uses linear signal processing to process the received signal and forward it to multiple users. This relaying strategy leverages MIMO technology to achieve high spectral efficiency and it does not require decoding and re-encoding of the real-time data at the relay. We studied the scenario where both the base station and the relay employ multiple antennas and each mobile user has one antenna.

Our study on this system was performed in both the information theoretics and the transceiver design. This provides a comprehensive solution for engineering the MIMO fixed relay system. We proposed upper and lower bounds on the achievable sum rate for this architecture assuming zero forcing dirty paper coding at the base station, neglecting the direct links from the base station to the users, and with certain structure in the relay. Motivated by the relay designs that are used to derive the achievable sum rate in the information theoretics, we also proposed an implementable system architecture. This architecture combines Tomlinson-Harashima precoding with adaptive modulation to adaptively determine the number of transmit streams and the QAM modulation. We also discussed solutions for feedback of channel information in the proposed systems. Through extensive simulations, we observed that the proposed system achieves sum rate performance that is close to decode-and-forward relaying though decoding is not required at the relay.

Chapter 5

Conclusions and Future Work

Using multiple antennas in the downlink of cellular systems has been well recognized as a promising means to enhance the system capacity. Designing the multiple antenna downlink, however, is a challenging task. This dissertation studied the design issues at both the physical layer and medium access layer for this system. In particular, three problems concerned with feedback reduction, interference suppression and relay-aided broadcast were investigated.

Chapter 2 presented a solution on scheduling and feedback reduction in the MIMO downlink. Multiuser diversity based scheduling requires feedback of channel information from the mobile users to the base station. The limited amount of resource in the uplink feedback channel, however, poses challenges on implementing feedback strategies for a large number of users. This chapter studied scheduling for the spatial multiplexing system with linear receivers. This decouples the downlink MIMO channel into multiple parallel spatial channels. The proposed strategy uses a contention based feedback for each spatial channel. Feedback is controlled by two parameters, i.e., a channel quality threshold and a feedback probability. The tail mass of users' channel distri-

butions is used as the channel quality threshold. Using this channel quality metric achieves temporal fairness for this system. Iterative algorithms were proposed to select the feedback parameters to maximize the sum throughput of the downlink.

Per-antenna scheduling in the multiple antenna downlink is simple to implement and it achieves a promising sum throughput for the downlink. This strategy, however, does not take advantages of precoding with multiple antennas. Optimum precoding strategy at the base station requires the channel state information of all users. Combining precoding with a contention based feedback strategy looks like a promising research direction.

Chapter 3 presented the design of a space-time receiver that uses multiple antennas to suppress the asynchronous interference from other cells in the OFDM downlink. The receiver uses a two stage interference suppression in the time domain and frequency domain to combat the asynchronous interferences. Design algorithms that configure the equalizer coefficients in the time domain and the frequency domain are proposed under the assumptions of perfect channel information or with training sequences. The formulation took both the error rate and capacity into consideration. For the training based system design, a novel algorithm that estimates the frequency offsets using training sequences was proposed.

The computation cost associated with equalizer design and frequency offset estimation for the receiver studied in this chapter may be expensive for real-time implementations. Future work will focus on reducing the implemen-

tation cost of the design algorithms. Literature on real-time equalization in digital subscriber line (DSL) systems may give sights on the implementation issue of this receiver.

The proposed receiver is a multiple antenna linear receiver designed for frequency selective channels with cochannel interference. It supports per-antenna based transmission. Clearly, the proposed framework in Chapter 2 for MIMO scheduling and feedback with linear receivers can be applied to this system. Another future direction is to evaluate the receiver design from an overall downlink throughput perspective.

Chapter 4 proposed a novel relay-aided broadcast system that uses fixed relays with linear signal processing. This system is designed to improve coverage for users under heavy signal attenuation. The system design problem was approached from both the information theoretic perspective and the transceiver design perspective. Results on lower and upper bounds of achievable sum rates were presented in this chapter. Reduced complexity algorithms are proposed to compute the bounds. From an implementation perspective, a Tomlinson-Harashima precoding strategy with adaptive QAM modulation and stream selection is proposed. The adaptive solution is simple and allows useful performance improvement for this system.

The results in Chapter 4 are for the relay system design with single receive antenna at each user. Generalizing this work to the multiple receive antenna case is a future research direction. Assuming linear precoding is used at both the base station and the relay, this system resembles the broadcast

system studied in Chapter 2. Henceforth, another aspect is to study the relay-aided broadcast with the feedback schemes as proposed in Chapter 2 as the future work.

This dissertation studied three design problems of multiple antenna downlink. The proposed solutions enhance throughput or error rate performance of the downlink system. These solutions can be applied to existing or future cellular communication systems such as the IEEE 802.16 systems.

Appendices

Appendix A

Appendix of Chapter 2

A.1 Derivation of the Average Sum Rate Expression

We use binary random variable S_j to denote the event that the j^{th} user is selected at the base station on the first spatial channel. When S_j takes 1, the j^{th} user is selected. We denote the number of users whose channel quality on the first channel is below the threshold η_1 by T. Thus the conditional probability that the base station captures one or more feedback packets in any of the feedback minislots given $\boldsymbol{\xi}_1 = \mathbf{x}$ can be represented as

$$P_c(T) = \sum_{u=1}^{\min\{M_t,T\}} \left(\begin{array}{c} T \\ u \end{array} \right) p_1^u (1-p_1)^{T-u} \tag{A.1}$$

where $T = \sum_{u=1}^{N} I\{\alpha_{1,u} > \eta_1\}$ and $I\{\cdot\}$ denotes the indicator function.

Thus the conditional probability of $S_j = 1$ given $\boldsymbol{\xi}_1 = \mathbf{x}$ is

$$\begin{aligned} P\{S_j = 1 | \boldsymbol{\xi}_1 = \mathbf{x}\} &= \frac{1}{T}(1 - [1 - P_c(T)]^K) I\{T > 0, \alpha_{1,j} < \eta_1\} \\ &+ \frac{1}{N}[1 - P_c(T)]^K I\{0 \le T \le N-1, \alpha_{1,j} \ge \eta_1\} \end{aligned} \tag{A.2}$$

Notice that the first term in the summation represents the probability of the j^{th} user being selected given its channel quality is below the threshold through the random access. The second term gives the probability of the j^{th} user

being selected given its channel quality is above the threshold. In this case, it is selected due to random selection at the base station when all feedback packages collide through all minislots or the channel quality of all users are above the threshold.

Based on (2.5) and (A.2), the joint probability density function of $\xi_{1,j}$, S_j and T (here, T represents a random variable) can be derived as

$$\begin{aligned} P_d\{\xi_{1,j} = x, S_j = 1, T = m\} &= f_{\xi_{1,j}}(x)\bar{P}(m)I\{m > 0, \alpha < \eta_1\} + f_{\xi_{1,j}}(x) \\ &\times \underline{P}(m)I\{0 \le m \le N-1, \alpha \ge \eta_1\} \end{aligned} \tag{A.3}$$

where

$$\bar{P}(m) = \left(\begin{array}{c} N-1 \\ m-1 \end{array} \right) \eta_1^{m-1}(1-\eta_1)^{N-m}\{\frac{1}{m}(1-[1-P_c(m)]^K) + \frac{1}{N}[1-P_c(m)]^K\} \tag{A.4}$$

$$\underline{P}(m) = \left(\begin{array}{c} N-1 \\ m \end{array} \right) \eta_1^{m}[1-\eta_1)]^{N-m-1}\frac{1}{N}[1-P_c(m)]^K \tag{A.5}$$

where $\alpha = 1 - F_{\xi_{1,j}}(x)$. Also we have $x = F^{-1}_{\xi_{1,j}}(1-\alpha)$.

Based on the probability density function in (A.3), the average system capacity of the first spatial channel can be derived as

$$\begin{aligned} C(p_1, \eta_1) &= \sum_{j=1}^{N} C_j(p_1, \eta_1) \\ &= \sum_{j=1}^{N} E[\log_2(1+\xi_{1,j})I\{S_j = 1\}] \\ &= \sum_{j=1}^{N} (\bar{C}_j(p_1, \eta_1) + \underline{C}_j(p_1, \eta_1)) \end{aligned} \tag{A.6}$$

where $C(p_1, \eta_1)$ represents the average sum rate on the first spatial channel, parameterized by p_1 and η_1. Based on (A.3), we have $\bar{C}_j(p_1, \eta_1) = \bar{R}_j \sum_{m=1}^{N} \bar{P}(m)$ and $\underline{C}_j(p_1, \eta_1) = \underline{R}_j \sum_{m=0}^{N-1} \underline{P}(m)$.

A.2 Derivative Expression of the Average Sum Rate

$$\frac{\partial \bar{C}_j}{\partial p_1} = -\bar{R}_j \sum_{m=1}^{N} \left(\begin{array}{c} N-1 \\ m-1 \end{array} \right) \eta_1^{m-1} (1-\eta_1)^{N-m} K (\frac{1}{N} - \frac{1}{m}) [1-P_c(m)]^{K-1} \frac{\partial P_c(m)}{\partial p_1}, \tag{A.7}$$

$$\frac{\partial \underline{C}_j}{\partial p_1} = -\underline{R}_j \sum_{m=0}^{N-1} \left(\begin{array}{c} N-1 \\ m \end{array} \right) \eta_1^{m} (1-\eta_1)^{N-m-1} \frac{K}{N} [1-P_c(m)]^{K-1} \frac{\partial P_c(m)}{\partial p_1}, \tag{A.8}$$

$$\begin{aligned} \frac{\partial \bar{C}_j}{\partial \eta_1} &= \frac{\partial \bar{R}_j}{\partial \eta_1} \sum_{m=1}^{N} \left(\begin{array}{c} N-1 \\ m-1 \end{array} \right) \eta_1^{m-1} (1-\eta_1)^{N-m} \\ &\times \{\frac{1}{m} + (\frac{1}{N} - \frac{1}{m})[1-P_c(m)]^K\} \\ &+ \bar{R}_j \sum_{m=2}^{N} \left(\begin{array}{c} N-1 \\ m-1 \end{array} \right) (m-1) \eta_1^{m-2} (1-\eta_1)^{N-m} \{\frac{1}{m} + (\frac{1}{N} - \frac{1}{m})[1-P_c(m)]^K\} \\ &- \bar{R}_j \sum_{m=1}^{N-1} \left(\begin{array}{c} N-1 \\ m-1 \end{array} \right) (N-m) \eta_1^{m-1} (1-\eta_1)^{N-m-1} \\ &\times \{\frac{1}{m} + (\frac{1}{N} - \frac{1}{m})[1-P_c(m)]^K\}, \end{aligned} \tag{A.9}$$

$$
\begin{aligned}
\frac{\partial \underline{C}}{\partial \eta_1} &= \frac{\partial \underline{R}_j}{\partial \eta_1} \sum_{m=0}^{N-1} \left(\begin{array}{c} N-1 \\ m \end{array} \right) \eta_1^m (1-\eta_1)^{N-m-1} \frac{1}{N} [1 - P_c(m)]^K \\
&+ \underline{R}_j \sum_{m=1}^{N-1} \left(\begin{array}{c} N-1 \\ m \end{array} \right) m \eta_1^{m-1} (1-\eta_1)^{N-m-1} \frac{1}{N} [1 - P_c(m)]^K \\
&- \underline{R}_j \sum_{m=0}^{N-2} \left(\begin{array}{c} N-1 \\ m \end{array} \right) (N-m-1) \eta_1^m (1-\eta_1)^{N-m-2} \\
&\times \frac{1}{N} [1 - P_c(m)]^K. \qquad \text{(A.10)}
\end{aligned}
$$

Appendix B

Appendix of Chapter 3

B.1 Derivative for the Cost Function of Min-SER

We denote the real part of any quantity as $(\cdot)^r$ or $Re\{\cdot\}$ and the imaginary part as $(\cdot)^i$ or $Im\{\cdot\}$. From (3.23), given a selection matrix $\mathcal{C}_i$, we can write the derivative of the cost function with respect to $\mathbf{t}_i^r$ as the following

$$\begin{aligned}\frac{\partial g_i(\mathbf{t}_i, \mathcal{C}_i)}{\partial \mathbf{t}_i^r} &= \frac{1}{|\mathcal{S}_i|}\sum_{p\in\mathcal{S}_i}\left[\frac{1}{|\mathbf{f}_{i,i}(p)|^2}\left(\frac{\partial \mathbf{G}_i(p,p)}{\partial \mathbf{w}_i^r}\frac{\partial \mathbf{w}_i^r}{\partial \mathbf{t}_i^r} + \frac{\partial \mathbf{G}_i(p,p)}{\partial \mathbf{w}_i^i}\frac{\partial \mathbf{w}_i^i}{\partial \mathbf{t}_i^r}\right)\right. \\ &\quad \left. - \frac{\mathbf{G}_i(p,p)}{|\mathbf{f}_{i,i}(p)|^4}\left(\frac{\partial |\mathbf{f}_{i,i}(p)|^2}{\partial \mathbf{w}_i^r}\frac{\partial \mathbf{w}_i^r}{\partial \mathbf{t}_i^r} + \frac{\partial |\mathbf{f}_{i,i}(p)|^2}{\partial \mathbf{w}_i^i}\frac{\partial \mathbf{w}_i^i}{\partial \mathbf{t}_i^r}\right)\right] \end{aligned} \tag{B.1}$$

$$\begin{aligned}\frac{\partial g_i(\mathbf{t}_i, \mathcal{C}_i)}{\partial \mathbf{t}_i^i} &= \frac{1}{|\mathcal{S}_i|}\sum_{p\in\mathcal{S}_i}\left[\frac{1}{|\mathbf{f}_{i,i}(p)|^2}\left(\frac{\partial \mathbf{G}_i(p,p)}{\partial \mathbf{w}_i^r}\frac{\partial \mathbf{w}_i^r}{\partial \mathbf{t}_i^i} + \frac{\partial \mathbf{G}_i(p,p)}{\partial \mathbf{w}_i^i}\frac{\partial \mathbf{w}_i^i}{\partial \mathbf{t}_i^i}\right)\right. \\ &\quad \left. - \frac{\mathbf{G}_i(p,p)}{|\mathbf{f}_{i,i}(p)|^4}\left(\frac{\partial |\mathbf{f}_{i,i}(p)|^2}{\partial \mathbf{w}_i^r}\frac{\partial \mathbf{w}_i^r}{\partial \mathbf{t}_i^i} + \frac{\partial |\mathbf{f}_{i,i}(p)|^2}{\partial \mathbf{w}_i^i}\frac{\partial \mathbf{w}_i^i}{\partial \mathbf{t}_i^i}\right)\right]. \end{aligned} \tag{B.2}$$

$$\frac{\partial \mathbf{G}_i}{\partial w_i(l)^r} = 2\sigma_n^2\sum_{j=1}^{M_r}\mathbf{Q}\mathbf{\Theta}(\epsilon_i, N, 0)^* Re\left\{\frac{\partial \mathbf{W}_{i,j}}{\partial w_i(l)^r}\mathbf{W}_{i,j}^H\right\}\mathbf{\Theta}(\epsilon_i, N, 0)\mathbf{Q}^H \tag{B.3}$$

$$\frac{\partial \mathbf{G}_i}{\partial w_i(l)^i} = 2\sigma_n^2\sum_{j=1}^{M_r}\mathbf{Q}\mathbf{\Theta}(\epsilon_i, N, 0)^* Re\left\{\frac{\partial \mathbf{W}_{i,j}}{\partial w_i(l)^i}\mathbf{W}_{i,j}^H\right\}\mathbf{\Theta}(\epsilon_i, N, 0)\mathbf{Q}^H \tag{B.4}$$

We also have the derivatives of the matrix $\mathbf{W}_{i,j}$ with respect to the real and imaginary parts of the l^{th} component $w_i(l)$ of the vector $\mathbf{w}_i$

$$\frac{\partial \mathbf{W}_{i,j}}{\partial w_i(l)^r} = \begin{bmatrix} 0 & ... & 1 & ... & 0 \\ \vdots & \vdots & \ddots & \ddots & \vdots \\ 0 & ... & ... & 1 & ... \end{bmatrix} \quad \frac{\partial \mathbf{W}_{i,j}}{\partial w_i(l)^i} = \begin{bmatrix} 0 & ... & i & ... & 0 \\ \vdots & \vdots & \ddots & \ddots & \vdots \\ 0 & ... & ... & i & ... \end{bmatrix}. \tag{B.5}$$

Let $(\mathbf{q}^{(p)})^T$ be the p^{th} row of the matrix $\bar{\mathbf{Q}}$, thus

$$\frac{\partial |\mathbf{f}_{i,i}(p)|^2}{\partial \mathbf{w}_i^r} = [2\mathbf{f}_{i,i}(p)^r Re\{(\mathbf{q}^{(p)})^T \mathcal{C}_i \mathcal{H}^T\} + 2\mathbf{f}_{i,i}(p)^i Im\{(\mathbf{q}^{(p)})^T \mathcal{C}_i \mathcal{H}^T\}] \tag{B.6}$$

$$\frac{\partial |\mathbf{f}_{i,i}(p)|^2}{\partial \mathbf{w}_i^i} = [-2\mathbf{f}_{i,i}(p)^r Im\{(\mathbf{q}^{(p)})^T \mathcal{C}_i \mathcal{H}^T\} + 2\mathbf{f}_{i,i}(p)^i Re\{(\mathbf{q}^{(p)})^T \mathcal{C}_i \mathcal{H}^T\}]. \tag{B.7}$$

$$\frac{\partial \mathbf{w}_i^r}{\partial \mathbf{t}_i^r} = Re\{\mathbf{U}_i^s(:, 2:(D_e+1))\} \tag{B.8}$$

$$\frac{\partial \mathbf{w}_i^i}{\partial \mathbf{t}_i^r} = Im\{\mathbf{U}_i^s(:, 2:(D_e+1))\} \tag{B.9}$$

$$\frac{\partial \mathbf{w}_i^r}{\partial \mathbf{t}_i^i} = -Im\{\mathbf{U}_i^s(:, 2:(D_e+1))\} \tag{B.10}$$

$$\frac{\partial \mathbf{w}_i^i}{\partial \mathbf{t}_i^i} = Re\{\mathbf{U}_i^s(:, 2:(D_e+1))\} \tag{B.11}$$

B.2 The Derivative of the MMSE Cost Function With Respect to the Frequency Offset

For a given Δ, the characteristic polynomial of the matrix $\mathbf{M}(\epsilon, \Delta)$ is given as

$$\phi(\lambda, \epsilon) = \det(\lambda \mathbf{I} - \mathbf{M}(\epsilon, \Delta)). \tag{B.12}$$

Let $\hat{\lambda}$ be the smallest eigenvalue of the matrix $\mathbf{M}(\epsilon, \Delta)$, and $\hat{\mathbf{z}}$ be the corresponding eigenvector. It must satisfy the characteristic equation

$$\phi(\hat{\lambda}, \epsilon) = 0. \tag{B.13}$$

Taking derivative to the implicit function with respect to ϵ , we have

$$\frac{\partial \phi}{\partial \lambda}\frac{\partial \lambda}{\partial \epsilon} + \frac{\partial \phi}{\partial \epsilon} = 0. \tag{B.14}$$

Thus we have

$$\frac{\partial \hat{\lambda}}{\partial \epsilon} = -\left(\left.\frac{\partial \phi}{\partial \lambda}\right|_{\lambda=\hat{\lambda}}\right)^{-1} \left.\frac{\partial \phi}{\partial \epsilon}\right|_{\lambda=\hat{\lambda}}. \tag{B.15}$$

Notice that we assume that $\left.\frac{\partial \phi}{\partial \lambda}\right|_{\lambda=\hat{\lambda}} \neq 0$ here, and it is equivalent to having the smallest eigenvalue without multiplicity. In particular,

$$\left.\frac{\partial \phi}{\partial \lambda}\right|_{\lambda=\hat{\lambda}} = \mathrm{Tr}[\mathrm{adj}(\hat{\lambda}\mathbf{I} - \mathbf{M}(\epsilon, \Delta))] \tag{B.16}$$

$$\left.\frac{\partial \phi}{\partial \epsilon}\right|_{\lambda=\hat{\lambda}} = -\mathrm{Tr}\left[\mathrm{adj}(\hat{\lambda}\mathbf{I} - \mathbf{M}(\epsilon, \Delta))\frac{\partial \mathbf{M}(\epsilon, \Delta)}{\partial \epsilon}\right], \tag{B.17}$$

where $\mathrm{Tr}(\cdot)$ denotes the trace of any matrix, and $\mathrm{adj}(\cdot)$ stands for the classical adjoint of any matrix. We can obtain that $\mathrm{adj}(\hat{\lambda}\mathbf{I} - \mathbf{M}(\epsilon, \Delta)) = \hat{\mathbf{z}}\hat{\mathbf{z}}^H$, since

$$\hat{\mathbf{z}}\hat{\mathbf{z}}^H(\hat{\lambda}\mathbf{I} - \mathbf{M}(\epsilon, \Delta)) = 0 = \det(\hat{\lambda}\mathbf{I} - \mathbf{M}(\epsilon, \Delta)). \tag{B.18}$$

Simply, we have

$$\frac{\partial \hat{\lambda}}{\partial \epsilon} = \hat{\mathbf{z}}^H \frac{\partial \mathbf{M}(\epsilon, \Delta)}{\partial \epsilon}\hat{\mathbf{z}}. \tag{B.19}$$

Notice that $\frac{\partial \mathbf{M}(\epsilon, \Delta)}{\partial \epsilon}$ can be derived from the derivative of $\mathbf{P}_{j,i}(\epsilon, \Delta, b)$ with respect to ϵ as

$$\frac{\partial \mathbf{P}_{j,i}(\epsilon, \Delta, b)}{\partial \epsilon} = \mathbf{Q}\mathbf{\Theta}(-\epsilon, \Delta, b)\mathbf{J}(b)\mathbf{R}_j(b, \Delta) \tag{B.20}$$

where $\mathbf{J} = \mathrm{diag}\{-j2\pi(N + L_{CP})b, ..., -j2\pi[(N + L_{CP})b + N - 1]\}$.

B.3 Derivative of the Training-based Equalizer Design

Let us define the real and imaginary parts of the vector $\mathbf{p}_i$ as $\mathbf{p}_i^r$ and $\mathbf{p}_i^i$, and $\mathbf{g}_i = [1, \mathbf{p}_i^T]^T$. We denote

$$\gamma(\mathbf{p}_i) = \mathbf{g}_i^H \mathbf{K}_i \mathbf{g}_i \tag{B.21}$$

where we drop the parameters to simplify the notation. From (3.46), the derivative of the cost function with respect to $\mathbf{p}_i^r$ and $\mathbf{p}_i^i$ can be derived as

$$\frac{\partial \gamma(\mathbf{p}_i)}{\partial \mathbf{p}_i^r} = \frac{\partial \gamma(\mathbf{p}_i)}{\partial \mathbf{f}_i^r}\frac{\partial \mathbf{f}_i^r}{\partial \mathbf{p}^r} + \frac{\partial \gamma(\mathbf{p}_i)}{\partial \mathbf{f}_i^i}\frac{\partial \mathbf{f}_i^i}{\partial \mathbf{p}^r} \tag{B.22}$$

$$\frac{\partial \gamma(\mathbf{p}_i)}{\partial \mathbf{p}_i^i} = \frac{\partial \gamma(\mathbf{p}_i)}{\partial \mathbf{f}_i^r}\frac{\partial \mathbf{f}_i^r}{\partial \mathbf{p}^i} + \frac{\partial \gamma(\mathbf{p}_i)}{\partial \mathbf{f}_i^i}\frac{\partial \mathbf{f}_i^i}{\partial \mathbf{p}^i}. \tag{B.23}$$

$$\begin{aligned}\mathbf{K}_i(\epsilon_i, \Delta_i, \mathbf{b}_{i,i}) &= \mathbf{D}_i^H[\bar{\mathbf{\Lambda}}_i - \bar{\mathbf{\Lambda}}_i\mathbf{P}_i(\epsilon_i,\Delta_i)(\mathbf{P}_i(\epsilon_i,\Delta_i)^H\bar{\mathbf{\Lambda}}_i\mathbf{P}_i(\epsilon_i,\Delta_i))^{-1} \\ &\quad \cdot\mathbf{P}_i(\epsilon_i,\Delta_i)^H\bar{\mathbf{\Lambda}}_i]\mathbf{D}_i.\end{aligned} \tag{B.24}$$

Let $\mathbf{k}_i(b) = \left[\frac{v_i(0,b)^*}{\mathbf{f}_{i,i}(0)}, ..., \frac{v_i(N-1,b)^*}{\mathbf{f}_{i,i}(N-1)}\right]^H$ and $\mathbf{v}_i(b) = [v_i(0,b), ..., v_i(N-1,b)]^T$, thus

$$\begin{aligned}\gamma(\mathbf{p}_i) &= \sum_{b=0}^{K-1}\|\mathbf{v}_i(b)\|^2 - [\mathbf{k}_i(0)^H, ..., \mathbf{k}_i(K-1)^H]\mathbf{P}_i(\mathbf{P}_i^H\bar{\mathbf{\Lambda}}_i\mathbf{P}_i)^{-1}\mathbf{P}_i^H \\ &\times [\mathbf{k}_i(0)^H, ..., \mathbf{k}_i(K-1)^H]^H\end{aligned} \tag{B.25}$$

where $\mathbf{v}_i = [v_i(0), ..., v_i(N-1)]^T$ is the transmitted data of the i^{th} stream. We can derive the following

$$\begin{aligned}\frac{\partial \gamma(\mathbf{p}_i)}{\partial \mathbf{f}_{i,i}(l)^r} &= -2Re\left\{\left[\frac{\partial \mathbf{k}_i(0)^H}{\partial \mathbf{f}_{i,i}(l)^r}, ..., \frac{\partial \mathbf{k}_i(K-1)^H}{\partial \mathbf{f}_{i,i}(l)^r}\right]\mathbf{P}_i(\mathbf{P}_i^H\bar{\mathbf{\Lambda}}_i\mathbf{P}_i)^{-1}\mathbf{P}_i^H\right. \\ &\cdot \left.[\mathbf{k}_i(0)^H, ..., \mathbf{k}_i(K-1)^H]^H\right\} \\ &\quad -[\mathbf{k}_i(0)^H, ..., \mathbf{k}_i(K-1)^H]\mathbf{P}_i(\mathbf{P}_i^H\bar{\mathbf{\Lambda}}_i\mathbf{P}_i)^{-1}\mathbf{P}_i^H\frac{\partial \bar{\mathbf{\Lambda}}_i}{\partial \mathbf{f}_{i,i}(l)^r} \\ &\quad \cdot\mathbf{P}_i(\mathbf{P}_i^H\bar{\mathbf{\Lambda}}_i\mathbf{P}_i)^{-1}\mathbf{P}_i^H[\mathbf{k}_i(0)^H, ..., \mathbf{k}_i(K-1)^H]^H\end{aligned} \tag{B.26}$$

$$\begin{aligned}\frac{\partial\gamma(\mathbf{p}_i)}{\partial\mathbf{f}_{i,i}(l)^i} &= -2Re\left\{\left[\frac{\partial\mathbf{k}_i(0)^H}{\partial\mathbf{f}_{i,i}(l)^i},...,\frac{\partial\mathbf{k}_i(K-1)^H}{\partial\mathbf{f}_{i,i}(l)^i}\right]\mathbf{P}_i(\mathbf{P}_i^H\bar{\mathbf{\Lambda}}_i\mathbf{P}_i)^{-1}\mathbf{P}_i^H\right.\\ &\left.\cdot\,[\mathbf{k}_i(0)^H,...,\mathbf{k}_i(K-1)^H]^H\right\}\\ &-[\mathbf{k}_i(0)^H,...,\mathbf{k}_i(K-1)^H]\mathbf{P}_i(\mathbf{P}_i^H\bar{\mathbf{\Lambda}}_i\mathbf{P}_i)^{-1}\mathbf{P}_i^H\frac{\partial\bar{\mathbf{\Lambda}}_i}{\partial\mathbf{f}_{i,i}(l)^i}\\ &\cdot\mathbf{P}_i(\mathbf{P}_i^H\bar{\mathbf{\Lambda}}_i\mathbf{P}_i)^{-1}\mathbf{P}_i^H[\mathbf{k}_i(0)^H,...,\mathbf{k}_i(K-1)^H]^H \qquad \text{(B.27)}\end{aligned}$$

where

$$\frac{\partial\mathbf{k}_i(b)}{\partial\mathbf{f}_{i,i}(l)^r} = [0,...,-\frac{v_i(l,b)^*}{\mathbf{f}_{i,i}(l)^2},...,0]^H \qquad \text{(B.28)}$$

$$\frac{\partial\mathbf{k}_i(b)}{\partial\mathbf{f}_{i,i}(l)^i} = [0,...,-i\frac{v_i(l,b)^*}{\mathbf{f}_{i,i}(l)^2},...,0]^H \qquad \text{(B.29)}$$

$$\frac{\partial\bar{\mathbf{\Lambda}}_i}{\partial\mathbf{f}_{i,i}(l)^r} = \mathbf{I}_{K\times K}\otimes\text{diag}\{0,...,2\mathbf{f}_{i,i}(l)^r,...,0\} \qquad \text{(B.30)}$$

$$\frac{\partial\bar{\mathbf{\Lambda}}_i}{\partial\mathbf{f}_{i,i}(l)^i} = \mathbf{I}_{K\times K}\otimes\text{diag}\{0,...,2\mathbf{f}_{i,i}(l)^i,...,0\}. \qquad \text{(B.31)}$$

Also we have

$$\frac{\partial\mathbf{f}_{i,i}^r}{\partial\mathbf{p}_i^r} = Re\{\bar{\mathbf{Q}}(:,2:(L_{CP}+1))\} \qquad \text{(B.32)}$$

$$\frac{\partial\mathbf{f}_{i,i}^i}{\partial\mathbf{p}_i^r} = Im\{\bar{\mathbf{Q}}(:,2:(L_{CP}+1))\} \qquad \text{(B.33)}$$

$$\frac{\partial\mathbf{f}_{i,i}^r}{\partial\mathbf{p}_i^i} = -Im\{\bar{\mathbf{Q}}(:,2:(L_{CP}+1))\} \qquad \text{(B.34)}$$

$$\frac{\partial\mathbf{f}_{i,i}^i}{\partial\mathbf{p}_i^i} = Re\{\bar{\mathbf{Q}}(:,2:(L_{CP}+1))\}. \qquad \text{(B.35)}$$

Appendix C

Appendix of Chapter 4

C.1 Proof of Proposition 4

From equation (4.8), we notice that the cost function

$$\begin{aligned} R_b(\mathbf{p}, g_s) &= \prod_{i=1}^{M_u} v_i d_i^{-1} p_i^{-1} \\ &= \prod_{i=1}^{M_u} (\|\mathbf{h}_{i,2}\|^2 g_s \sigma_1^2 + \sigma_2^2) g_s^{-1} |\mathbf{G}_{eq}(i,i)|^{-2} p_i^{-1} \\ &= \sum_{t=0}^{M_u} a_t g_s^{-t} \prod_{i=1}^{M_u} p_i^{-1} \end{aligned} \tag{C.1}$$

where $a_t \geq 0$. Therefore $\sum_{t=0}^{M_u} a_t g_s^{-t} \prod_{i=1}^{M_u} p_i^{-1}$ is a posynomial [113].

We notice that the term $\mathrm{Tr}\{\mathbf{H}_1 \mathbf{Q}_{eq}^H \mathbf{\Theta} \mathbf{Q}_{eq} \mathbf{H}_1^H + \mathbf{I}\sigma_1^2\} g_s = \sum_{t=1}^{M_u} b_t p_t g_s + M_r \sigma_1^2 g_s$, where $b_t \geq 0$. This is a posynomial. We also observe that $\sum_{i=1}^{M_u} p_i$ is a posynomial. Therefore, the optimization has the structure of minimizing a posynomial subject to posynomial upper bound inequality constraints. We conclude that the optimization in (4.8) is a standard geometric program [113].

C.2 An Iterative Algorithm for All-Pass Relay Design

By taking the transformation $\mathbf{p^t} = \log(\mathbf{p})$ and $g_s^t = \log(g_s)$, the problem (4.8) can be transformed into the following convex optimization problem [113]

$$\begin{gathered}\min_{\mathbf{p}^t, g_s^t} R_b(\mathbf{p}^t, g_s^t) \\ \text{s.t.} \quad \log(\textstyle\sum_{i=1}^{M_u} e^{p_i^t}) \leq \log(P_t), \\ \log(\mathrm{Tr}\{\mathbf{H}_1 \mathbf{Q}_{eq}^H \mathbf{\Theta}^t \mathbf{Q}_{eq} \mathbf{H}_1^H + \mathbf{I}\sigma_1^2\}) + g_s^t \leq \log(P_r) \end{gathered} \tag{C.2}$$

where $\mathbf{\Theta}^t = \mathrm{diag}\{e^{p_1^t}, ..., e^{p_{M_u}^t}\}$. This problem can be solved using interior point methods. A standard procedure for solving this problem can be found from [77]. We briefly describe the procedure here.

Using the logarithmic barrier function defined as

$$\begin{aligned}\phi(\mathbf{p}^t, g_s^t) &= -\log[\log(P_t) - \log(\sum_{i=1}^{M_u} e^{p_i^t})] \\ &- \log[-\log(\mathrm{Tr}\{\mathbf{H}_1 \mathbf{Q}_{eq}^H \mathbf{\Theta}^t \mathbf{Q}_{eq} \mathbf{H}_1^H + \mathbf{I}\sigma_1^2\}) \\ &- g_s^t + \log(P_r)]. \end{aligned} \tag{C.3}$$

With the barrier function, we solve an unconstrained optimization problem

$$\min_{\mathbf{p}^t, p_s^t} -R_b(\mathbf{p}^t, g_s^t) + \frac{1}{t}\phi(\mathbf{p}^t, g_s^t) \tag{C.4}$$

where $t > 0$. The problem can be solved by the steepest descent algorithm with Armijo step size selection [77]. By increasing t, the optimizer to the unconstrained convex optimization problem converges to the solution to the constrained optimization problem [77]. Finally, the permutation that corresponds to the maximum sum rate is selected.

Bibliography

[1] A. Paulraj and T. Kailath, "U. S. #5345599: increasing capacity in wireless broadcast systems using distributed transmission/directional reception (DTDR)," Sept. 1994.

[2] E. Telatar, "Capacity of multi-antenna gaussian channels," *Eur. Trans. Telecom. ETT*, vol. 10, no. 6, pp. 585–596, 1999.

[3] G. J. Foschini and M. J. Gans, "On limits of wireless communications in a fading environment when using multiple antennas," *Wireless Personal Communications*, vol. 6, no. 3, pp. 311–335, March 1998.

[4] D. Gesbert, M. Shafi, D.-S. Shiu, P. J. Smith, and A. Naguib, "From theory to practice: An overview of MIMO space-time coded wireless systems," *IEEE Jour. Select. Areas in Commun.*, vol. 21, no. 3, pp. 281–302, April 2003.

[5] A. Paulraj, R. Nabar, and D. Gore, *Introduction to Space-Time Wireless Communications*, Cambridge University Press, 2003.

[6] "IEEE 802.16 Task Group 3," http://grouper.ieee.org/groups/802/16/tg3/.

[7] "3GPP Home Page," http://www.3gpp.org.

[8] "IEEE 802.11n," [Online]. Available: http://grouper.ieee.org/groups /802/11.

[9] T. M. Cover and J. A. Thomas, *Elements of Information Theory*, John Wiley and Sons, New York, 1991.

[10] V. Tarokh, N. Seshadri, and A. R. Calderbank, "Space-time codes for high data rate wireless communication: Performance criterion and code construction," *IEEE Trans. Inf. Th.*, vol. 44, no. 2, pp. 744–765, March 1998.

[11] V. Tarokh, H. Jafarkhani, and A. R. Calderbank, "Space-time block codes from orthogonal designs," *IEEE Trans. Inf. Th.*, vol. 45, no. 5, pp. 1456–1467, Jul. 1999.

[12] H. Bolcskei, D. Gesbert, and A. J. Paulraj, "On the capacity of OFDM-based spatial multiplexing systems," *IEEE Trans. Commun.*, vol. 50, no. 2, pp. 225 –234, Feb. 2002.

[13] D. J. Love, R. W. Heath, Jr., and T. Strohmer, "Grassmannian beamforming for multiple-input multiple-output wireless systems," *IEEE Trans. Inform. Theory*, vol. 49, pp. 2735–2747, Oct. 2003.

[14] W. Yu, W. Rhee, S. Boyd, and J. Cioffi, "Iterative water-filling for vector multiple access channels," in *Proc. International Symposium on Information Theory*, June 2001, p. 322.

[15] G. Caire and S. Shamai, "On the achievable throughput of a multi-antenna Gaussian broadcast channel," *IEEE Trans. Inform. Theory*, vol. 49, no. 7, pp. 1691–1706, July 2003.

[16] S. Vishwanath, N. Jindal, and A. Goldsmith, "Duality, achievable rates, and sum-rate capacity of Gaussian MIMO broadcast channels," *IEEE Trans. Inf. Th.*, vol. 49, no. 10, pp. 2658–2668, Oct. 2003.

[17] W. Yu and J. M. Cioffi, "Sum capacity of a Gaussian vector broadcast channel," in *Proc. Int. Symp. on Info. Theo.*, Jul. 2002, p. 498.

[18] P. Viswanath and D. N. C. Tse, "Sum capacity of the vector Gaussian broadcast channel and uplink-downlink duality," *IEEE Trans. Inf. Th.*, vol. 49, no. 8, pp. 1912–1921, Aug. 2003.

[19] M. Sharif and B. Hassibi, "On the capacity of MIMO broadcast channels with partial side information," *IEEE Trans. Inform. Theory*, vol. 51, no. 2, pp. 506–522, Feb. 2005.

[20] B. Wang, J. Zhang, and A. Host-Madsen, "On the capacity of MIMO relay channels," *IEEE Trans. Inform. Theory*, vol. 51, no. 1, pp. 29–43, Jan. 2005.

[21] A. Host-Madsen and J. Zhang, "Capacity bounds on power allocation in wireless relay channel," *IEEE Trans. Inform. Theory*, pp. 29–43, Jan. 2005.

[22] C. K. Lo, S. Vishwanath, and R. W. Heath, Jr., "Sum-rate bounds for MIMO relay channels using precoding," in *Proc. Glob. Telecom. Conf.*, 2005.

[23] S. Vishwanath and S. A. Jafar, "On the capacity of vector Gaussian interference channels," in *IEEE Information Theory Workshop*, San Antonio, TX, Oct. 2004, pp. 365–369.

[24] E. G. Larsson and P. Stoica, *Space-Time Block Coding for Wireless Communications*, Cambridge University Press, New York, 2003.

[25] A. Paulraj, R. Nabar, and D. Gore, *Introduction to Space-Time Wireless Communications*, Cambridge University Press, New York, 2003.

[26] R. F. H. Fischer, *Precoding and Signal Shaping for Digital Transmission*, Wiley-IEEE Press, July 2002.

[27] E. Visotsky and U. Madhow, "Space-time transmit precoding with imperfect feedback," *IEEE Trans. Inf. Th.*, vol. 47, no. 6, pp. 2632–2639, Sept. 2001.

[28] N. Jindal, W. Rhee, S. Vishwanath, S. A. Jafar, and A. Goldsmith, "Sum power iterative water-filling for multi-antenna gaussian broadcast channels," *IEEE Trans. Inform. Theory*, vol. 51, no. 4, pp. 1570–1580, April 2005.

[29] R. W. Heath Jr., M. Airy, and A. J. Paulraj, "Multiuser diversity for MIMO wireless systems with linear receivers," in *Proc. of the Asilomar*

Conf. on Signals, Systems and Computers, Nov. 2001, vol. 2, pp. 1194 –1199.

[30] P. Viswanath, D.N.C. Tse, and R. Laroia, "Opportunistic beamforming using dumb antennas," *IEEE Trans. Inf. Th.*, vol. 48, no. 6, pp. 1277–1294, June 2002.

[31] A. Sang, X. Wang, M. Madihian, and R. D. Gitlin, "Donwlink scheduling schemes in cellular packet data systems of multiple-input multiple-output antennas," in *Proc. Glob. Telecom. Conf.*, Dallas, TX, Nov. 29 - Dec. 3 2004, vol. 6, pp. 4021–4027.

[32] C. Windpassinger, R. F. H. Fischer, T. Vencel, and J. B. Huber, "Precoding in multiantenna and multiuser communications," *IEEE Trans. Wireless Commun.*, vol. 3, no. 4, pp. 1305–1316, July 2004.

[33] T. Yoo and A. Goldsmith, "Optimality of zero-forcing beamforming with multiuser diversity," in *Proc. Int. Conf. on Commun.*, May 2005, vol. 1, pp. 542–546.

[34] Z. Tu and R. S. Blum, "Multiuser diversity for a dirty paper approach," *IEEE Commun. Lett.*, vol. 7, no. 8, pp. 370–372, Aug. 2003.

[35] R. Chen, R. W. Heath Jr., and J. G. Andrews, "Transmit selection diversity for unitary precoded multiuser spatial multiplexing systems with linear receivers," accepted subject to minor revisions to IEEE Trans. on Signal Processing, Jan. 2005.

[36] J. N. Laneman and G. W. Wornell, "Exploiting distributed spatial diversity in wireless networks," in *Proc. of Allerton Conf. on Comm. Cont. and Comp.*, Monticello, IL, Oct. 2000.

[37] A. Sendonaris, E. Erkip, and B. Aazhang, "User cooperation diversity. part I. system description," *IEEE Trans. Commun.*, vol. 51, no. 11, pp. 1927–1938, Nov. 2003.

[38] R. U. Nabar, H. Bolcskei, and F. W. Kneubuhler, "Fading relay channels: Performance limits and space-time signal design," *IEEE J. Select. Areas Commun.*, vol. 22, no. 6, pp. 1099–1109, August 2004.

[39] O. Munoz, J. Vidal, and A. Agustin, "Non-regenerative MIMO relaying with channel state information," in *Proc. Int. Conf. Acoust., Speech and Sig. Proc.*, March 2005, vol. 3, pp. 361–364.

[40] B. Rankov and A. Wittneben, "On the capacity of relay-assisted wireless MIMO channels," in *Proc. of IEEE Workshop on Signal Processing Advances in Wireless Comm.*, July 2004, pp. 323–327.

[41] T. Rappaport, *Wireless Communications: Principles and Practice*, Prentice Hall, second edition, 1996.

[42] R. Knopp and P. Humblet, "Information capacity and power control in single-cell multiuser communications," in *Proc. Int. Conf. on Commun.*, June 1995, vol. 1, pp. 331–335.

[43] D. Gesbert and M. Slim-Alouini, "How much feedback is multi-user diversity really worth?," in *Proc. Int. Conf. on Commun.*, June 2004, pp. 234–238.

[44] J. G. Andrews, "Interference cancellation for cellular systems: a contemporaray overview," *IEEE Wireless Commun. Mag.*, vol. 12, no. 2, pp. 19–29, April 2005.

[45] M. B. Breinholt, M. D. Zoltowski, and T. A. Thomas, "Space-time equalization and interference cancellation for MIMO-OFDM," in *Proc. of the Asilomar Conf. on Signals, Systems and Computers*, Nov. 2002, vol. 2, pp. 1688–1693.

[46] T. A. Thomas and F. W. Vook, "Multi-user frequency-domain channel identification, interference suppression, and equalization for time-varying broadband wireless communications," in *Sensor Array and Multichannel Signal Processing Workshop 2000. Proceedings of the 2000 IEEE*, March 2000, pp. 444–448.

[47] J.-W. Liang, J.-T. Chen, and A. J. Paulraj, "A two-stage hybrid approach for CCI/ISI reduction with space-time processing," *IEEE Commun. Lett.*, vol. 1, no. 6, pp. 163–165, Nov. 1997.

[48] T. Tang and R. W. Heath, Jr., "Space-time interference cancellation in MIMO-OFDM systems," accepted to *IEEE Trans. on Veh. Technol.*, 2005.

[49] R. Pabst, B. H. Walke, D. C. Schultz, D. C. Herhold, H. Yanikomeroglu, S. Mukherjee, H. Viswanathan, M. Lott, W. Zirwas, M. Dohler, H. Aghvami, D. D. Falconer, and G. P. Fettweis, "Relay-based deployment concepts for wireless and mobile broadband radio," *IEEE Commun. Mag.*, vol. 42, no. 9, pp. 80–89, Sept. 2004.

[50] H. Hu, H. Yanikomeroglu, D. D. Falconer, and S. Periyalwar, "Range extension without capacity penalty in cellular networks with digital fixed relays," in *Proc. Glob. Telecom. Conf.*, Nov. 29 - Dec. 3 2004, vol. 5, pp. 3053–3057.

[51] M. Airy, R. W. Heath, Jr., and S. Shakkottai, "Multiuser diversity for the multiple antenna broadcast channel with linear receivers: asymptotic analysis," in *Proc. of the Asil. Conf. on Sig. Sys. and Comp.*, 7-10, Nov. 2004, vol. 1, pp. 886–890.

[52] M. Airy, A. Forenza, R. W. Heath, Jr., and S. Shakkottai, "Practical costa precoding for the multiple antenna broadcast channel," in *Proc. Glob. Telecom. Conf.*, 29 Nov. - 3 Dec. 2004, vol. 6, pp. 3942–3946.

[53] M. Johansson, "Benefits of multiuser diversity with limited feedback," in *Proc. of IEEE Workshop on Signal Processing Advances in Wireless Comm.*, June 2003, pp. 155–159.

[54] S. Sanayei, A. Nosratinia, and N. Al-Dhahir, "Opportunistic dynamic subchannel allocation in multiuser OFDM networks with limited feedback," in *IEEE Information Theory Workshop*, Oct. 2004, pp. 182–186.

[55] X. Qin and R. Berry, "Opportunistic splitting algorithms for wireless networks," in *IEEE INFOCOM 2004*, March 2004, vol. 3, pp. 1662–1672.

[56] T. Tang and R. W. Heath, Jr., "Opportunistic feedback for downlink multiuser diversity," *IEEE Commun. Lett.*, vol. 9, no. 10, pp. 948–950, Oct. 2005.

[57] G. de Veciana and S. Patil, "Measurement-based opportunistic feedback and scheduling for wireless systems," in *Proc. of Allerton Conf. on Comm. Cont. and Comp.*, Oct. 2005.

[58] O.-S. Shin and K. B. Lee, "Antenna-assisted round robin scheduling for MIMO cellular systems," *IEEE Commun. Lett.*, vol. 7, no. 3, pp. 109–111, March 2003.

[59] J. Jiang, R. M. Buehrer, and W. H. Tranter, "High-speed downlink packet transmission with spatial multiplexing and scheduling," March 2004, vol. 4, pp. 2148–2152.

[60] D. Park, H. Seo, H. Kwon, and B.G. Lee, "A new wireless packet scheduling algorithm based on the CDF of user transmission rates," in *Proc. Glob. Telecom. Conf.*, Dec. 2003, vol. 1, pp. 528–532.

[61] M. Airy, S. Shakkottai, and R. W. Heath Jr., "How bad is spatially greedy scheduling in multi-user mimo systems?," in *Proc. of the Asilomar Conf. on Signals, Systems and Computers*, Nov. 2003.

[62] Jaehak Chung, Chan-Soo Hwang, Kiho Kim, and Young Kyun Kim, "A random beamforming technique in MIMO systems exploiting multiuser diversity," *IEEE Jour. Select. Areas in Commun.*, vol. 21, no. 5, pp. 848 –855, June 2003.

[63] Chiung-Jang Chen and Li-Chun Wang, "Coverage and capacity enhancement in multiuser MIMO systems with scheduling," in *Proc. Glob. Telecom. Conf.*, 29 Nov.-3 Dec. 2004, vol. 1, pp. 101–105.

[64] V. K. N. Lau, "Proportional fair space-time scheduling for wireless communications," *IEEE Trans. Commun.*, vol. 53, no. 8, pp. 1353–1360, Aug. 2005.

[65] N. Sharma and L. H. Ozarow, "A study of opportunism for multiple-antenna systems," *IEEE Trans. Inform. Theory*, vol. 51, no. 5, pp. 1804–1814, May 2005.

[66] T. Yoo and A. Goldsmith, "Optimality of zero-forcing beamforming with multiuser diversity," in *Proc. Int. Conf. on Commun.*, May 2005, vol. 1, pp. 542–546.

[67] M. Fuchs, G. Del Galdo, and M. Haardt, "A novel tree-based scheduling algorithm for the downlink of multi-user MIMO systems with ZF beamforming," in *Proc. Int. Conf. Acoust., Speech and Sig. Proc.*, March 2005, vol. 3, pp. iii/1121 – iii/1124.

[68] P. Svedman, S. K. Wilson, L. J. Cimini, Jr., and B. Ottersten, "A simplified opportunistic feedback and scheduling scheme for OFDM," in *Proc. Veh. Technol. Conf.*, May 2004, vol. 4, pp. 1878–1882.

[69] X. Liu, E. Chong, and N. Shroff, "A framework for opportunistic scheduling in wireless networks," *Computer Networks Journal (Elsevier)*, vol. 41, no. 4, pp. 451–474, 2003.

[70] D. W. Bliss, A. M. Chan, and N. B. Chang, "MIMO wireless communication channel phenomenology," *IEEE Trans. Antennas Propagat.*, vol. 52, no. 8, pp. 2073–2082, Aug. 2004.

[71] B. M. Hochwald, T. L. Marzetta, and V. Tarokh, "Multi-antenna channel hardening and its implications for rate feedback and scheduling," *IEEE Jour. Select. Areas in Commun.*, vol. 21, no. 5, pp. 684 –702, June 2003.

[72] R. W. Heath, Jr., T. Strohmer, and A. J. Paulraj, "On quasi-orthogonal signatures for CDMA systems," *IEEE Trans. Inform. Theory*, vol. 52, no. 3, pp. 1217–1226, 2006.

[73] B. Hassibi and B. M. Hochwald, "How much training is needed in multiple-antenna wireless links?," *IEEE Trans. Inform. Theory*, vol. 49, no. 4, pp. 951–963, April 2003.

[74] L. Tong, B. M. Sadler, and M. Dong, "Pilot-assisted wireless transmissions: general model, design criteria, and signal processing," *IEEE*

Signal Processing Mag., vol. 21, no. 6, pp. 12–25, Nov. 2004.

[75] A. J. van der Veen and A. Paulraj, "An analytical constant modulus algorithm," *IEEE Trans. Signal Processing*, vol. 44, no. 5, pp. 1136–1155, May 1996.

[76] R. Djapic, A. J. van der Veen, and L. Tong, "Synchronization and packet separation in wireless ad hoc networks by known modulus algorithms," *IEEE J. Select. Areas Commun.*, vol. 23, no. 1, pp. 51–64, Jan. 2005.

[77] S. Boyd and L. Vandenberghe, *Convex Optimization*, Cambridge University Press, 2004.

[78] D. P. Bertsekas, *Nonlinear Programming*, Athena Scientific, 2nd edition, 1999.

[79] G. Casella and R. L. Berger, *Statistical Inference*, Duxbury Press, 2nd edition, June 2001.

[80] J. C. Spall, *Introduction to Stochastic Search and Optimization: Estimation, Simulation and Control*, John Wiley & Sons, 2003.

[81] J. S. Rustagi, *Optimization Techniques in Statistics*, Academic Press, 1994.

[82] T. A. Thomas and F. W. Vook, "Asynchronous interference suppression in broadband cyclic-prefix communications," in *IEEE Wireless Communications and Networking Conference*, March 2003, pp. 568–572.

[83] *Wireless LAN Medium Access Control (MAC) and Physical Layer (PHY) Specification*, IEEE Std. 802.11, 1997.

[84] L. Hanzo, M. Munster, B. J. Choi, and T. Keller, *OFDM and MC-CDMA for Broadband Multi-user Communications, WLAN and Broadcasting*, Wiley, 2003.

[85] T. Tang and R. W. Heath, Jr., "Joint frequency offset estimation and interference cancellation in MIMO-OFDM systems," in *Proc. of IEEE Vehicular Technology Conf.*, Los Angeles, CA, Sept. 2004, pp. 1553–1557.

[86] C. Tellambura, I. R. Johnson, Y. J. Guo, and S. K. Barton, "Equalization and frequency offset correction for HIPERLAN," in *Proc. of International Symposium on Personal, Indoor and Mobile Radio Communications*, Helsinki, Finland, Sep. 1997, pp. 796–800.

[87] Lang Tong, "Joint blind signal detection and carrier recovery over fading channels," in *Proc. Int. Conf. Acoust., Speech and Sig. Proc.*, May 1995, vol. 2, pp. 1205–1208.

[88] M. Morelli and U. Mengali, "Carrier-frequency estimation for transimissions over selective channels," *IEEE Trans. Commun.*, vol. 48, pp. 1580–1589, 2000.

[89] M. Luise, M. Marselli, and R. Reggiannini, "Low-complexity blind carrier frequency recovery for OFDM signals over frequency-selective radio

channels," *IEEE Trans. Commun.*, vol. 50, no. 7, pp. 1182 – 1188, July 2002.

[90] Y. Yao and G. B. Giannakis, "Blind carrier-frequency offset estimation of SISO, MIMO and multi-user OFDM," *IEEE Trans. Commun.*, vol. 53, no. 1, Jan. 2005, to appear.

[91] O. Besson and P. Stoica, "On parameter estimation of MIMO flat-fading channels with frequency offsets," *IEEE Trans. on Signal Processing*, vol. 51, pp. 602–613, 2003.

[92] T. Cui and C. Tellambura, "Joint channel and frequency offset estimation and training sequence design for MIMO systems over frequecy selective channels," in *Proc. IEEE Glob. Telecom. Conf.*, Dallas, TX, Nov. 29 - Dec. 3 2004.

[93] K. Cho and D. Yoon, "On the general expression of one- and two-dimensional amplitude modulations," *IEEE Trans. Commun.*, vol. 50, no. 7, pp. 1074 – 1080, July 2002.

[94] Y. Ding, T. N. Davidson, Z.-Q. Luo, and K. M. Wong, "Minimum BER block precoder for zero-forcing equalization," *IEEE Trans. on Sig. Proc.*, vol. 51, no. 9, pp. 2410–2423, Sept. 2003.

[95] R. Baldick, *Optimization of Engineering Systems Course Notes*, The University of Texas at Austin, http://www.ece.utexas.edu/∼baldick/.

[96] "ETSI TR 101 112 V3.2.0 UMTS 30.03," April 1998.

[97] A. Saleh, A. Rustako, and R. Roman, "Distributed antennas for indoor radio communications," *IEEE Trans. Commun.*, vol. 35, no. 12, pp. 1245–1251, Dec. 1988.

[98] H. Bolukbasi, H. Yanikomeroglu, H. Falconer, and S. Periyalwar, "On the capacity of cellular fixed relay networks," in *Electrical and Computer Engr., 2004. Canadian Conf. on*, May 2004, vol. 4, pp. 2217–2220.

[99] J. N. Laneman, G. W. Wornell, and D. N. C. Tse, "An efficient protocol for realizing cooperative diversity in wireless networks," in *Proc. Int. Symp. on Info. Theo.*, June 2001, p. 294.

[100] A. Sendonaris, E. Erkip, and B. Aazhang, "User cooperation diversity. part II. implementation aspects and performance analysis," *IEEE Trans. Commun.*, vol. 51, no. 11, pp. 1939–1948, Nov. 2003.

[101] J. N. Laneman and G. W. Wornell, "Energy efficient antenna sharing and relaying for wireless networks," in *IEEE Wireless Communications and Networking Conference*, Oct. 2000, pp. 7–12.

[102] M. Hu, J. Zhang, and J. Sadowsky, "Traffic aided opportunistic scheduling for wireless networks: Algorithms and performance bounds," *Computer Networks Journal*, Nov. 2004.

[103] M. O. Hasna and M.-S. Alouini, "A performance study of dual-hop transmissions with fixed gain relays," *IEEE Trans. Wireless Commun.*, vol. 3, no. 6, pp. 1963–1968, Nov. 2004.

[104] A. So and B. Liang, "Effect of relaying on capacity improvement in wireless local area networks," in *IEEE Wireless Communications and Networking Conference*, March 2005, vol. 3, pp. 1539–1544.

[105] G. J. Foschini, "Layered space-time architecture for wireless communication in a fading environment when using multiple antennas," *The Bell System Technical Journal*, vol. 1, no. 2, pp. 41–59, 1996.

[106] S. Catreux, V. Erceg, D. Gesbert, and R. W. Heath Jr., "Adaptive modulation and MIMO coding for broadband wireless data networks," *IEEE Comm. Mag.*, vol. 40, no. 6, pp. 108–115, June 2002.

[107] A. Agustin, O. Muhoz, and J. Vidal, "A game theoretic approach for cooperative MIMO schemes with cellular reuse of the relay slot," in *Proc. Int. Conf. Acoust., Speech and Sig. Proc.*, May 2004, vol. 4, pp. 581–584.

[108] H. Shi, T. Abe, T. Asai, and H. Yoshino, "A relaying scheme using QR decomposition with phase control for MIMO wireless networks," in *Proc. Int. Conf. on Commun.*, May 2005, vol. 4, pp. 2705–2711.

[109] X. Tang and Y. Hua, "Optimal waveform design for MIMO relaying," in *Proc. of IEEE Workshop on Signal Processing Advances in Wireless Comm.*, 2005.

[110] H. Bolcskei and R. U. Nabar, "Realizing MIMO gains without user cooperation in large single-antenna wireless networks," in *Proc. Int.*

Symp. on Info. Theo., July 2004, p. 18.

[111] A. Ribeiro, X. Cai, and G. B. Giannakis, "Opportunistic multipath for bandwidth-efficient cooperative networking," *IEEE Trans. Wireless Commun.*, 2006, to appear.

[112] R. A. Horn and C. R. Johnson, *Matrix Analysis*, Cambridge University Press, 1985.

[113] M. Chiang, *Geometric programming for communication systems*, vol. 2, Short monograph in Foundations and Trends in Communication and Information Theory, July 2005.

[114] G. Dirmic and N. D. Sidiropoulos, "On downlink beamforming with greedy user selection: performance analysis and a simple new algorithm," *IEEE Trans. Signal Processing*, vol. 53, no. 10, pp. 3857–3868, Oct. 2005.

[115] D. J. Love, R. W. Heath, Jr., W. Santipach, and M. L. Honig, "What is the value of limited feedback for MIMO channels?," *IEEE Commun. Mag.*, vol. 42, no. 10, pp. 54–59, Oct. 2003.

[116] F. W. Vook, X. Zhuang, K. L. Baum, T. A. Thomas, and M. C. Cudak, "Signalling methodologies to support closed-loop transmit processing in TDD-OFDMA," July 2004, IEEE C802.16e-04/103r2.

Index

Vita

Taiwen Tang received the B.E. in electronic engineering from Beijing University of Posts and Telecommunications, Beijing, China in 2001, and the M.S. in electrical and computer engineering from Colorado State University, Fort Collins, Colorado in 2003. He is currently pursuing the Ph.D. degree in the Department of Electrical and Computer Engineering, The University of Texas at Austin.

From August 2001 to July 2003, he was a member of the Radar and Communications Group in Colorado State University, working on remote sensing with dual polarized meteorological Radar systems. Since August 2003, he has been a research assistant in the Wireless Networking and Communications Group of The University of Texas at Austin. His current research interests are in wireless digital communications and wireless networks with emphases on MIMO-OFDM communications and feedback protocols and scheduling algorithms in wireless networks. His industrial experience includes internship in Beceem Communications Inc., Santa Clara, CA, participating in IEEE 802.16 d/e system development and standard contributions, in the summer of 2004.

Permanent address: 2000 Burton Dr. 154, Austin, Texas 78741

This dissertation was typeset with LaTeX[†] by the author.

[†]LaTeX is a document preparation system developed by Leslie Lamport as a special

version of Donald Knuth's TEX Program.